ARCHEAN CRUSTAL EVOLUTION IN THE BARBERTON MOUNTAIN LAND, SOUTH AFRICA: U-Pb AND Nd ISOTOPIC CONSTRAINTS

By

SANDRA L. KAMO, B.Sc.

A Thesis

Submitted to the School of Graduate Studies

in Partial Fulfilment of the Requirements

for the Degree

Master of Science

McMaster University

MASTER OF SCIENCE (1992) **McMaster University**

(Geology) **Hamilton, Ontario**

TITLE: Archean Crustal Evolution in the Barberton Mountain Land: U-Pb and Nd Isotopic Constraints

AUTHOR: Sandra L. Kamo

B.Sc. (University of Toronto)

SUPERVISORS: Dr. D.W. Davis

Dr. A.P. Dickin

Dr. R.H. McNutt

NUMBER OF PAGES: x, 114

ABSTRACT

New U-Pb ages from the Barberton Mountain Land document an 800 m.y. period of Archean magmatism (ca. 3540 Ma to ca. 2740 Ma) that can be divided into five distinct episodes. Magmatic activity during Episode I includes tonalite-trondhjemite gneisses such as the Steynsdorp pluton (3509 +8/-7 Ma) and a tectonically interleaved sliver (3538 +4/-2 Ma) located at the base of the Onverwacht Group. Trondhjemitic magmatism of Episode II is synchronous with volcanism and inferred D_1 thrusting of the Onverwacht Group and is represented by plutons such as the Doornhoek (3448 ± 4 Ma), Theespruit (3443 +4/-3 Ma), and Stolzburg (3459 +5/-4 Ma). A quartz-feldspar porphyry dyke, related to Episode II, intrudes the Komati Formation of the Onverwacht Group and yields an age of 3467 +12/-7 Ma. D_2-related thrusting, volcanism, sedimentation, and tonalitic plutonism in the north-central part of the Barberton greenstone belt (BGB) occurred during Episode III and are recorded by an ignimbrite which was deposited between the Fig Tree and Moodies Groups during regional deformation (3227 ± 1 Ma), by pre- and post-tectonic porphyries (3227 Ma), and by the emplacement of the Kaap Valley tonalite (3227 ± 1 Ma). Episode IV is characterized by the intrusion of large sheet-like potassic batholiths to the north and south of the BGB and syenitic plutonism at ca. 3107 Ma, and by D_3-related deformation at the northern margin of the BGB.

Gold mineralization also appears to coincide in time with this episode. The last known period of Archean magmatic activity in the BGB is represented by late phase granite magmatism at ca. 2740 Ma (Episode V).

Epsilon Nd values range from +1.3 to -0.7 in rocks varying in composition from gabbro to granodiorite that were emplaced during Episodes I to IV. A gabbro from the Komati Formation, with a baddeleyite age of 3352 +6/-5 Ma, has an ϵ_{Nd} of +1.3, which is the only value to fall on a depleted mantle growth curve. This value is similar to ϵ_{Nd} data obtained by others for ca. 3450 Ma basalts from the Onverwacht Group. Three Episode IV plutons have identical ϵ_{Nd} values of -0.5, and a granite pluton from Episode V has an ϵ_{Nd} of -4.3, indicating a source compatible with remelting of older crust.

In summary, the protracted evolution of the Barberton Mountain Land occurred in a series of discrete events widely separated in time. Each event is characterized by a number of geological processes (magmatism, volcanism, sedimentation) that appear to coincide in time with thrust-related deformation as a result of compressional tectonics. The duration of the main period of crustal growth occurred over ≈365 m.y. from ca. 3470 Ma, with the formation of the main Onverwacht sequence and its associated tonalitic-trondhjemitic rocks through ca. 3230 Ma, with the intrusion of the Kaap Valley tonalite and D_2 thrust-related deformation, to ca. 3105 Ma, with the widespread emplacement of sheet-like potassic batholiths bordering the Barberton greenstone belt.

ACKNOWLEDGEMENTS

I wish to acknowledge the instruction, advice, and knowledge gained from my supervisors Dr. R.H. McNutt, Dr. A.P. Dickin, and especially Dr. D.W. Davis. Sample collecting for this thesis was thoughtfully guided by Dr. M.J. de Wit, Dr. L.J. Robb and Dr. C.E.J. de Ronde. Appreciation is also extended to all employees of the Jack Satterly Geochronology Laboratory for their interest and encouragement throughout the duration of this project. In particular, I wish to thank Dr. T.E. Krogh for continued employment throughout this part-time endeavour, and Dr. L.M. Heaman for helpful suggestions and guidance, particularly in the early stages of writing. Finally, I wish to thank my husband for his spirited and independent nature which kept him occupied kayaking/skiing when I was busy studying/picking zircons.

TABLE OF CONTENTS

LIST OF FIGURES

LIST OF TABLES

LIST OF ACRONYMS

AGC	Ancient Gneiss Complex
BGB	Barberton Greenstone Belt
BML	Barberton Mountain Land
CHUR	Chondritic Uniform Reservoir
DM	Depleted Mantle
IF	Initial Frantz
FF	Final Frantz
LIL	Large Ion Lithophile
LREE	Light Rare Earth Elements
SHRIMP	Sensitive High-Resolution Ion Microprobe
TTG	Tonalite - Trondhjemite Granitoid

CHAPTER 1:

INTRODUCTION

The Barberton greenstone belt (BGB), contained within the Barberton Mountain Land (BML), South Africa (Figs. 1 and 2), is one of six Archean metavolcanic belts on the Kaapvaal craton; these are the Pietersburg, Sutherland, Murchison, Amalia, Muldersdrif and Barberton belts. Of these, the BGB is the largest, best preserved, and best exposed greenstone succession. It hosts some of the world's oldest plutonic and supracrustal sequences and many of the classic exposures of Archean geology are preserved within it. Therefore, clues to understanding the geological development of this ca. 3.1 - 3.5 Ga granite-greenstone terrane provide key information on the growth and evolution of Earth's early crust. It is for these reasons and the fact that it hosts numerous gold deposits, that the BGB continues to be one of the most widely studied greenstone belts in the world.

Models for the geological evolution of the BGB remain controversial. Early geological mapping by A.L. Hall (1918) and by Visser et al. (1956) provided comprehensive accounts of the geology of the BGB, but it was not until the late 1960's that further mapping studies (Viljoen and Viljoen, 1969a,b) provided the basis for a 20 km thick "continuous" stratigraphic evolution model i.e. wherein temporal and/or tectonic discontinuities are not recognized (Viljoen and Viljoen, 1969a). This stratigraphy, originally known as the Swaziland Supergroup (Fig. 3), was officially

adopted (SACS, 1980) with the name: "Barberton Sequence" and was subsequently incorporated into many models of Archean terrestrial processes (Anhaeusser, 1978; Glikson, 1979; Windley, 1984; Nisbet, 1987; Condie, 1989). Although part of the stratigraphy has also been named the "Jamestown ophiolite complex" (de Wit et al., 1987b), the entire stratigraphy of the BGB is most commonly referred to in the literature as the "Swaziland Supergroup".

Recently, the BGB has been the focus of a number of detailed structural and sedimentological studies (e.g. Williams and Furnell, 1979; de Wit, 1982, 1983; de Wit et al., 1983, 1987a; Lamb, 1984; Lowe et al., 1985; de Ronde, 1991) as well as geochronological studies (e.g. Armstrong et al., 1990; de Ronde et al., 1991; Kröner et al., 1991). These new studies contradict the continuous stratigraphy model because they show that portions of the BGB represent a litho-tectonic complex in which parts of the original stratigraphy were repeated due to horizontal shortening. In addition, a geophysical study indicated that the greenstone belt has a maximum thickness of 8 km (de Beer et al., 1988) which is much less than the 20 km of continuous stratigraphy suggested by Viljoen and Viljoen (1969a). Further, de Wit et al. (1987a) reported that felsic igneous rocks, that comprise parts of the Hooggenoeg and Theespruit Formations, are mainly shallow level intrusions and subsurface domes that have been emplaced within thrust zones that have repeated the stratigraphy in these formations.

Precise isotopic dating techniques applied to geologically well-defined problems frequently provide the essential data needed for resolving controversies of

this nature. New developments in dating techniques that have enabled the analysis of individual single grains of zircon (or parts thereof) have provided a tool that has enhanced our ability to: (1) investigate the crustal pre-history of a rock by analyzing xenocrystic zircon grains, (2) unravel complicated sequences of events in heterogeneously deformed terranes, (3) determine the original crystallization ages of rocks that have been variously contaminated through derivation by partial melting of an older source, or by incorporation of wall rock during emplacement, and (4) perform provenance studies on detrital zircons. These advances have been critical in establishing the chronological sequences of events in the BML and other Archean granite-greenstone belts.

In addition to providing chronological information, isotopic studies are useful for evaluating the relative importance of reworking processes during periods of crustal growth. The application of isotopic techniques, such as high precision U-Pb radiometric dating and the study of Nd isotopic variations to the BGB, provides an exceptional opportunity to constrain evolutionary models for the development of Archean greenstone belts.

At the onset of this project there was a clear need for a systematic U-Pb study of the BGB and the surrounding granitoid terrane. Extensive granitoid batholiths and plutons surround the BGB and are exposed in an area at least three times that of the BGB yet, with the exception of limited bulk conventional U-Pb and a few Ar/Ar and Sm-Nd data, only whole-rock Rb-Sr data existed for defining the magmatic evolution in the Barberton Mountain Land. These data were useful as a

reconnaissance tool and for establishing a general framework for the sequence of magmatic events in the BML (Allsop et al., 1962; de Gasparis, 1967; Davies, 1971; Barton, 1983; Barton et al., 1983). However, these data are generally imprecise and, because the BML has had a protracted magmatic evolutionary history, the Rb-Sr systematics of the older plutons have frequently been affected by thermal perturbation(s) and/or hydrothermal alteration associated with the emplacement of younger plutons. Numerous published examples exist elsewhere where the Rb-Sr systematics in rocks have been disturbed even when the dated units lack evidence for post-crystallization disturbance (e.g. Bickford and Mose, 1975; Page, 1978; Heaman et al., 1986; Beakhouse et al., 1988). In addition, most of the existing Rb-Sr and Sm-Nd geochronologic data had errors greater than 50-100 m.y. so even major tectonic and plutonic events were impossible to resolve. For example, Sm-Nd whole-rock isochron ages of 3560 ± 240 Ma (Jahn et al., 1982) and 3526 ± 48 Ma (Hamilton et al., 1979; 1983) for the Onverwacht Group volcanic rocks, long considered the best estimates for the time of volcanism, are not only relatively imprecise, but are presently believed to be ≈100 m.y. too old, as shown in Chapters 4 and 5. The currently accepted age for volcanism is≈ 3440-3490 Ma (Lopez-Martinez et al., 1984; Brévart et al., 1986; Kröner and Todt, 1988; Armstrong et al., 1990) obtained by other dating methods.

The present study will precisely define geochronological relationships of plutonic rocks from the Barberton Mountain Land using U-Pb isotope dilution analyses of zircon, sphene, monazite, rutile and baddeleyite. Initial Nd ratios of

whole rocks will be used to constrain petrogenesis. Specifically, the thesis objectives are:

(i) To elucidate the chronology and duration of granitoid magmatism within and surrounding the BGB using the U-Pb method.

(ii) To determine precise U-Pb ages for key stratigraphic units within the BGB to help resolve the existing controversy concerning the tectonic repetition of BGB stratigraphy.

(iii) To determine Nd isotopic variations in some of the plutonic rocks in order to evaluate the relative contributions from mantle and crustal sources in the generation of these rocks.

(iv) To integrate age and isotopic data with known field relationships in order to understand the sequence of igneous and tectonic events which formed the BGB.

FIGURE 1.

Location map for the Barberton greenstone belt (BGB). The Ancient Gneiss Complex (AGC) is located just south of the BGB.

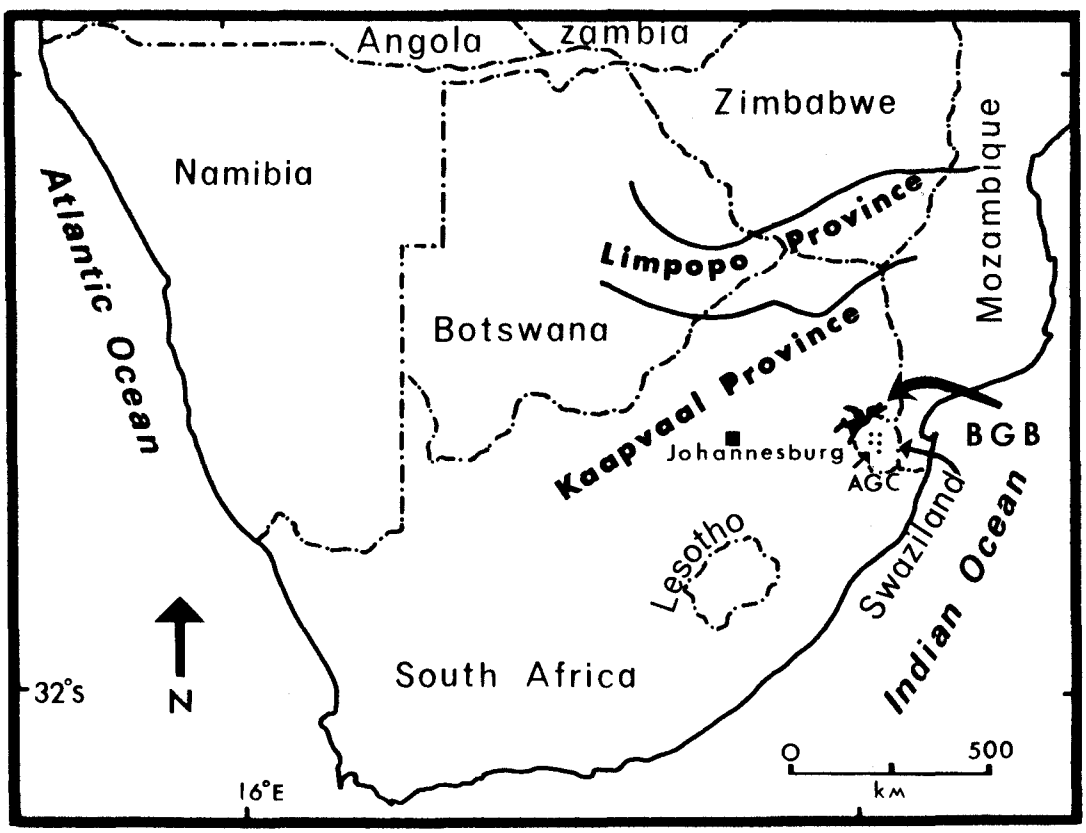
Angola
zambia
Zimbabwe
Mozambique
Namibia
Atlantic Ocean
Limpopo Province
Botswana
Kaapvaal Province
Johannesburg
AGC
BGB
Lesotho
Swaziland
Indian Ocean
South Africa
32°s
N
16°E
0
500
km

FIGURE 2.

Simplified geological map of the Barberton Mountain Land (from Robb et al., 1983). Type locality for the Komati formation is shown.

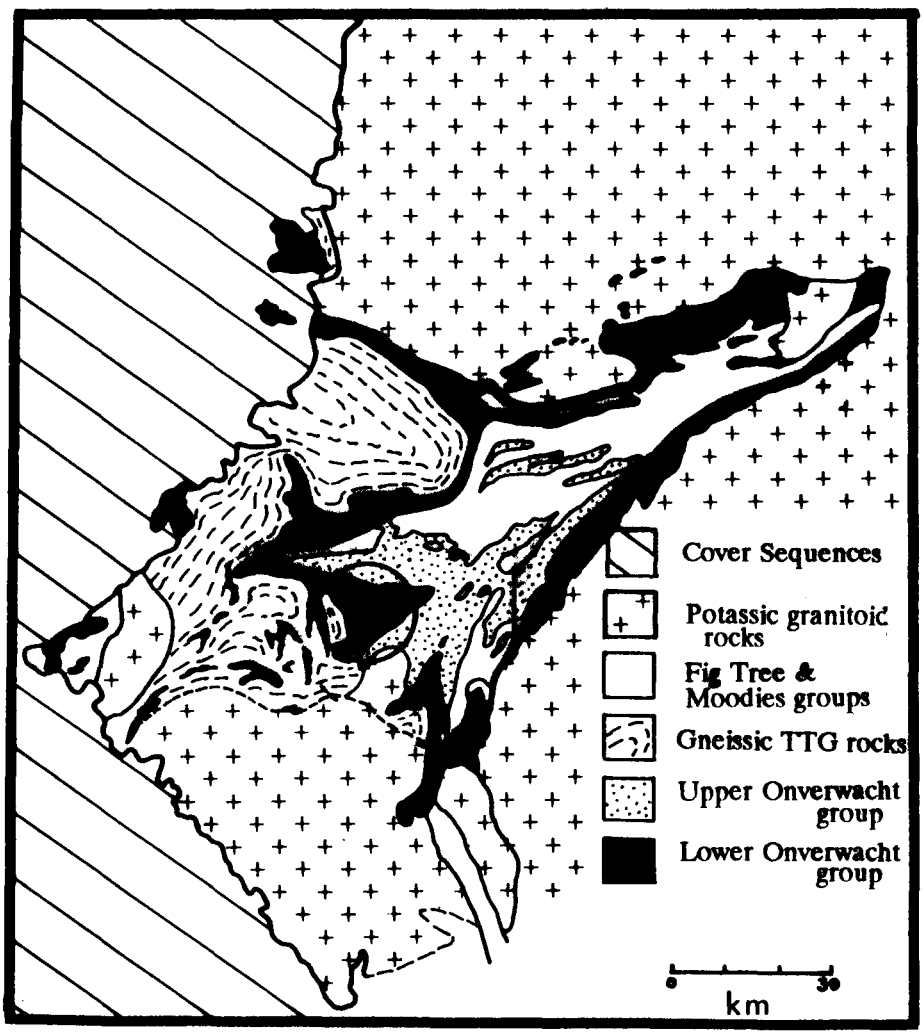
Cover Sequences
Potassic granitoid rocks
Fig Tree & Moodies groups
Gneissic TTG rocks
Upper Onverwacht group
Lower Onverwacht group
0
30
km

CHAPTER 2:

GENERAL GEOLOGY OF THE BARBERTON MOUNTAIN LAND

The BML is located ≈400 km east of Johannesburg on the northwest border of Swaziland (see Fig. 1). There are two major components of the BML: the BGB, exposed over a distance of approximately 50 km by 130 km, and the surrounding granitoid rocks. The BGB comprises the Barberton Sequence (Viljoen and Viljoen, 1969a; Anhaeusser, 1973; SACS, 1980), where the type stratigraphy is best preserved in a sequence of rocks from the southern part of the belt (Fig. 2). Here, the classical chronostratigraphy comprises volcano-sedimentary assemblages of the Onverwacht, Fig Tree, and Moodies Groups, represented schematically in Figure 3. Mafic and ultramafic lavas of the lower Onverwacht Group, called the Tjakastad Subgroup, comprise three formations: the Sandspruit, Theespruit, and Komati Formations. These units are dominated by komatiites and basaltic komatiites (Viljoen and Viljoen, 1969b; Viljoen et al., 1983) with minor banded chert and iron-formation, felsic tuff and agglomerate, calc-silicate rocks, and soda-rich porphyry intrusions. Separating the Tjakastad Subgroup from the overlying Geluk Subgroup is a chert-carbonate unit termed the Middle Marker (Viljoen and Viljoen, 1969b). The three formations of the Geluk Subgroup, the Hooggenoeg, Kromberg, and Zwartkoppie Formations, are dominated by mafic and felsic lava, tuff, agglomerate and porphyries.

Two predominantly sedimentary units lie above the Onverwacht Group: the argillaceous Fig Tree Group and the Moodies Group conglomerates (Visser et al., 1956; SACS, 1980).

Recently, the "classical" Barberton stratigraphy has been revised in order to accomodate structural and geochronological constraints that indicate that sections of the BGB have been repeated due to horizontal shortening within a compressional tectonic environment (Fig. 4). These observations further indicate that this thrust-related "litho-tectonic" complex (i.e. lithologic "packages" of stratigraphy bounded by faults) as documented along both the northwestern and southeastern margins of the belt (Fripp et al., 1980; Lamb, 1984; Paris, 1985) was tectonically transported in a northwesterly direction.

The BGB is almost entirely surrounded by felsic intrusive rocks. The northern and southwestern margins of the BGB are intruded by tonalitic and trondhjemitic gneisses. These elliptical gneissic bodies exhibit chemical variations and have been classified into two groups based on their Sr and REE signatures, the origins of which may be related to the depths at which partial melting occurred (Robb and Anhaeusser, 1983). Extensive sheet-like potassic intrusions predominate to the north and south of the exposed BGB. These flat-lying intrusions comprise a variety of compositions such as granodiorites, adamellites, granites and syenites. Smaller granitoid plutons intrude both supracrustal rocks and the tonalite-trondhjemite gneisses in the extreme southwestern part of the BGB. Most of the supracrustal rocks have been variously altered, either by low grade metamorphism, metasomatism,

or hydrothermal processes.

Complex migmatites characterize the granite-greenstone interfaces and are located mainly at the northern and southwestern margins of the BGB. These have been described in detail by Anhaeusser and Robb (1980) and Robb (1983a). They represent a complicated mixture of tonalitic or trondhjemitic magmas containing remnants of greenstone lithologies, syntectonic anatectites and mafic dykes.

Located to the south of the BML, in central and northern Swaziland, are the high-grade tonalite-trondhjemite gneisses of the Ancient Gneiss Complex (AGC)(Hunter, 1973).

Cover sequences surrounding the BML comprise early Proterozoic volcanic and sedimentary sequences mainly from the Transvaal Supergroup.

FIGURE 3.

Generalized stratigraphy of the Barberton greenstone belt as proposed by Viljoen and Viljoen (1969), SACS (1980) and Anhaeusser (1973). This "layer cake" model was believed to represent 20 km of continuous stratigraphy. Formation descriptions are from Anhaeusser et al. (1983).

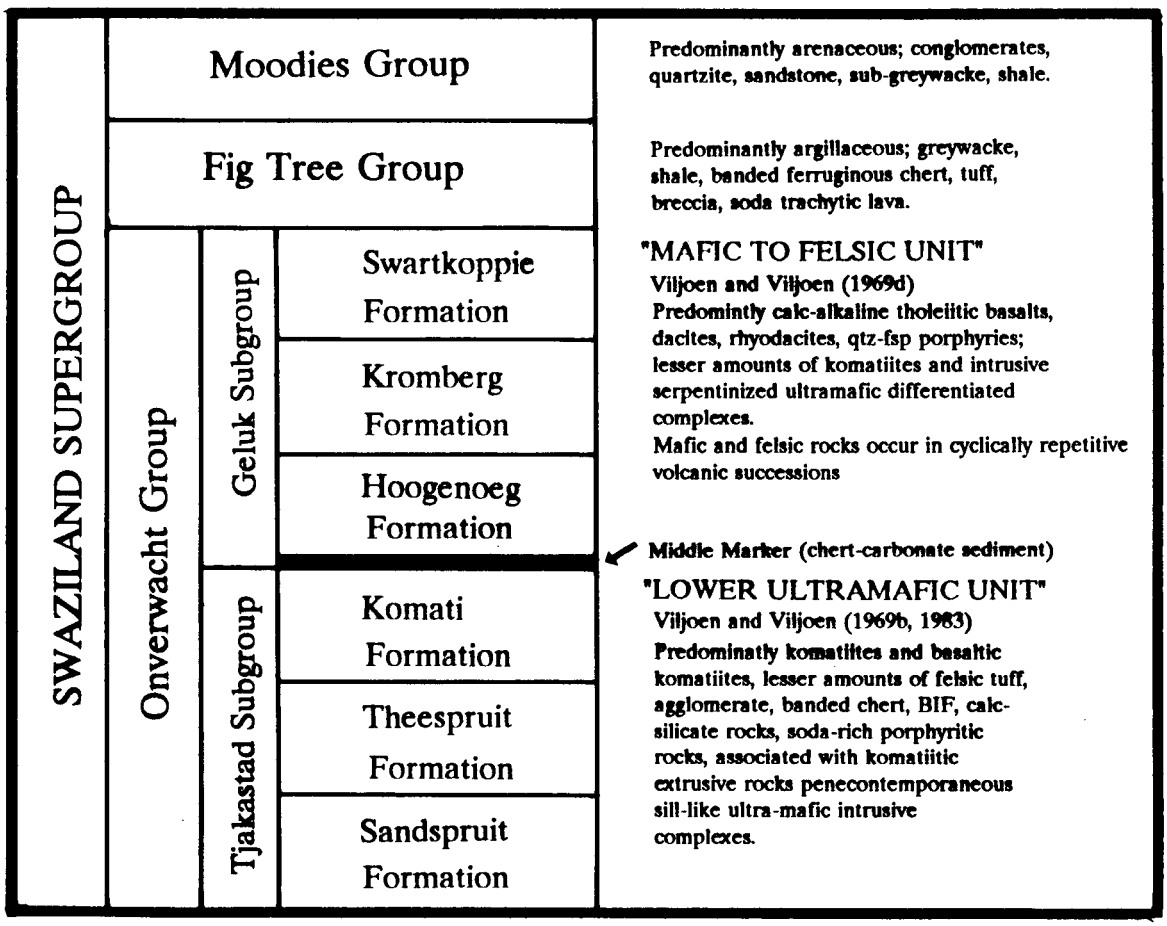
SWAZILAND SUPERGROUP
Moodies Group
Predominantly arenaceous; conglomerates, quartzite, sandstone, sub-greywacke, shale.
Fig Tree Group
Predominantly argillaceous; greywacke, shale, banded ferruginous chert, tuff, breccia, soda trachytic lava.
Onverwacht Group
Geluk Subgroup
Swartkoppie Formation
Kromberg Formation
Hoogenoeg Formation
"MAFIC TO FELSIC UNIT"
Viljoen and Viljoen (1969d)
Predominantly calc-alkaline tholeiitic basalts, dacites, rhyodacites, qtz-fsp porphyries; lesser amounts of komatiites and intrusive serpentinized ultramafic differentiated complexes.
Mafic and felsic rocks occur in cyclically repetitive volcanic successions
Middle Marker (chert-carbonate sediment)
Tjakastad Subgroup
Komati Formation
Theespruit Formation
Sandspruit Formation
"LOWER ULTRAMAFIC UNIT"
Viljoen and Viljoen (1969b, 1983)
Predominatly komatiites and basaltic komatiites, lesser amounts of felsic tuff, agglomerate, banded chert, BIF, calc-silicate rocks, soda-rich porphyritic rocks, associated with komatiitic extrusive rocks penecontemporaneous sill-like ultra-mafic intrusive complexes.

CHAPTER 3:

OVERVIEW OF GEOLOGIC CONCEPTS FOR THE BARBERTON MOUNTAIN LAND

Almost 75 years have elapsed since the pioneering work of A.L. Hall was published in 1918. Interest in the geology of the BML has persisted throughout this period of time and interpretations regarding the evolution of the BML have changed dramatically. For the last 30 years the Onverwacht Group of rocks has been the central focus of interest and new ideas. It was in the Komati River valley of the BML that komatiites were first recorded by Viljoen and Viljoen (1969b) and since that time they have been widely documented, particularly in Archean terranes, and much progress has since been made in understanding the nature and origin of these rocks (see Arndt and Nisbet, 1982). Komatiites are generally believed to have formed by very high degrees of melting, thereby acquiring chemical and isotopic characteristics similar to their mantle source. They, therefore, provide evidence concerning the evolution of the early mantle and crust. This evidence forms the basis for ideas about the origin and nature of ancient oceanic crust (e.g. Sleep and Windley, 1982; Arndt, 1983; Nisbet and Fowler, 1983), and thus provides insight into Archean plate tectonic processes.

The identification of basement to the Barberton Sequence remains obscure; and, until recently, the genetic relationship between the AGC and the BGB was

unknown. However, age data for the AGC, which was once thought to be derived by partial melting of the Onverwacht Group volcanics (Anhaeusser, 1975; Glikson and Jahn, 1985), indicate that it is older than the BGB, based on single grain zircon dating by Compston and Kröner (1988), Kröner and Todt (1988) and Kröner et al. (1989). Temporally, it is possible that the AGC represents basement to the BGB although there is presently no direct evidence for this.

Two opposing interpretations exist on the nature and origin of the Komati Formation. Viljoen and Viljoen (1969a,b) and Viljoen et al.(1983) interpret the Komati Formation as being an extrusive pile of komatiitic flows, citing textural evidence and implications based on geochemical modelling to support their view. In contrast, the Komati Formation has been interpreted by de Wit and Stern (1980) and de Wit et al. (1987b) as a "pseudo-stratigraphy" comparable to Phanerozoic ophiolite sequences. These workers suggest that mafic-ultramafic rocks from the Komati and Kromberg Formations form an Archean oceanic crustal sequence consisting of a high temperature tectono-metamorphic peridotite overlain by an intrusive-extrusive igneous section, capped by a chert-shale sequence. Where Viljoen and Viljoen (1969c) interpret high MgO contents and high Ca/Al_2O_3 ratios as a reflection of clinopyroxene and olivine fractionation and accumulation, de Wit et al. (1987b) emphasize the role of regional metasomatic alteration from hydrothermal interaction with the Archean ocean which hydrated and chemically altered the entire simatic sequence. Thus, the chemical signatures of the komatiites, 95% of which de Wit et al. regard as being metamorphosed into serpentinites, result from large-scale

mobilization of elements rather than reflecting the original igneous chemistry.

Pervasive Si, Ca, Ba and Fe metasomatism have, in fact, been well documented in the Onverwacht Group and its overlying sediments (e.g. Lowe and Knauth, 1977; de Wit and Stern, 1980; de Wit et al., 1982; Hart and de Wit, 1984; Paris et al., 1985; Lowe et al., 1985; Lowe and Byerly, 1986; de Wit et al., 1987b; Duchac and Hanor, 1987; de Ronde,1991). Metasomatism likely occurred early because ^{40}Ar-^{39}Ar step-heating plateau ages of 3330 ± 40 Ma (York et al., 1981) and 3489 ± 68 Ma (Lopez Martinez et al., 1984) on serpentinized komatiites from the lower Onverwacht Group are close to the accepted crystallization ages .

Extensive metasomatism in Onverwacht Group rocks has led to erroneous lithologic interpretations of the upper part of the Onverwacht Group. The Geluk Subgroup volcanic rocks were interpreted as cyclically alternating mafic-to-felsic extrusions (Viljoen and Viljoen, 1969c). Williams and Furnell (1979) interpreted the cycles as a random and complex interfingering of the products of adjacent extrusive centres. In fact, some of the "felsic" units have been identified as silicified mafic-ultramafic rocks (de Wit et al., 1982; Paris et al., 1985; Lowe et al., 1985; Duchac and Hanor, 1987; Hanor and Duchac, 1990) and some have intrusive contacts (de Wit et al., 1987a).

Numerous chert horizons are intercalated within the Onverwacht and Fig Tree Groups (Hall, 1918; Visser, 1956; Viljoen and Viljoen, 1969b). Some of the more prominent units are the Middle Marker, located between the upper and lower Onverwacht Group, and the Swartkoppie, Msauli, and Skokokla chert units, located

near the top of the Onverwacht Group. Although once believed to be a product of Onverwacht Group volcanism, either as altered silicic tuffs (Viljoen and Viljoen, 1969b; Anhausser, 1973) or as ultramafic flows that were syndepositionally altered from interaction with the prevailing hydrosphere or atmosphere (Byerly et al., 1983; Lowe and Byerly, 1986), these highly silicified zones have been identified as secondary silica replacements of pre-existing sediments (Lowe and Knauth, 1977; Stanistreet et al., 1981; Lowe, 1982) and of volcanic rocks (de Wit et al., 1982; Paris et al., 1985; Duchac and Hanor, 1987; Hanor and Duchac, 1990; de Ronde, 1991). The silicified komatiitic rocks preserve ghosts of spinifex and cumulates of olivine and pyroxene of the original ultramafic rocks and are enriched in Si, K, Rb and Ba, depleted in Fe, Mg, Ca, Na, Mn, Sr, Zn, Ni, while Al, Ti, P, Cr, Zr, Y, Nb remained immobile (Duchac and Hanor, 1987). The metasomatic process converted original olivine, pyroxene and plagioclase to quartz, mica and chlorite (Duchac and Hanor, 1987). Similar interpretations have been reported by Jahn et al. (1981) from the Pilbara craton.

The model for silicification of Fig Tree sediments and Onverwacht volcanic rocks involves hydrothermal alteration of the sea floor and overlying sediments from seawater convecting through Archean oceanic crust (Corliss et al., 1979; de Wit, 1982; Paris et al., 1985). Silica and other elements leached from sea floor rocks enrich hydrothermal fluids that circulate in cells through the oceanic crust and along the ocean floor mainly through porous, unconsolidated sediments. The high geothermal gradient needed to drive the inferred convection cells may be related to

shallow-level igneous activity (de Wit, 1982; de Wit et al., 1987a). Characteristically light $\delta^{18}O$ values may reflect temperature-dependent isotopic shifts associated with exhalative activity (Paris et al., 1985). An exhalative environment also accounts for the presence of postulated relict mineralized chimneys situated above serpentinized ultramafic rocks, analogous to "black smokers" currently forming on the ocean floor. Discharges of iron-oxides and silica-rich flocculates from these vents occur along strike as laminated iron-oxide facies banded iron-formation (de Ronde, 1991). These vent structures were described by de Wit et al. (1982) along with exceptionally well-preserved "mudpool" structures (formed by gas streaming subaerially through mud pools) that bear a remarkable resemblance to those currently forming in the Taupo volcanic zone, New Zealand (de Wit et al., 1982; de Ronde, 1991).

Structural deformation in the BGB is polyphase and complex. At the northern margin of the belt, three phases of deformation have been recognized (Ramsay, 1963; Viljoen, 1964; Fripp et al., 1980). Shear zones at the northern margin may be linked to a low angle south-dipping sole thrust at the base of the belt (Fripp et al., 1980). Recent studies focussed on the southern part of the belt indicate stratigraphic thickening by imbricate thrusting (e.g. de Wit, 1982, 1983; de Wit et al., 1983, 1987a; Lamb, 1984; Lowe et al., 1985; de Ronde, 1991). De Wit et al. (1982) recognized the juxtaposition of turbiditic sediments (Stanistreet et al., 1981) and subaerially derived mudpool structures (i.e. sediments from two spatially distinct environments) separated by a strongly foliated flaser-banded chert unit (fuchsite + carbonate + quartz) interpreted to represent an early (D_1) shear zone. These chert units have

been interpreted by de Wit (1982) as evidence for horizontal translation along thrust planes which led to the formation of nappe structures and inverted stratigraphy within the Barberton stratigraphic column. Olistostromes, comprising chaotic breccias within ferruginous cherts and shale units, were cited as further evidence by de Wit (1982) for horizontal mass translation.

An opposing viewpoint is given by Dokka and Lowe (1984) and Lowe et al. (1985) who recognize stratigraphic duplication in the uppermost Onverwacht Group and Fig Tree Group, but consider the underlying stratigraphy to be an intact 12 km succession.

In addition to sea-floor metamorphism, contact metamorphism between the BGB and surrounding granitoids, and burial metamorphism have also been documented within the BGB (Anhaeusser et al., 1969; Cloete, 1990).

High-level felsic intrusions, co-magmatic with the surrounding trondhjemitic terrane, were emplaced contemporaneously with thrusting in the southern part of the BGB (de Wit et al., 1987a; Armstrong et al., 1990).

Sedimentological studies of units within the Onverwacht Group indicate an oceanic environment for volcanism accompanied by minimal sedimentation. Above the Middle Marker, however, pyroclastic, volcaniclastic, biochemical and orthochemical sediments are commonly found. Fig Tree Group sediments, consisting of abundant submarine-fan greywackes and mudstones, paraconformably overlie the Onverwacht Group. Moodies Group sediments in turn overly the Fig Tree Group and consist of braided alluvial and shallow-marine sediments (Eriksson, 1980).

Together the Fig Tree and Moodies Groups were once suggested to have accumulated along a passive continental margin that formed from intracontinental rifting (Eriksson, 1980). However, recent evidence indicates that these sedimentary sequences accumulated in a foredeep-type basin, formed from internal shortening during uplift (Lamb, 1984; Jackson et al., 1987; Nocita, 1989). Lamb (1984) documented large synsedimentary folds in the Fig Tree Group in the southern part of the BGB. As well, Fig Tree and Moodies Group sediments contain recycled Onverwacht Group oceanic volcanic and sedimentary components, as well as older Fig Tree Group components, indicative of an active tectonic environment (Jackson et al., 1987). Finally, the AGC, also an important source terrane for the sediments, records structures that indicate progressive northwestward uplift around 3.4 Ga ago (Jackson, 1984).

CHAPTER 4:

PREVIOUS GEOCHRONOLOGY

The last decade has seen an unprecedented growth in the amount and quality of isotopic data for the BML. Just as geochemical studies stimulated new ideas and dramatically improved our general understanding of geological processes, the growth of isotopic data in Archean terranes has provided critically important data to test new evolutionary models, leading geologists a step further towards understanding Archean geological processes.

(i) Early work

Early contributions to the geochronology of the BML provided broad constraints on the timing of magmatism. Whole-rock Rb-Sr studies on granitoid rocks and migmatitic gneisses (Allsop et al., 1962; de Gasparis, 1967; Davies, 1971) and a bulk conventional U-Pb zircon study (i.e. ages determined by isotope dilution on milligram fractions of zircon; Oosthuyzen, 1970) established a general framework for the magmatic evolution of the granitoid terrane adjacent to the BGB and showed that the granites to the north, which were once thought to represent basement to the BGB, are actually younger (ca. 3000 Ma) than the supracrustal rocks of the BGB. Rb-Sr studies in the BML and AGC revealed that the emplacement of granitoid

rocks occurred episodically from 3500 Ma to 2750 Ma. Based on these data, Anhaeusser and Robb (1981) envisioned continental growth occurring in three cycles at ca. 3500 Ma, ca. 3200 Ma and ca. 2900 Ma, wherein each cycle was characterized by distinctive physical, chemical and isotopic characteristics each representing a wide range of events and processes.

(ii) Recent advances

Precise and accurate ages are imperative for detailing igneous, deformational and metamorphic histories of greenstone belts that have, in some cases, occurred over geologically short durations (e.g. Corfu et al., 1989). Recent analytical advances, particularly in the U-Pb method, such as zircon abrasion and low contamination techniques permitting the analysis of microgram quantities of zircon, baddeleyite and monazite (i.e. single grains or parts thereof), as well as the development of the SHRIMP ion-microprobe (acronym for Sensitive High Resolution Ion Microprobe, Compston et al., 1984; Williams et al., 1984) and the single grain evaporation ("Kober") technique (Kober 1986; 1987), have stimulated a renewed interest in the BML, resulting in a dramatic increase and improvement in the number and quality of isotopic studies in this region.

A summary of recent age data for rocks within the BGB and the granitoid plutons intruding and surrounding it is presented in Tables 1 and 2.

(iii) Age of major volcanism: the Onverwacht group

Currently, the best age estimate for the lower Onverwacht group is≈3450-3490 Ma based on: (1) ^{40}Ar-^{39}Ar ages of metavolcanic rocks from the Komati Formation (Lopez Martinez et al., 1984), and (2) a Pb-Pb age using komatiitic basalts from the Komati Formation (Brévart et al., 1986). Armstrong et al. (1990) reported maximum ages of 3472 ± 5 Ma and 3482 ± 5 Ma for the Komati Formation, based on a number of single zircon U-Pb ages from an interflow sediment within the Komati Formation and xenocrystic zircons from a metagabbro that intrudes the Komati Formation (see Fig. 4), respectively. Zircon ages from the metagabbro, however, ranged from 3511 ± 5 Ma to 3357 ± 10 Ma, and were interpreted to result from inherited and metamorphic zircons, respectively. U-Pb baddeleyite and zircon data obtained in the present study from the same rock unit yield an age of 3352 +6/-5 Ma, which is considered the crystallization age for this rock for reasons given in Chapter 7.

Volcanic and sedimentary units of the Hooggenoeg Formation from the upper Onverwacht group have yielded U-Pb zircon evaporation ages ranging from 3451 ± 15 Ma to 3416 ± 5 Ma (Kröner and Todt, 1988; Kröner et al., 1991) and a U-Pb zircon SHRIMP age of 3445 ± 8 Ma (Armstrong et al., 1990). Felsic volcanism spanned at least 30 m.y. based on the age range obtained by Kröner et al. (1991) from dacitic tuffs and agglomerates from this formation.

Recent age determinations for the trondhjemitic suite that intrudes the BGB at its southwest margin reveal ages similar to those for the Onverwacht volcanic rocks. Two of these intrusions, the Theespruit pluton, dated at 3437 ± 6 Ma

(Armstrong et al., 1990) and 3440 ± 5 Ma (Kröner et al., 1991), and the Stolzburg pluton dated at 3445 ± 4 Ma (Kröner et al., 1991), intrude mafic-ultramafic units of the Hooggenoeg Formation (Robb and Anhaeusser, 1983; de Wit et al., 1987a). These ages are comparable to ages of felsic volcanism in the upper Onverwacht Group and support the hypothesis of de Wit et al. (1987a) that the gneissic trondhjemitic suite is co-magmatic with some high-level felsic volcanic units within the greenstone succession. If, as previously suggested, the generation of these sodic intrusions is syntectonic, i.e. formed by partial melting of simatic rocks over which the lower Onverwacht rocks were overthrust (de Wit et al., 1987a), then these ages also constrain the timing of thrusting in this part of the BGB.

(iv) Evidence for pre-Onverwacht Group crust

Recent U-Pb single zircon investigations on rocks within the Barberton greenstone belt present evidence for a pre-Onverwacht crustal history. For example, a tectonically interleaved thrust slice of gneissic tonalite within the Theespruit formation yields a zircon age of 3538 ± 6 Ma (Armstrong et al., 1990; this study), 50-100 m.y. older than the Onverwacht Group and the oldest rock yet dated within the Barberton sequence. These gneisses record deformation and metamorphism which predates that within the greenstone belt (de Wit, 1983). Single xenocrystic zircon grains from felsic metavolcanic rocks from the Hooggenoeg and Theespruit Formations, yield ages ranging from 3470-3520 Ma (Kröner et al., 1991; Armstrong et al., 1990). This may indicate the presence of an early sialic basement when rocks

of the Onverwacht were emplaced.

(v) Temporal relationships between the BGB and the AGC

An early prevailing question on the genetic relationship between the BGB and the AGC was: did the AGC represent basement to the BGB or was it derived by partial melting of the BGB? Data obtained by Barton et al. (1980) on orthogneisses of the AGC suggested an age of 3555 ± 111 Ma which coincided with the then accepted Sm-Nd age for the Onverwacht Group of 3540 Ma by Hamilton et al. (1979). These data suggested that the orthogneissic component of the AGC was coeval with, and possibly derived from, the lower Onverwacht Group volcanics. However, the Onverwacht Group is now considered to be ≈3450-3490 Ma, as previously discussed. Recent data from zircons from tonalitic orthogneisses of the AGC, analyzed by U-Pb SHRIMP (Compston and Kröner, 1988; Kröner et al., 1989), yielded many pre-3500 Ma ages, as well as the oldest age yet measured at 3644 Ma from a gneissic tonalite inlier of the AGC, located on the southern margin of the BGB. These data have established that some components of the AGC are older than the lower BGB by up to 200 m.y. and, thus, cannot be derived by partial melting of the greenstones as was previously proposed by Anhaeusser (1975) and Glikson and Jahn (1985). In a separate study by Kröner and Compston (1988), granitic clasts from the Moodies Group yielded U-Pb SHRIMP ages of ca. 3570 Ma. These clasts have evolved, potassic granitoid compositions and pronounced negative Eu anomalies (Reimer et al., 1985), demonstrating that a mature source terrane, significantly older

than the volcanic rocks, fed sedimentation in the BGB. Age determinations on gneisses from central Swaziland with similar ages of 3560 Ma (U-Pb SHRIMP; Kröner et al., 1989) were obtained on tonalitic-trondhjemitic plutons rather than K-rich intrusions, so the source for the granitic clasts remains undiscovered. In this same study it was shown that 3560 Ma gneisses contain K-rich lenses that are 3200 Ma, indicating that intense ductile deformation occurred after 3.2 Ga. It has been suggested by Jackson et al. (1987) and Kröner et al. (1989) that granites, which were the source of some Moodies Group clasts, were emplaced at high crustal levels and were subsequently eroded during ductile deformation, thrusting, crustal thickening and uplift. For a review of the isotopic evidence and geological implications of the relationship between the BGB and the AGC, see Kröner and Todt (1988).

(vi) Ages for deposition and provenance of clastic sediments: the Fig Tree and Moodies Groups

Recent single zircon U-Pb evaporation ages for what have been interpreted as dacitic tuffs and agglomerates from the Fig Tree Group, indicate that felsic volcanism spanned at least 35 m.y. from 3259 ± 5 Ma to 3225 ± 3 Ma (Kröner et al., 1991). This age range may correspond to deposition of associated greywackes in the Fig Tree Group which would demonstrate that deposition of the major sedimentary sequences in the BGB was at least 200 m.y. younger than deposition of rocks from the Onverwacht Group. The extrusive nature of some of these rocks, however, has been contested by the results of recent mapping (C. de Ronde, pers.

comm.) and they may, in fact, only constrain *minimum* ages for the time of Fig Tree sedimentation if shown to be intrusive in nature. The youngest age obtained by Kröner et al. (1991) corresponds to the timing of felsic magmatism within the north-central part of the greenstone belt. The Kaap Valley pluton was emplaced at 3227 Ma (this study; Tegtmeyer and Kröner, 1987; Armstrong et al., 1990), the same age as that determined by de Ronde et al. (1991) for two undeformed feldspar-quartz porphyries in this north-central part of the belt. These porphyries are interpreted by de Ronde (1991) to cross-cut regionally deformed (D_2) Fig Tree sediments and intrude up a D_2-related thrust fault(s). If these interpretations are correct, the age of 3227 Ma places a minimum on the time of D_2 deformation and on thrusting in the north-central BGB, and may provide evidence for regional crustal uplift accompanying sedimentation at this time. The above age determinations have also shown that the BGB has evolved over a protracted period of time (>200 m.y.) and that thrusting was diachronous within this time span.

The last stage of mid-Archean sedimentation in the BGB appears to have been the deposition of the Moodies Group. Although this has not been directly dated, it is possible that in some locations it was deposited as a result of tectonism associated with thrusting and emplacement of the Kaap Valley pluton at 3227 Ma (see Chapter 7).

TABLE 1.

Summary of selected age data of units from:
(a) the Onverwacht Group, and (b) the Fig Tree and Moodies Groups.

(Notes: w-r = whole-rock; im = SHRIMP technique; evap^{n} = single zircon Pb evaporation technique)

Table 1a.

Unit	Rock Type	Age (Ma) 2σ errors	Dating Method	Source
Lower Onverwacht Group				
Theespruit Fm	tonalitic wedge tectonically emplaced	3438 ± 6	U-Pb zircon im	Armstrong et al. (1990)
Theespruit Fm	volcaniclastic sediment	<3453 ± 6	U-Pb zircon im	Armstrong et al. (1990)
Komati Fm	komatiitic metabasalt	3489 ± 34	$^{40}Ar/^{39}Ar$ step-heating, w-r and amphibolite concentrate	Lopez-Martinez et al. (1984)
Komati Fm	komatiitic basalt (+tholeiite)	3460 ± 70	Pb-Pb w-r isochron	Brévart et al. (1986)
Komati Fm	interflow sediment	3472 ± 5	U-Pb zircon im	Armstrong et al. (1990)
Upper Onverwacht Group				
Hoogenoeg Fm	felsic volcaniclastic, metaquartzite	3438 ± 12 to 3451 ± 15	U-Pb zircon evap[n]	Kröner and Todt (1988)
Hoogenoeg Fm	dacitic volcanic	3445 ± 8	U-Pb zircon im	Armstrong et al. (1990)
Hoogenoeg Fm	dacitic tuff	3445 ± 3 to 3416 ± 5	U-Pb zircon evap[n]	Kröner et al. (1991)

Table 1b.

Rock Type	Age (Ma) 2σ errors	Dating Method	Interpretation	Source
Fig Tree Group				
greywacke	3453 ± 9	U-Pb zircon ion microprobe	Age represents that of the stratigraphically underlying source terrane (Onverwacht felsic metavolcanics)	Kröner and Compston (1988)
dacitic tuffs and agglomerates	3259 ± 5 to 3225 ± 3	U-Pb zircon evaporation	Age range represents duration of felsic volcanism	Kröner et al. (1991)
Moodies Group				
gneissic granitoid pebbles from conglomerate	3570 ± 6 to 3518 ± 11	U-Pb zircon evaporation	Age range suggests AGC and felsic volcanics of Onverwacht gp are the source terranes	Kröner and Compston (1988)

TABLE 2.

Summary of previous geochronology of plutonic rocks from the Barberton Mountain Land.

(Notes: bc = bulk conventional isotope dilution technique, see Chapt.4(i) for definition; see also notes for Table 1.

Plutonic Unit	Age (Ma) 2σ errors	Dating Method	Source
Gneissic tonalite sliver Theespruit Fm	3538 ± 6	U-Pb Zr im	Armstrong et al.(1990)
Steynsdorp	3490 ± 4	U-Pb Zr evap[n]	Kröner et al. (1991)
Stolzburg	3445 ± 4	U-Pb Zr evap[n]	Kröner et al. (1991)
	3408 +89/-95	Pb-Pb w-r	Robb et al. (1986)
	3481 ± 92	Rb-Sr w-r	Barton et al. (1983)
Doornhoek	3191 ± 46	Rb-Sr w-r	Barton et al. (1983)
Theespruit	3440 ± 5	U-Pb Zr evap[n]	Kröner et al. (1991)
	3437 ± 6	U-Pb Zr im	Armstrong et al. (1990)
	3475 +148/-165	Pb-Pb w-r	Robb et al. (1986)
	3432 ± 135	Rb-Sr w-r	Barton et al. (1983)
	3250 ± 80	U-Pb bc	Oosthuyzen (1970)
Kaap Valley	3226 ± 14	U-Pb Zr im	Armstrong et al. (1990)
	3229 ± 5	U-Pb Zr bc	Tegtmeyer & Kröner (1987)
	3211 +94/-102	Pb-Pb w-r	Robb et al. (1986)
	3191 +77/-81	Pb-Pb w-r	"
	3491 ± 166	Rb-Sr w-r	Barton et al. (1983)
	3310 ± 80	U-Pb bc	Oosthuyzen (1970)
Dalmein	3201 ± 43	Rb-Sr w-r	Barton et al. (1983)
	3290 ± 160	U-Pb bc	Oosthuyzen (1970)
Mpuluzi	3028 ± 14	Rb-Sr w-r	Barton et al. (1983)
	3075 ± 200	U-Pb bc	Oosthuyzen (1970)
	3005 ± 120	Rb-Sr w-r	Allsopp et al. (1962)
Nelspruit	3160 ± 100	U-Pb bc	Oosthuyzen (1970)
Hebron	3211 ± 133	Rb-Sr w-r	E. Barton (unpublished)
Stentor	3250 ± 30	U-Pb bc	Tegtmeyer & Kröner (1987)
Boesmanskop	2848 ± 31	Rb-Sr w-r	Barton et al. (1983)
	3130 ± 60	U-Pb bc	Oosthuyzen (1970)
Mpageni	2810 ± 160	U-Pb bc	Oosthuyzen (1970)
	2496 ± 176	Rb-Sr w-r	De Gasparis (1967)

FIGURE 4.

Proposed stratigraphic sections of the Barberton greenstone belt (from Armstrong et al., 1990).

Viljoen and Viljoen, 1969a
SACS, 1980
Anhaeusser, 1973

Williams and Furnell, 1979

de Wit et al., 1983; 1987a

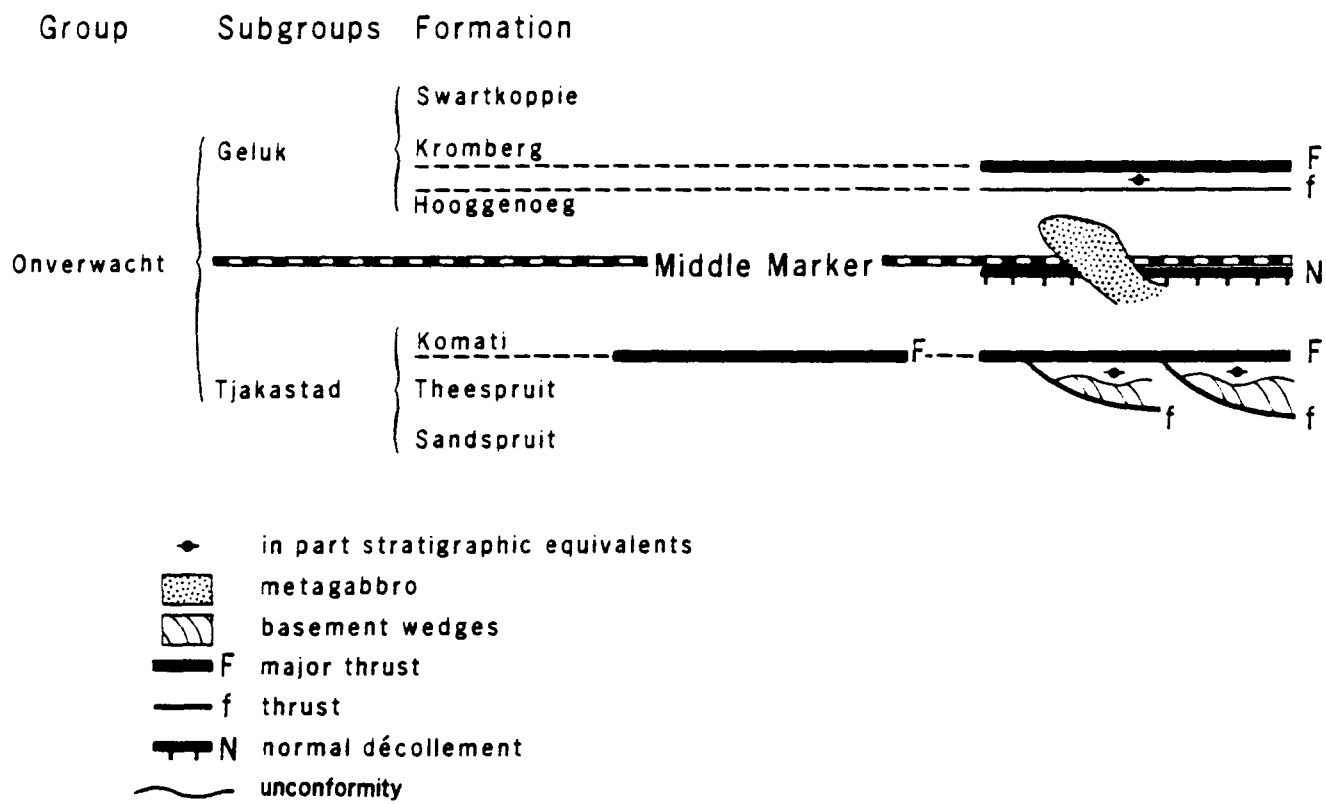

CHAPTER 5:

U-Pb GEOCHRONOLOGY

(i) SAMPLING RATIONALE

Granitoid plutons having a wide range in chemical composition and covering most of the exposed granitoid terrane in the BML were sampled for U-Pb analysis. Key units from within the BGB were sampled in order to place constraints on the time of deformation in the north-central part of the greenstone belt and to elucidate stratigraphic relationships in the Barberton Sequence. These samples have been divided into three groups based on geochemistry and rock association. Sample locations for Groups I and II are indicated in Figure 5 and Group III rocks in Figure 6.

GROUP I: Tonalite-trondhjemite suite

The Kaap Valley is the largest pluton (30 km diameter) in the BML and the only one of tonalitic composition (Robb et al., 1986). It is a homogenous, hornblende-rich tonalite thought to have been diapirically emplaced (Robb et al., 1986). Two samples were obtained, a hornblende-biotite-rich interior phase (**B87-32**), and a hornblende-rich mafic marginal phase (**B87-14**). The proximity of this tonalite to the many gold deposits in the BGB, and hence its potential genetic relationship to them, make it an important unit to study isotopically. Also, by dating

minerals with lower blocking temperatures than zircon, such as sphene (≈500°C), it was hoped that a cooling rate could be estimated, which may indicate the depth of emplacement.

Five samples were collected from the gneissic trondhjemitic terrane located to the southwest of the BGB in order to establish its chronological relationship to the Onverwacht Group volcanics. These trondhjemites are characterized by a strong foliation that parallels the trondhjemite - greenstone contact. Isotopic data obtained on these units, in combination with previous geochemical studies, could help to establish a better understanding of the derivation of these rocks. The units sampled are the Theespruit (**B87-4**), Doornhoek (**B87-21**), Steynsdorp (**B87-24**) and two phases of the Stolzburg (**B87-1, 2**) plutons, sampled from the same outcrops.

GROUP II: Potassic granitoid batholiths and related intrusions

Extending to the north and south of the BGB are extensive, potassic, sheet-like intrusions that are polyphase and are comprised predominantly of granodiorite and adamellite as well as some trondhjemite and granite (Fig. 5). A homogeneous, undeformed and strongly porphyritic phase of the Nelspruit batholith (**B87-17**) is located north of the BGB. Intrusive into the central portion of the Nelspruit batholith is a medium- to fine-grained equigranular-textured grey granodioritic intrusion called the Hebron pluton (**B87-19**).

Another multi-phase, sheet-like, high-K batholith, located to the south of the BGB, called the Mpuluzi batholith (**B87-25**), was also sampled. Together with the

Nelspruit batholith, these intrusions are believed to represent components of the second phase of magmatism of the "three magmatic cycle" model as defined by Anhaeusser and Robb (1981), i.e. an early phase of trondhjemitic plutonism at ca. 3.5 Ga, followed by a second cycle of potash-rich batholiths at ca. 3.2 Ga, and ends with the emplacement of granite and syenite plutons at ca. 2.9 Ga. U-Pb zircon dating of these crustally extensive intrusions (**B87-17,19 & 25**) will determine whether they are time-correlative.

The Stentor pluton (**B87-15**), located at the southern margin of the Nelspruit gneisses and migmatites, is strongly deformed and has mylonitic fabrics along its contact with the northern margin of the BGB (Visser et al., 1956; Fripp et al., 1980; Robb et al., 1983). Fripp et al. (1980) note late south-dipping thrust faults that are present both in the greenstones and the pluton. Thus, the age of this pluton provides a maximum estimate for thrusting at the northern margin of the BGB.

Two late intrusions located in the southwestern part of the BGB were sampled. The Boesmanskop syeno-granitic complex (**B87-20**) cuts GROUP I trondhjemitic gneisses, and the Dalmein granodiorite (**B87-22**) intrudes Onverwacht Group metavolcanics and metasediments. Ages for these units place minimum time constraints on magmatism and deformation in this part of the BGB. The precise timing of the Boesmanskop intrusion is of particular interest because Archean syenites have not been widely reported; thus, isotopic data for this unit and for those that it intrudes may help in understanding its petrogenesis. Detailed mineralogical and petrological descriptions of these rocks are given by Anhaeusser et al. (1983) for

the Boesmanskop complex, and Robb (1983b) for the Dalmein pluton.

The Mpageni pluton (**B87-16**) is the only rock of granitic (sensu stricto) composition that was obtained. It is an undeformed, small, circular, coarse-grained intrusion that truncates gneisses and migmatites of the Nelspruit batholith.

GROUP III: Samples from the Barberton greenstone belt

These samples were collected from: (1) exposures of the classical stratigraphy, located in the southwestern BGB, and (2) from the north-central part of the belt.

A strongly foliated and lineated wedge of tonalitic gneiss (**B87-5**) that has been tectonically emplaced (de Wit, 1983) into the lower Onverwacht Group stratigraphy (Theespruit Formation) was sampled. Based on a recent zircon U-Pb ion-microprobe study (Armstrong et al., 1990), it represents the oldest unit yet dated from the BGB at ca. 3540 Ma and supports the suggestion that an internal unconformity exists between rocks of the Onverwacht Group and older sialic gneisses (de Wit et al., 1983; Armstrong et al., 1990). A precise age for this unit will (1) provide a comparison between data obtained by single zircon U-Pb conventional and SHRIMP ion-microprobe methods, and (2) confirm whether pre-Onverwacht Group units exist within the BGB.

A highly altered quartz-phyric felsic rock (**B87-6**), situated within komatiites of the Komati Formation, is one of the same units used in Hamilton et al.'s (1979) Sm-Nd isochron where it was assumed to be genetically linked to the komatiites. However, geochemical analysis and detailed mapping by de Wit (pers. comm., 1987)

indicate that this unit is not co-magmatic with the ultramafic lavas and may represent a later felsic intrusion. U-Pb zircon dating of this unit provides a test for this hypothesis.

B87-7 is fresh quartz-feldspar porphyry that intrudes the type locality of the Komati Formation komatiites. It will, therefore, provide a minimum age for the Komati Formation.

A medium-grained metagabbro (**B87-8**) intrusive into the Komati sequence has been studied in detail by de Wit et al. (1987b). It reportedly grades upward from an olivine cumulate rock into gabbro, transects the Middle Marker and merges with pillow lavas of the Hooggenoeg Formation (Fig. 4). If correct, an age for this sample should provide a direct date for the Hooggenoeg Formation and a minimum for the Komati Formation and the Middle Marker.

B87-11 is a sample from an ignimbritic unit situated between the Fig Tree and Moodies Groups sediments in the north-central BGB. Its contact with the underlying Fig Tree Group sediments grades from a conformable to an unconformable relationship, reflecting deposition in a tectonically active environment (de Wit, 1983; de Wit et al., 1983). This sample provides a direct age for deformation as well as a minimum age for Fig Tree Group sedimentation, and a maximum age for deposition of the Moodies Group conglomerates, at this location. An undeformed feldspar porphyry (**B87-10**) that intrudes B87-11 was also sampled.

A number of undeformed porphyries within the north-central BGB are shown by de Ronde (1991) to have intruded into shear zones interpreted to be D_2-related

thrust faults. These shear zones are characterized by strongly foliated ultramafic contacts and sometimes flaser-banded and schistose green coloured fuchsite-carbonate-quartz-bearing chert (de Wit, 1982). U-Pb data previously obtained on two undeformed porphyries suggests an emplacement age of ca. 3230 Ma (de Ronde et al., 1991) which provides a minimum estimate for D_2-related thrusting in this area. In order to further bracket thrust-related deformation, a deformed feldspar porphyry (**B87-27**) was sampled from the same area to provide a maximum age for thrusting.

FIGURE 5.

Sample location map for Group I (tonalite-trondhjemite suite) and Group II (potassic granitoid batholiths and related intrusions) rocks (from Anhaeusser et al., 1983).

Group I samples: Kaap Valley (B87-14, -32), Theespruit (B87-4), Doornhoek (B87-21), Steynsdorp (B87-24), Stolzburg (B87-1, -2) plutons.

Group II samples: Nelspruit (B87-17) and Mpuluzi (B87-25) batholiths, Hebron (B87-19), Stentor (B87-15), Boesmanskop (B87-20), Dalmein (B87-22), Mpageni (B87-16) plutons.

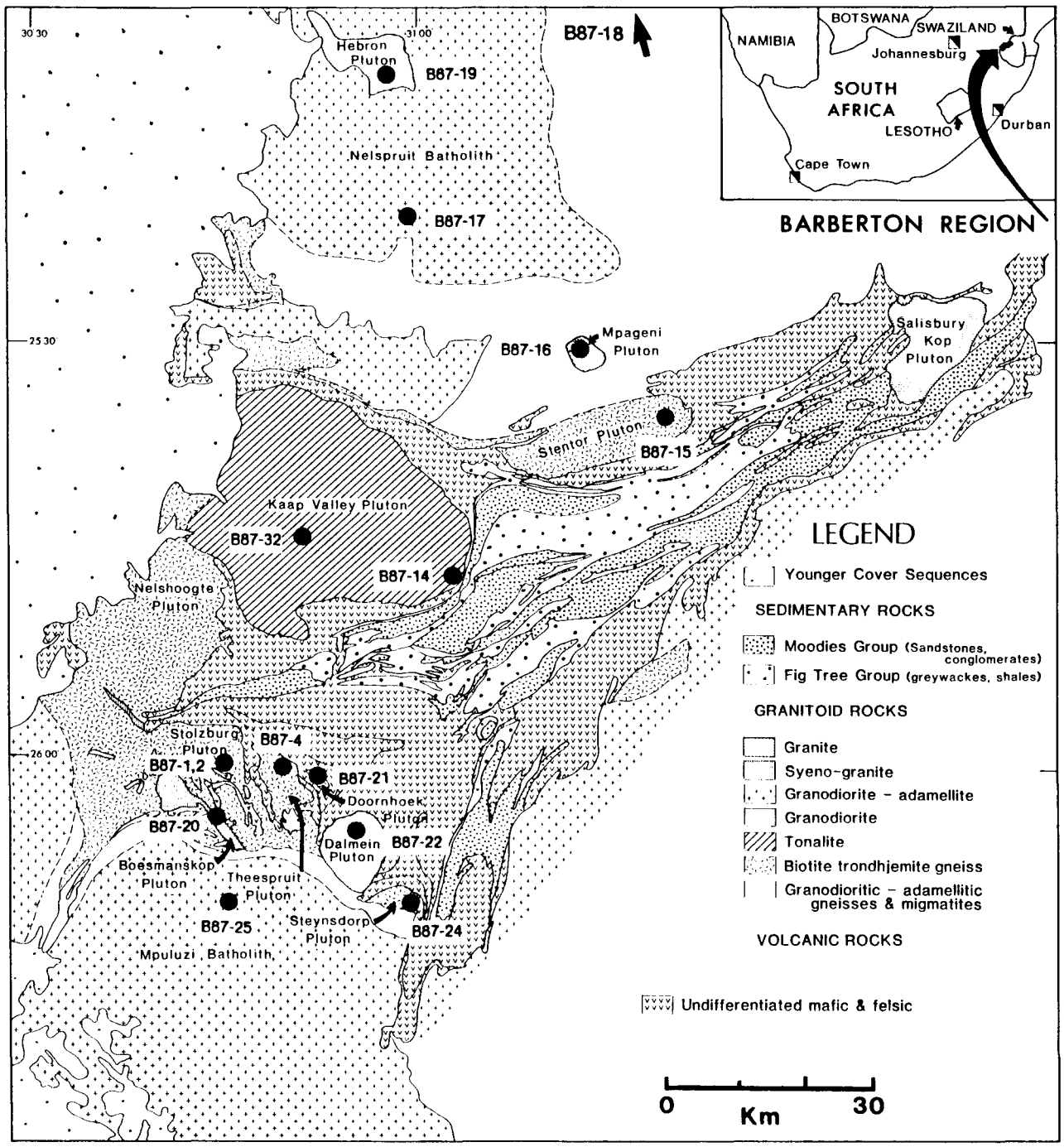
30 30
31 00
25 30
26 00
B87-18
Hebron Pluton
B87-19
Nelspruit Batholith
B87-17
B87-16
Mpageni Pluton
Salisbury Kop Pluton
Stentor Pluton
B87-15
Kaap Valley Pluton
B87-32
B87-14
Nelshoogte Pluton
Stolzburg Pluton
B87-4
B87-1,2
B87-21
Doornhoek Pluton
B87-20
Dalmein Pluton
B87-22
Boesmanskop Pluton
Theespruit Pluton
B87-25
Steynsdorp Pluton
B87-24
Mpuluzi Batholith
BOTSWANA
SWAZILAND
NAMIBIA
Johannesburg
SOUTH AFRICA
LESOTHO
Durban
Cape Town
BARBERTON REGION
LEGEND
Younger Cover Sequences
SEDIMENTARY ROCKS
Moodies Group (Sandstones, conglomerates)
Fig Tree Group (greywackes, shales)
GRANITOID ROCKS
Granite
Syeno-granite
Granodiorite - adamellite
Granodiorite
Tonalite
Biotite trondhjemite gneiss
Granodioritic - adamellitic gneisses & migmatites
VOLCANIC ROCKS
Undifferentiated mafic & felsic
0
Km
30

FIGURE 6.

Sample location map for rock samples from Group III rocks (from de Wit, 1983).

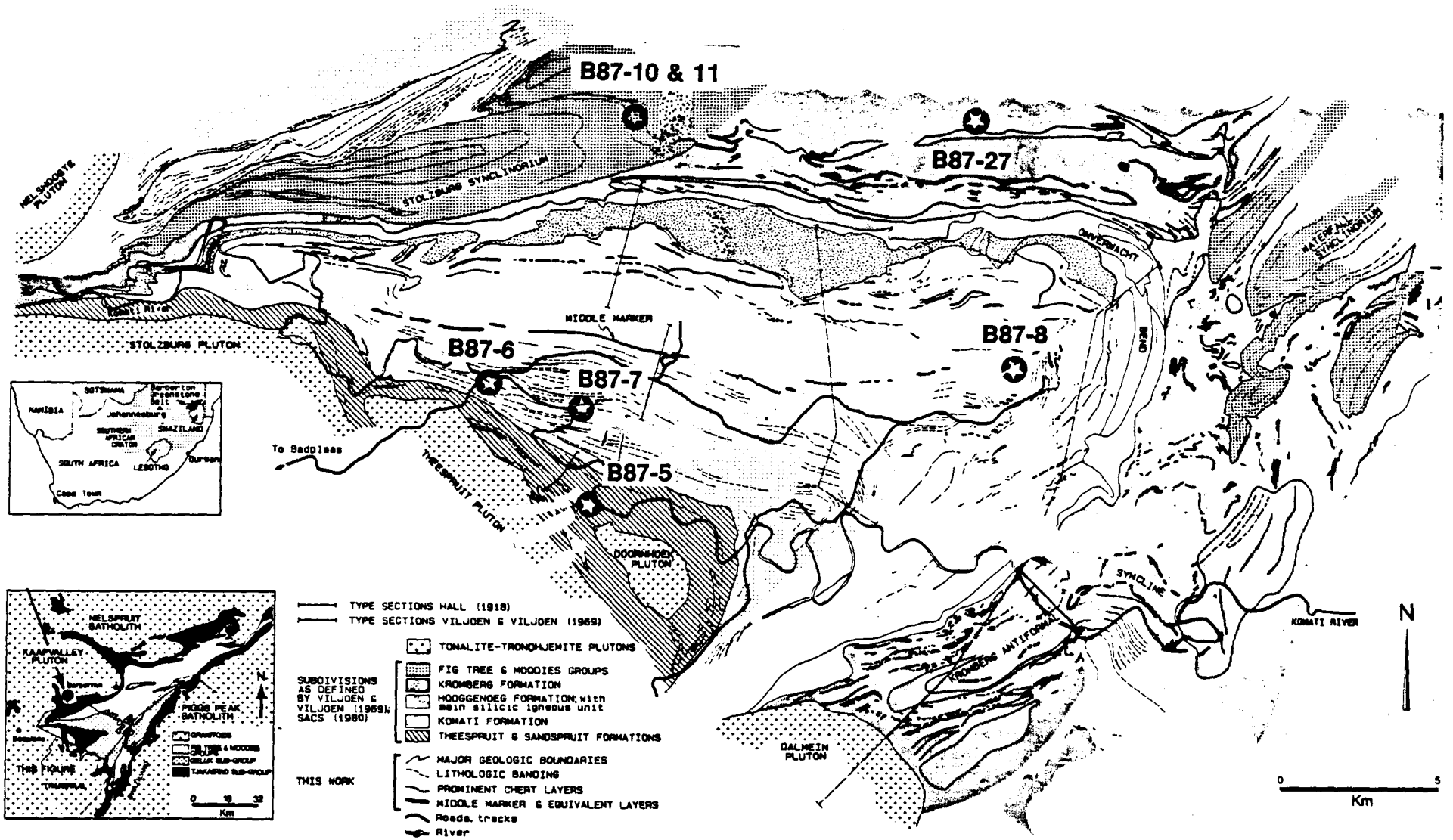
B87-10 & 11
B87-27
B87-8
B87-6
B87-7
B87-5
NELSPRUIT PLUTON
STOLZBURG SYNCLINORIUM
STOLZBURG PLUTON
MIDDLE MARKER
To Sadiaas
THEESPRUIT PLUTON
DOORNHOEK PLUTON
ONVERWACHT
SHEBA
MAJESTIC SYNCLINORIUM
SYNCLINE
KROMBERG ANTIFORMAL
GALMEIN PLUTON
KOMATI RIVER
N
0
5
Km
BOTSWANA
NAMIBIA
SWAZILAND
SOUTH AFRICA
LESOTHO
Cape Town
Durban
KAAPVALLEY PLUTON
PIGGS PEAK BATHOLITH
THIS FIGURE
TRANSVAAL
0 10 32
Km
TYPE SECTIONS HALL (1918)
TYPE SECTIONS VILJOEN & VILJOEN (1969)
TONALITE-TRONDHJEMITE PLUTONS
SUBDIVISIONS AS DEFINED BY VILJOEN & VILJOEN (1969); SACS (1980)
FIG TREE & MOODIES GROUPS
KROMBERG FORMATION
HOOGGENOEG FORMATION; with main silicic igneous unit
KOMATI FORMATION
THEESPRUIT & SANDSPRUIT FORMATIONS
THIS WORK
MAJOR GEOLOGIC BOUNDARIES
LITHOLOGIC BANDING
PROMINENT CHERT LAYERS
MIDDLE MARKER & EQUIVALENT LAYERS
Roads, tracks
River

(ii) ANALYTICAL PROCEDURE

Generalized procedures for sample preparation, dissolution and chemical separation are presented schematically in Figure 7.

(a) Sample preparation

Rock samples, weighing 20-40 kg, were crushed in a steel jaw- crusher before being pulverized to -80 mesh powder (<0.18 mm) in a steel Bico disk mill. A Wilfley table was then used to obtain a heavy mineral concentrate.

The heavy mineral concentrate was passed through a 70 mesh (200 micron) disposable nylon sieve and the <70 mesh fraction was allowed to fall approximately 2 cm in front of the pole pieces of a Frantz isodynamic separator at full magnetic field strength to extract magnetite and steel particles from the disk mill. This concentrate was then processed further using conventional heavy liquid (sodium polytungstate and/or bromoform, and methylene iodide) and magnetic separation techniques (Frantz isodynamic separator). Minerals that have specific gravities greater than methylene iodide (3.33 g/cm^3) and that are non-magnetic when initially passed through the Frantz, with the trough at a 10° tilt and the magnetic current at 1.8 A (called an initial Frantz or IF), are further separated magnetically by maintaining the magnetic current at 1.8 A and progressively decreasing the degree of side tilt (5°,3°,1°,0°) of the trough through subsequent passes (called a final frantz or FF). If sulfides were present in these final concentrates then a pyrite flotation technique or a hot 4N HNO_3 acid wash was used to separate or eliminate them.

The least magnetic zircons correspond to the least cracked and altered, lowest U zircons with the fewest inclusions. Rutile is concentrated at FF @ 5° and 3° tilt on the Frantz. Sphene, depending on its colour, can be found at IF @ 1.0 A (if dark brown) to FF @ 5° tilt (if pale brown to colourless). The colour range is generally associated with a range in U concentration; the darker brown, higher U grains contain more LREE which renders the mineral paramagnetic. The magnetic susceptibility of monazite is greater than that of most other heavy minerals due to its enrichment in LREE and it is recovered from the IF @ 1.0 A fraction. Inclusion- and crack-free baddeleyite is generally non-magnetic and is concentrated with the best quality zircons.

The final concentration process involves individual selection of the best quality grains, under a binocular microscope, using fine-tipped tweezers. The grains are picked under alcohol avoiding those that have cracks, along which alteration might be present. In most cases, zircon crystals that are crack-free, inclusion- free, euhedral and low in U, yield concordant results when given an air abrasion treatment according to the procedure of Krogh (1982).

For sphene, grains that are higher in U are favourable in order to obtain higher ratios of radiogenic Pb to common Pb. Unlike zircon, sphene incorporates significant common Pb upon crystallization. The smaller the ratio of radiogenic Pb to common Pb, the greater must be the model-dependent correction for the isotopic composition of the common Pb. Particular care was taken to avoid cloudiness and

surface alteration which is common in sphene. The air abrasion technique was applied to all sphene fractions. Monazite generally has very high radiogenic Pb concentrations (>1000 ppm) and therefore only a single grain or a fragment of a grain (1-3 μg) for Archean samples is needed to yield a strong signal in the mass spectrometer. Air abrasion of monazite can, in some cases, increase concordancy (Corfu and Muir, 1989).

Baddeleyite is selected with attention focussed on eliminating grains with minor alteration parallel to striations. Air abrasion does not appear to improve concordancy in baddeleyite (Kamo et al., 1989) and since it usually occurs with a bladed, platey habit, which is not amenable to air abrasion, non-abraded baddeleyite was analyzed in this study. Rutile is frequently very low in U (2 - 10 ppm) and it incorporates common Pb when it crystallizes; thus ratios of radiogenic Pb to common Pb tend to be lower than they are in minerals such as zircon, monazite and baddeleyite. Corrections for the isotopic composition of the initial common Pb must, therefore, be considered carefully. Rutile is brittle and is therefore abraded very gently for a relatively short duration.

After air abrasion with pyrite all zircon fractions were washed in hot 4N HNO_3 in order to dissolve the pyrite and remove any FeS_2 dust from the sample grains. Pyrite is not needed for abrasion of monazite, rutile and sphene because these minerals are significantly softer than zircon and will not polish. Thus, only a very weak (2N) HNO_3 wash for a short time (5 minutes) is required to pre-clean the

grains.

After a final picking, the grains are cleaned before bomb dissolution. This final cleaning process involves a hot (130°F) distilled 4N HNO_3 bath in 10 ml Pyrex beakers on a hot plate, followed by rinsing with doubly distilled H_2O, and distilled acetone. Distillation of all reagents was carried out under sub-boiling conditions. For sphene and monazite this final cleaning process is less vigorous because the surfaces of sphene are etched in hot 4N HNO_3 and the possibility of differential Pb and U leaching must be considered. Monazite is a phosphate which is soluble in strong HNO_3; therefore both sphene and monazite are washed in weak HNO_3 (1-2N for sphene and 0.5N for monazite).

Multi-grain samples were then weighed on clean disposible aluminum boats on a Cahn microbalance. The weights for single grains were estimated by eye and are probably accurate to about ± 50%.

(b) Chemical procedures

Clean Teflon bombs (Krogh, 1973) that have Pb blanks routinely in the 2-6 pg range are used for sample dissolution. Zircon, rutile, and baddeleyite are dissolved in bombs for 5 days with HF (+HNO3) at 220°C. Sphene and monazite are both dissolved in Savillex vials, sphene in HF (+HNO3) and monazite in 6.2N HCl, on a hot plate for 2-3 days at 130°C. All samples were spiked with a mixed $^{205}Pb/^{235}U$ tracer prior to dissolution (Parrish and Krogh, 1987). Before extraction of Pb and

U, sample solutions are dried down and then re-dissolved in 3.1N HCl at high temperature for at least 12 hours in order to convert the fluorides to chlorides, to ensure total dissolution of REE. Pb - U separation for zircon and sphene follow Krogh (1973) and Corfu and Andrews (1987), respectively. Chemical separation for zircon, baddeleyite, and monazite involves purification of Pb and U using anion exchange resin on columns 1/10th the volume of those described in Krogh (1973). The Pb and U elutions were obtained using 6.2N HCl and H_2O, respectively. For sphene and rutile, purification is achieved using 1N HBr for Pb and 8N HNO_3 and 6.2N HCl for U.

The maintenance of low Pb and U blanks for the total procedure is critical so that blank corrections are insignificant. In the routine analysis of single grains or small fractions of zircon, the total amount of Pb is almost entirely radiogenic; thus, the total amount of common Pb for each analysis gives a within-run measurement of blank. Recent total laboratory blanks for Pb and U at the Royal Ontario Museum geochronology laboratory are in the 2.0 - 8.0 pg and 0.5 - 2.0 pg range, respectively.

(c) Data collection

Low laboratory blanks coupled with high transmission mass spectrometry allow precise analysis of low U (50-100 ppm) Archean zircon samples of less than 0.002 mg. This also results from the fact that subnanogram quantities of elements have higher ionization efficiency than larger samples (Edwards et al., 1987).

Pb and U were loaded together onto an outgassed Re filament using H_3PO_4 and Si-gel. A high transmission extended-focussing VG354 mass spectrometer in peak jumping collection mode was used for data collection. Most data collection, except for sphene and monazite, was performed using the Daly photomultiplier detector. The Faraday collector was used to measure the $^{207}Pb/^{206}Pb$ ratio on large multi-grain zircon fractions or on high U single grains, whenever possible. A Daly to Faraday conversion factor of 0.35% per AMU was used and mass fractionation corrections of 0.13% per AMU for Pb and U were applied.

Initial Pb compositions for all analyses were calculated using the Stacey and Kramers (1975) two-stage terrestrial Pb evolution model. In most cases, common Pb corrections for zircon, monazite, and baddeleyite are negligible.

Minimum errors of 0.05% for the $^{207}Pb/^{206}Pb$ ratio and 0.25% for the Pb/U ratio (1 σ), based on replicate analyses, are largely due to uncertainty in thermal fractionation (taken as 0.13%/amu). These errors may be enlarged based on the reproducibility of the ratios within a given sample. Larger errors are assigned to sphene and rutile because a larger common Pb correction, used in calculating the radiogenic $^{207}Pb/^{206}Pb$ ratio, is necessary. All plotted error ellipses in Figures 8, 9 and 10 are 2σ.

Age regressions were calculated using the program of Davis (1982). A random linear data distribution, with correctly chosen errors, would be expected to produce an average probability of fit of 50%. If a regression yields less than 10%

probability of fit, then the discordia line is recalculated after expanding the errors in proportion to the discordance of the data points until an acceptable probability of fit (40 - 50%) is obtained (Davis, 1982). The decay constants used are those of Jaffey et al. (1971). All errors are quoted at the 95% confidence level.

FIGURE 7.

Schematic presentation of generalized procedures for sample preparation, dissolution and chemical separation of minerals used for U-Pb dating.

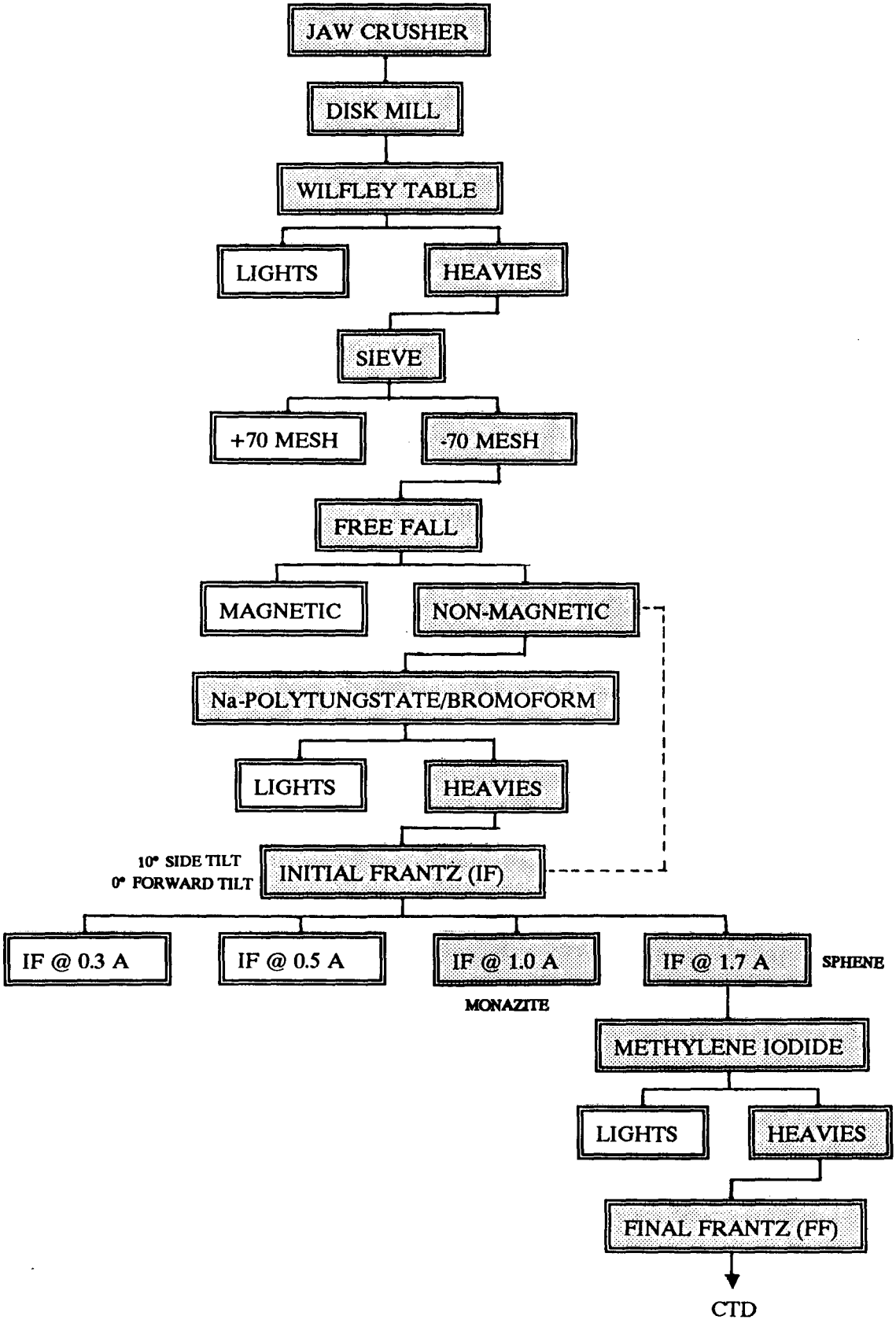
JAW CRUSHER
DISK MILL
WILFLEY TABLE
LIGHTS
HEAVIES
SIEVE
+70 MESH
-70 MESH
FREE FALL
MAGNETIC
NON-MAGNETIC
Na-POLYTUNGSTATE/BROMOFORM
LIGHTS
HEAVIES
10° SIDE TILT
0° FORWARD TILT
INITIAL FRANTZ (IF)
IF @ 0.3 A
IF @ 0.5 A
IF @ 1.0 A
MONAZITE
IF @ 1.7 A
SPHENE
METHYLENE IODIDE
LIGHTS
HEAVIES
FINAL FRANTZ (FF)
CTD

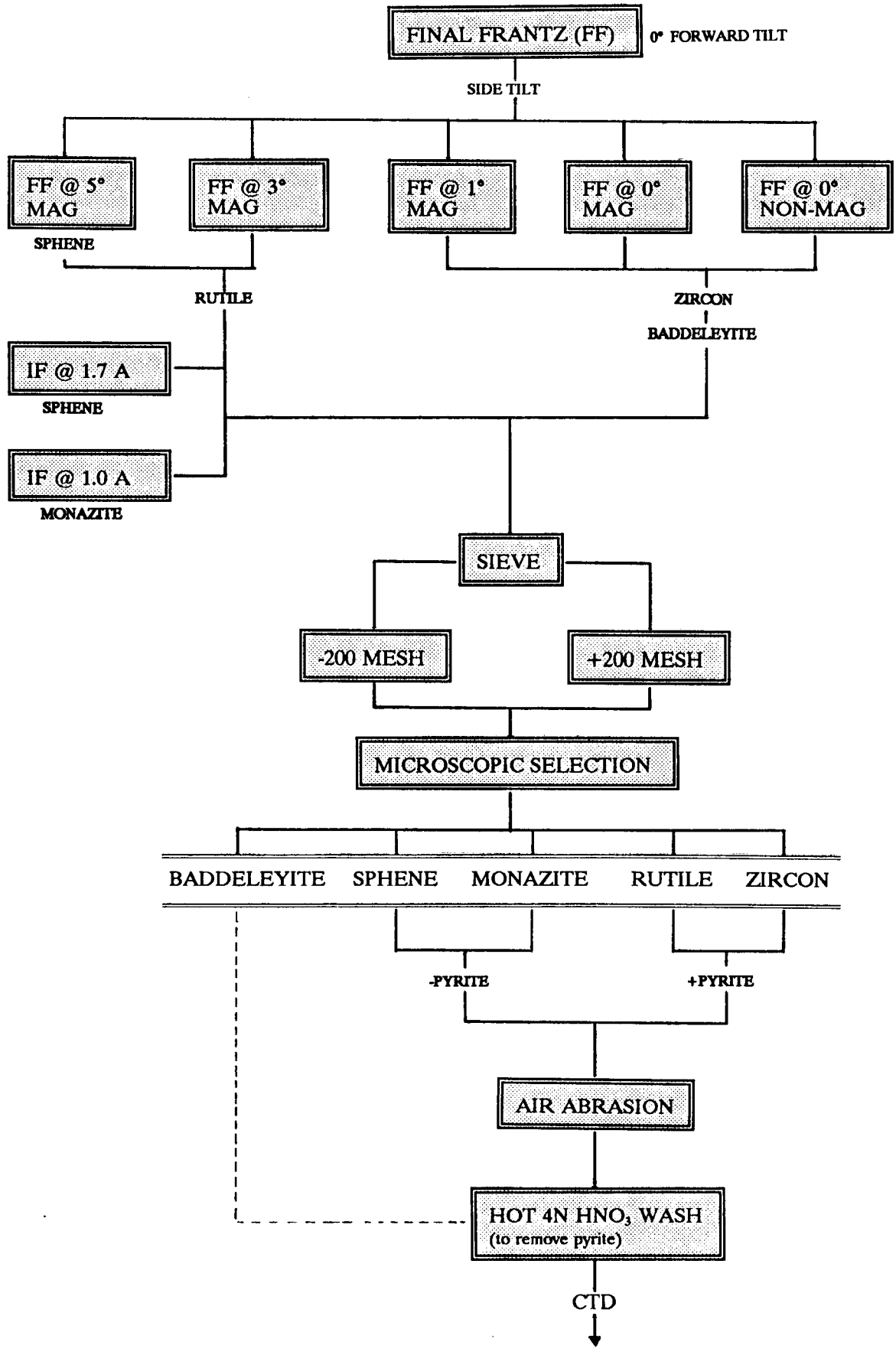
FINAL FRANTZ (FF)
0° FORWARD TILT
SIDE TILT
FF @ 5° MAG
SPHENE
FF @ 3° MAG
FF @ 1° MAG
FF @ 0° MAG
FF @ 0° NON-MAG
RUTILE
ZIRCON
BADDELEYITE
IF @ 1.7 A
SPHENE
IF @ 1.0 A
MONAZITE
SIEVE
-200 MESH
+200 MESH
MICROSCOPIC SELECTION
BADDELEYITE
SPHENE
MONAZITE
RUTILE
ZIRCON
-PYRITE
+PYRITE
AIR ABRASION
HOT 4N HNO_3 WASH
(to remove pyrite)
CTD

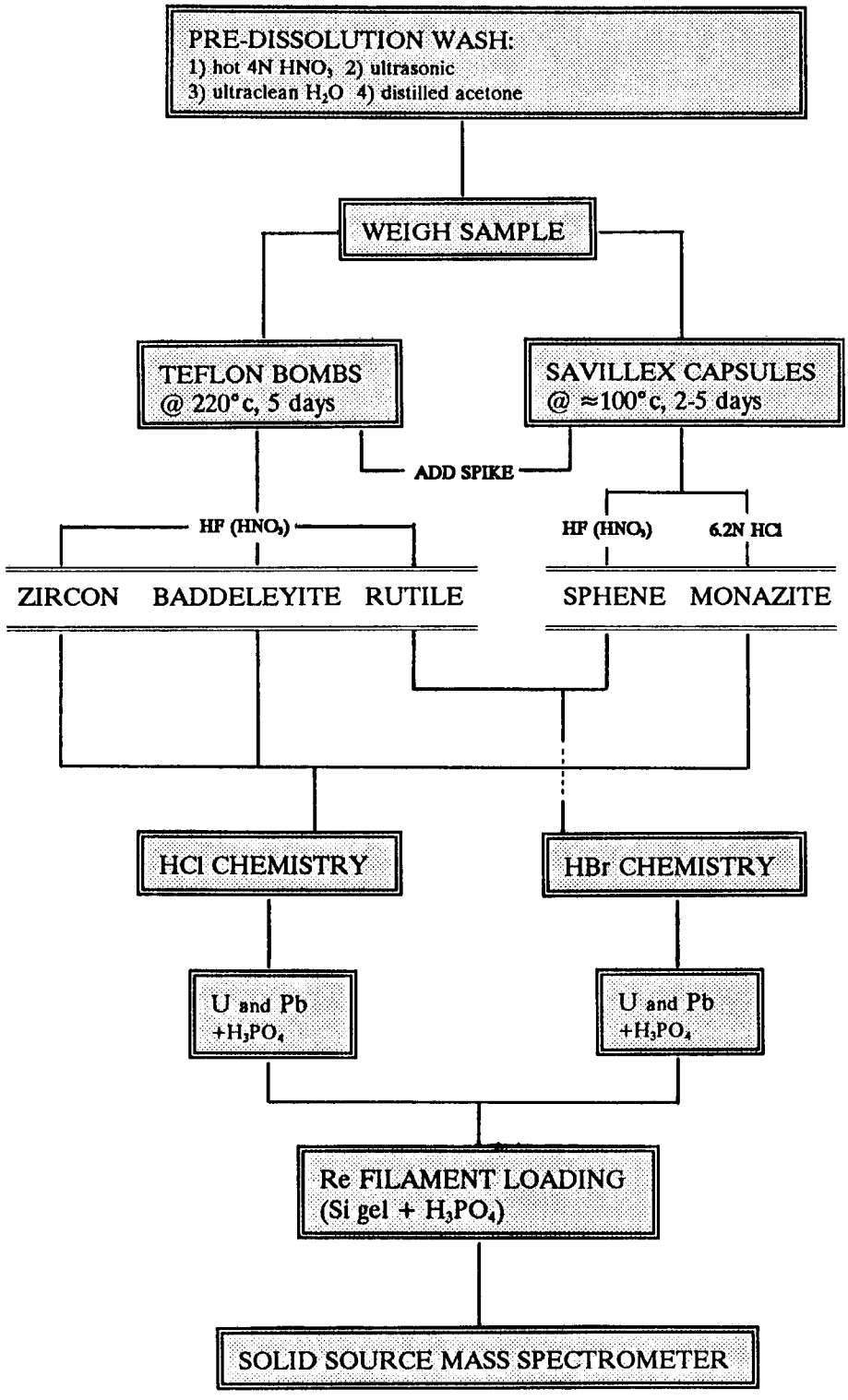
PRE-DISSOLUTION WASH:
1) hot 4N HNO3 2) ultrasonic
3) ultraclean H2O 4) distilled acetone
WEIGH SAMPLE
TEFLON BOMBS
@ 220°c, 5 days
SAVILLEX CAPSULES
@ ≈100°c, 2-5 days
ADD SPIKE
HF (HNO3)
HF (HNO3)
6.2N HCl
ZIRCON BADDELEYITE RUTILE
SPHENE MONAZITE
HCl CHEMISTRY
HBr CHEMISTRY
U and Pb
+H3PO4
U and Pb
+H3PO4
Re FILAMENT LOADING
(Si gel + H3PO4)
SOLID SOURCE MASS SPECTROMETER

(iii) ANALYTICAL CONSIDERATIONS

Few of the zircon populations analyzed in this study were free of complications, such as:

(1) severe Pb-loss, even after abrading the outer surfaces to remove surface corollated Pb-loss,

(2) inheritance, either as xenocrystic zircons, or as cores mantled by magmatic zircon,

(3) small sample yield.

Such difficulties were frequently overcome by analyzing either sphene, monazite, or baddeleyite, when present in the rocks. These minerals are usually concordant and can provide, at the very least, minimum ages for crystallization. Although zircon inheritance can provide meaningful information about the source rocks, it also complicates efforts to obtain the crystallization age. This was generally overcome by avoiding zircons that were larger than the general population i.e. those that may have survived a crustal melting process, or by selecting elongate or needle-like zircons that had longitudinal cracks, sometimes indicative of a core-free grain. Needle-like grains are broken into more equant shapes before abrasion in order to effectively remove the surfaces.

(iv) RESULTS

Tables 3 - 5 give the age data for three time spans in the order of decreasing age. All age results are summarized in Table 6.

(a) Table 3: ca. 3540-3350 Ma

Pre-Onverwacht Group sialic crust

Tonalitic gneiss sliver (B87-5) (Figure 8a):

Zircons analyzed in this sample were pink, euhedral, magmatically-zoned grains. These were extracted from a homogeneous zircon population with no apparent evidence of inheritance. Three out of four analyses (1 concordant) give a high probability of fit yielding an upper intercept age of 3538 +4/-2 Ma and a lower intercept age of about 350 Ma. This age is identical to the SHRIMP ion-microprobe age obtained by Armstrong et al. (1990). The fourth data point is more discordant and seems to have been affected by earlier Pb loss than the others. Th/U ratios (as calculated from $^{208}Pb/^{206}Pb$) are rather variable, possibly due to crystal zoning.

Steynsdorp Pluton (B87-24) (Figure 8b):

This sample yielded abundant zircon that can be grouped into a population of larger (+200 mesh) severely cracked, heterogeneous, brown to pale brown grains with distinctly rounded edges, and a population of smaller (-200 mesh) euhedral pale brown to pale pink grains. A population of very well-rounded, amorphous grains, having the appearance of metamorphic zircons, is also present, but these were not analyzed. Some grains have severely rounded edges resulting from resorption. Two

low U (65-80 ppm) multi-grain fractions of the euhedral, -200 mesh, pale pink variety were less discordant than two pale brown, slightly cracked, single grain analyses from the larger grain size population. These four analyses yield an upper intercept age of 3509 +8/-7 Ma.

One sphene analysis of pale yellow, slightly cloudy fragments gave a distinctly younger concordant $^{207}Pb/^{206}Pb$ age of 3192 Ma. The Th/U ratio is relatively low compared to magmatic sphene which does not fractionate Th/U. This may be indicative of a hydrothermal origin since Th is much less mobile than U (which is very soluble) in hydrothermal systems.

Onverwacht Group-associated early felsic magmatism

Stolzburg Pluton (B87-1, older phase) (Figure 8c):

This homogeneous population of brown to pale brown euhedral zircon yielded an upper intercept age of 3459 +5/-4 Ma. Four fractions, three multi-grain and one single zircon grain, gave results ranging from 4% to 15% discordant along the regression line. Due to the possible presence of an inherited component, fraction #12, consisting of 7 abraded brown zircon grains, was omitted from the regression, although the scatter of data points may also be due to multiple ages of Pb loss.

Quartz-feldspar porphyry (Komati Fm) (B87-7) (Figure 8d):

Three fractions of zircon (#14, #15 & #16) were regressed with sphene fraction #18 to yield an upper intercept age of 3467 + 12/-7 Ma. Fraction #14 plots slightly above the concordia curve but still within error of concordia. This is

probably due to the imprecise calibration of the position of the magnet of the mass spectrometer, resulting in a poorly defined U peak shape, which does not affect the $^{207}Pb/^{206}Pb$ age. This was a temporary situation that affected only three analyses in this study. Single zircon fraction #17 is severely discordant (26%) and appears to have suffered a complicated lead loss history and was, therefore, omitted from the regression. A second sphene fraction (#19) may not have undergone complete dissolution resulting in the discordant (14%) data point. Lead loss in sphene is uncommon because it probably does not accumulate the same type of radiation damage-induced alteration as zircon. Chemical alteration to leucoxene appears to result in the complete loss of both Pb and U (Richards et al., 1988).

The age of this unit is bracketed between the oldest sphene $^{207}Pb/^{206}Pb$ age of 3458 Ma and the youngest concordant zircon $^{207}Pb/^{206}Pb$ age of 3476 Ma.

Doornhoek Pluton (B87-21) (Figure 8e):

A heavy mineral population of zircon, monazite, sphene, and garnet was concentrated at 0.5 A on the Frantz at 10° tilt. The zircon population comprised many with pink cores and yellow overgrowths, some milky cracked grains, and a number of small, clear, pink grains. Two fractions of the latter type were analyzed: a 4.6% discordant single abraded grain (#22) with a $^{207}Pb/^{206}Pb$ age of 3439 Ma, and a fraction of two small abraded zircons (#23) with very small cracks was 29% discordant with a $^{207}Pb/^{206}Pb$ age of 3331 Ma. Monazite, which was identified by X-ray diffraction, was severely and ubiquitously cracked, therefore portions of these

grains were separated by breaking the grains along the cracks and then abraded to remove unwanted material from the surfaces of the cracks. Two near concordant fractions (#20 & #21) yielded similar $^{207}Pb/^{206}Pb$ ages at 3446 Ma and 3439 Ma, respectively. When regressed with zircon fraction #22, an age of 3448 +/-4 Ma was obtained.

One fraction of pale yellow sphene which gave a $^{207}Pb/^{206}Pb$ age of 3217 Ma and is 5.1% discordant, may be recording a later hydrothermal alteration event. An attempt was made to analyze grains of clear, yellow, euhedral garnet, which also appeared (petrographically) to have formed late, but insufficient radiogenic Pb was present.

Theespruit Pluton (B87-4) (Figure 8f):

Sphene in this sample is honey brown in colour and occurs in large fragments that are cracked and contain dark inclusions. Two fractions (#25 and #26) of crack- and inclusion-free abraded sphene yielded a concordant point at 3443 Ma and a 3% discordant point with a $^{207}Pb/^{206}Pb$ age of 3438 Ma. Zircons in this uniform population were severely cracked and medium brown in colour. Clear, single fragments between the cracks of these grains (#28 and #29) and 3 small, clear, crack-free, euhedral grains (#27), yielded results that had similar $^{207}Pb/^{206}Pb$ ages as the sphene, but were more discordant. An age regression involving all five sphene and zircon analyses gives an upper intercept age of 3443 +4/-3 Ma.

Mafic magmatism

Metagabbro (Komati Fm) (B87-8) (Figure 8g):

Five tiny blades (40-60 μm) of baddeleyite were recovered from this sample and these had an unusually low U concentration of $\approx$56 ppm. The analysis yielded a 1% discordant data point with a $^{207}Pb/^{206}Pb$ age of 3347 Ma. Analysis of clear, pale yellow, skeletal zircon (i.e. tabular plates), that are common in mafic pegmatitic rocks where zircon is a late phase, was 9% discordant with a $^{207}Pb/^{206}Pb$ age of 3315 Ma. The discordance of this analysis is attributed to surface diffusion of lead from these grains, which had relatively high surface-to-volume ratios and were not abraded due to their platey habit. The upper intercept age for these two analyses is 3352 +6/- 5 Ma.

A second zircon population of xenocrystic grains, distinguished by its assortment of grains of variable size, colour, habit and degree of resorption, is also present. Although ages from these grains can provide useful information on the age of the underlying crust, none of these were analyzed in this study since the object was to obtain the crystallization age of the rock. However, Armstrong et al. (1990) reported a number of older U-Pb zircon SHRIMP analyses that range from 3523 ± 6 Ma to 3482 ± 5 Ma on a very similar population of zircons from the same rock unit. In terms of crystal habit and Th/U ratios, these grains were typical of zircons that crystallized from felsic melts.

TABLE 3.

U-Pb age data for rock samples from ca. 3540-3350 Ma.

(Notes: Z=zircon; S=sphene; M=monazite; B=baddeleyite; grains were selected from the least magnetic fractions; all fractions were abraded unless otherwise noted; a=includes blank + zircon common Pb but corrected for 0.117 mol fraction of common Pb in the ^{205}Pb spike; b=corrected for fractionation and blank; c=corrected for fractionation, blank, common Pb; ^{238}U decay constant=$0.15513X10^{-9}$/year; ^{238}U decay constant=$0.98485X10^{-9}$/year; $^{238}U/^{235}U=137.88$)

TABLE 3

U-Pb data for ca. 3540-3350 Ma rocks from the Barberton Mountain Land.

Description fraction no.	Weight (μg)	Concentration U (ppm)	Concentration Pb (ppm)	Common Pb (pg)	Atomic ratios $^{206}Pb/^{204}Pb$	Atomic ratios $^{208}Pb/^{206}Pb$	$^{206}Pb/^{238}U$	$^{207}Pb/^{235}U$	$^{207}Pb/^{206}Pb$	Age (Ma) $^{207}Pb/^{206}Pb$
TONALITE GNEISS WEDGE B87-5										
1. Z, 1 gr	1	135	132	4	1791	0.2318	0.7339	31.7194	0.31346	3538
2. Z, 1 gr	4	64	57	4	2931	0.1232	0.7125	30.7317	0.31283	3535
3. Z, 1 gr	1	127	113	6	961	0.1439	0.7083	30.5385	0.31269	3534
4. Z, 3 gr	5	63	55	7	2056	0.2037	0.6695	28.0879	0.30430	3492
STEYNSDORP PLUTON B87-24										
5. Z, 10 gr	9	81	69	14	2277	0.1104	0.7014	29.8436	0.30605	3501
6. Z, 5 gr	10	67	55	12	2407	0.1251	0.6679	27.9641	0.30368	3489
7. Z, 1 gr	1	149	105	3	2291	0.0743	0.5982	24.3959	0.29767	3448
8. Z, 1 gr	2	93	63	10	678	0.0915	0.5641	22.8881	0.29429	3440
9. S	195	23	16	207	893	0.0157	0.6404	22.1773	0.25118	3192
STOLZBURG PLUTON (older phase) B87-1										
10. Z, 30 gr	3	179	149	6	4203	0.1075	0.6888	28.1284	0.29617	3450
11. Z, 9 gr	4	39	32	2	945	0.1045	0.6736	27.3146	0.29409	3439
12. Z, 7 gr	10	152	120	5	12385	0.1166	0.6466	26.2555	0.29448	3441
13. Z, 1 gr	1	398	298	2	6518	0.0924	0.6291	25.1101	0.28947	3415

QTZ-FSP PORPHYRY DYKE (Komati fm) B87-7										
14. Z, 2 gr	2	85	74	15	550	0.1102	0.7172	29.7777	0.30114	3476
15. Z, 1 gr	1	108	93	13	402	0.1259	0.7013	28.6858	0.29667	3453
16. Z, 11 gr	1	532	441	9	2688	0.1098	0.6864	27.7770	0.29349	3436
17. Z, 1 gr	1	175	120	5	1411	0.1102	0.5728	22.0574	0.27927	3359
18. S	38	30	25	85	595	0.1110	0.6891	28.2111	0.29691	3454
19. S	112	40	30	53	3252	0.1250	0.6040	24.7854	0.29763	3458
DOORNHOEK PLUTON B87-21										
20. M, 4 fr	12	2178	8887	38	30388	5.4528	0.6981	28.4218	0.29530	3446
21. M, 4 fr	1	3940	17158	6	29163	5.9876	0.6904	27.9852	0.29398	3439
22. Z, 1 gr	1	52	41	5	502	0.0873	0.6721	27.2425	0.29396	3439
23. Z, 2 gr	2	531	314	31	1067	0.1561	0.4802	18.1597	0.27427	3331
24. S	50	26	19	79	663	0.1040	0.6140	21.5960	0.25509	3217
THEESPRUIT PLUTON B87-4										
25. S	76	36	32	102	1223	0.1498	0.7035	28.5886	0.29471	3443
26. S	62	26	22	109	669	0.1128	0.6838	27.7034	0.29384	3438
27. Z, 3 gr	2	86	71	9	886	0.1170	0.6766	27.4678	0.29443	3441
28. Z, 1 gr	1	319	260	16	867	0.1131	0.6743	27.1236	0.29175	3427
29. Z, 1 gr	2	917	650	6	11694	0.1349	0.5795	22.8771	0.28630	3398
METAGABBRO (Komati fm) B87-8										
30. B	3	56	42	2	3321	0.0107	0.6735	25.7328	0.27709	3347
31. Z	8	175	143	33	1647	0.2845	0.6122	22.9234	0.27155	3315

FIGURE 8a-g.

Concordia diagrams for rocks from ca. 3540-3350 Ma.

(Notes: Zr=zircon; NM0°=non-magnetic @ 0° tilt on Frantz; -200 mesh=<70 microns)

Tonalitic Gneiss Sliver

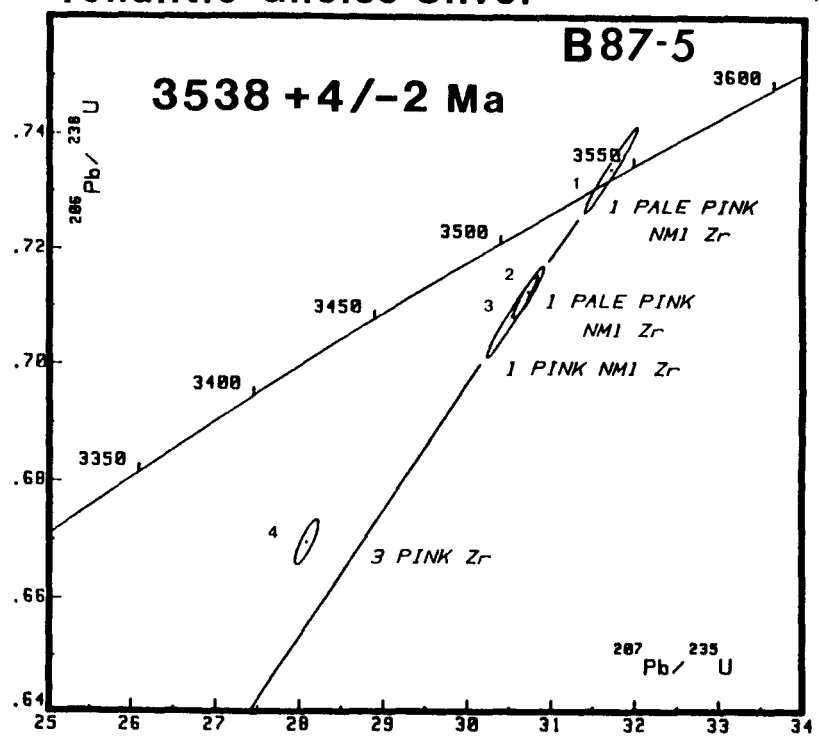

Steynsdorp Pluton

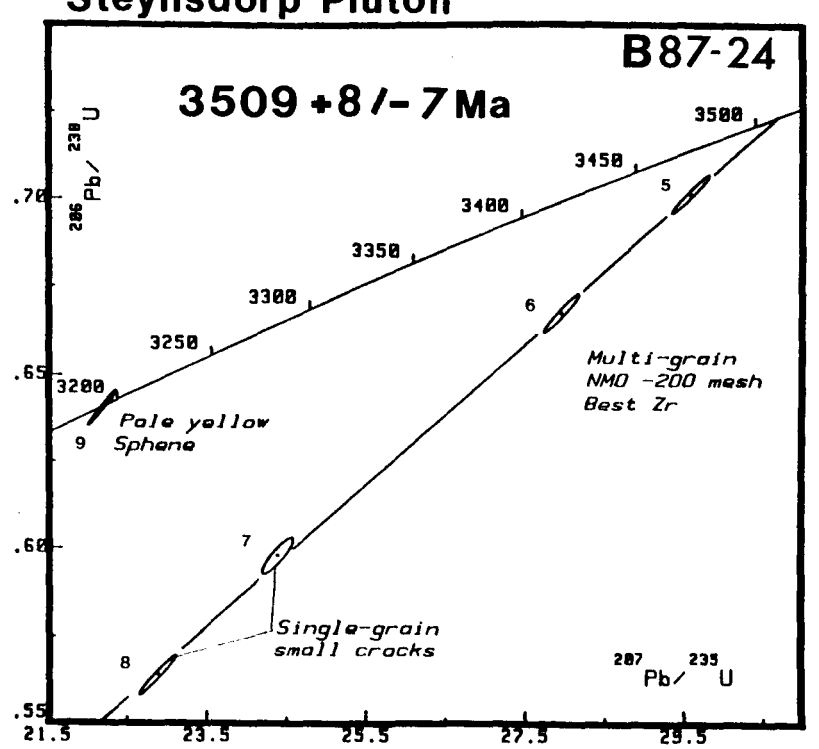

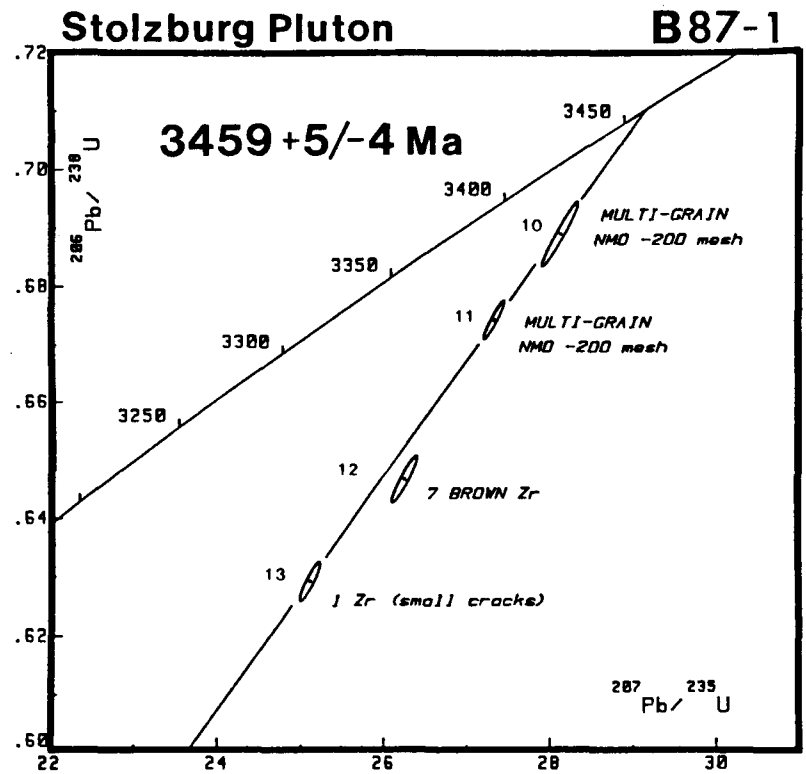
Stolzburg Pluton
B87-1
c
3459 +5/-4 Ma
206 Pb/ 238 U
207 Pb/ 235 U
3450
3400
3350
3300
3250
10
MULTI-GRAIN
NMD -200 mesh
11
MULTI-GRAIN
NMD -200 mesh
12
7 BROWN Zr
13
1 Zr (small cracks)
.72
.70
.68
.66
.64
.62
.60
22
24
26
28
30

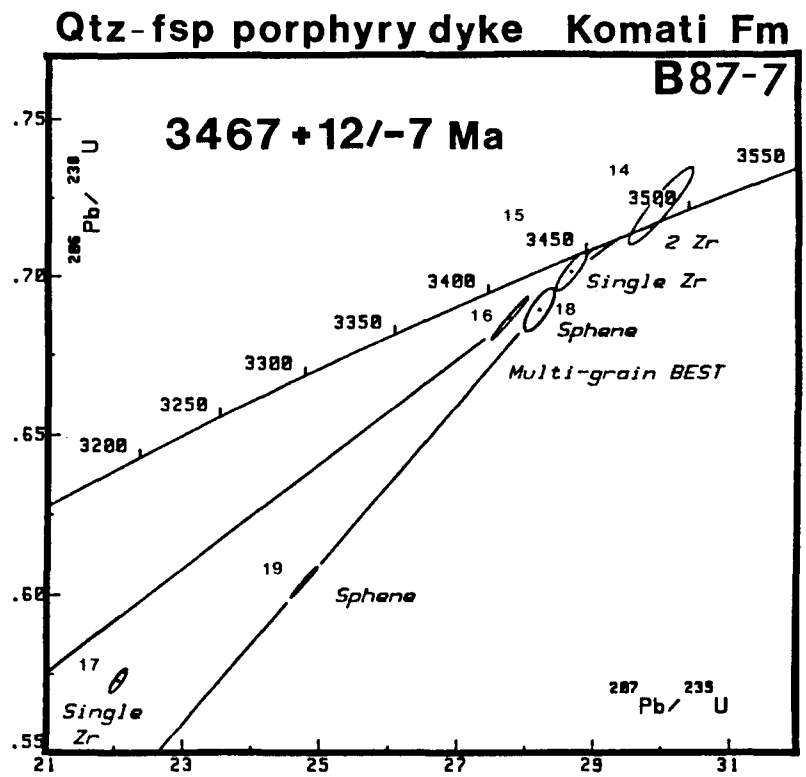
Qtz-fsp porphyry dyke Komati Fm
B87-7
d
3467 +12/-7 Ma
206 Pb/ 238 U
207 Pb/ 235 U
3550
3500
3450
3400
3350
3300
3250
3200
14
15
2 Zr
Single Zr
16
18
Sphene
Multi-grain BEST
19
Sphene
17
Single Zr
.75
.70
.65
.60
.55
21
23
25
27
29
31

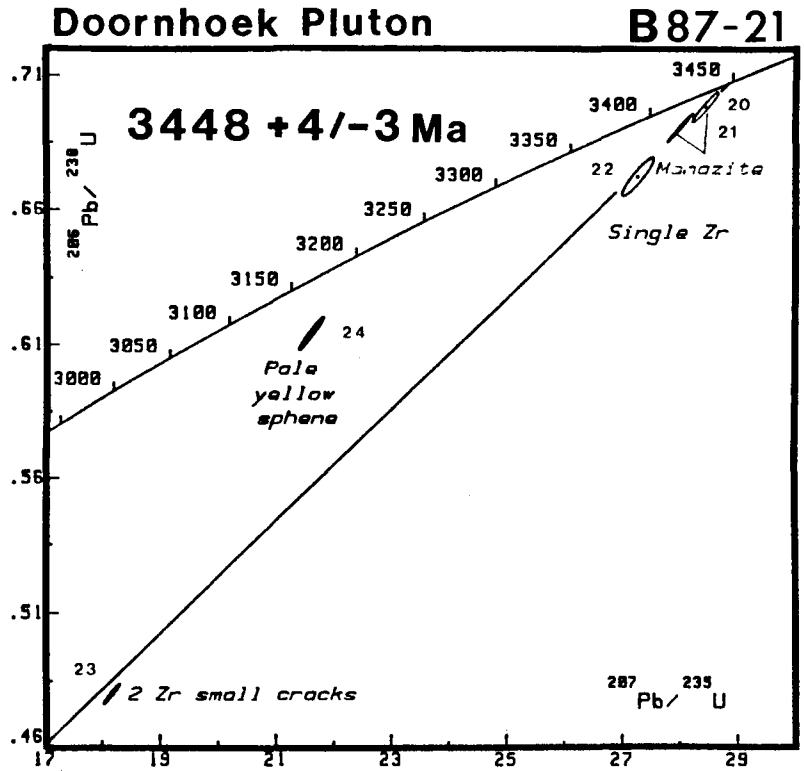
Doornhoek Pluton
B87-21
3448 +4/-3 Ma
3450
3400
3350
3300
3250
3200
3150
3100
3050
3000
20
21
22
Monazite
Single Zr
24
Pale yellow sphene
23
2 Zr small cracks
.71
.66
.61
.56
.51
.46
17
19
21
23
25
27
29

e

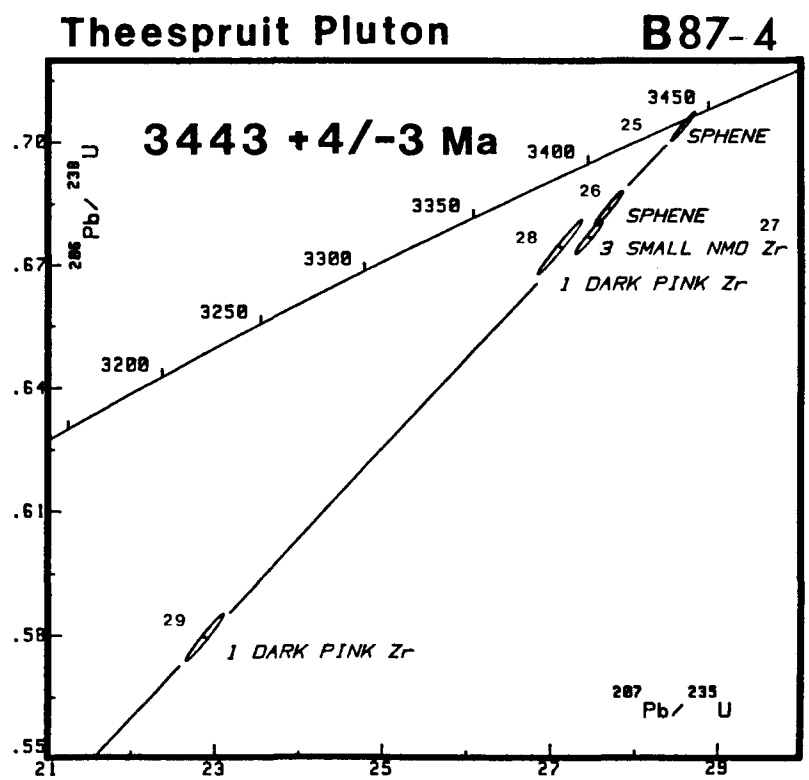
Theespruit Pluton
B87-4
3443 +4/-3 Ma
3450
3400
3350
3300
3250
3200
25
SPHENE
26
SPHENE
27
3 SMALL NMO Zr
28
1 DARK PINK Zr
29
1 DARK PINK Zr
.70
.67
.64
.61
.58
.55
21
23
25
27
29

f

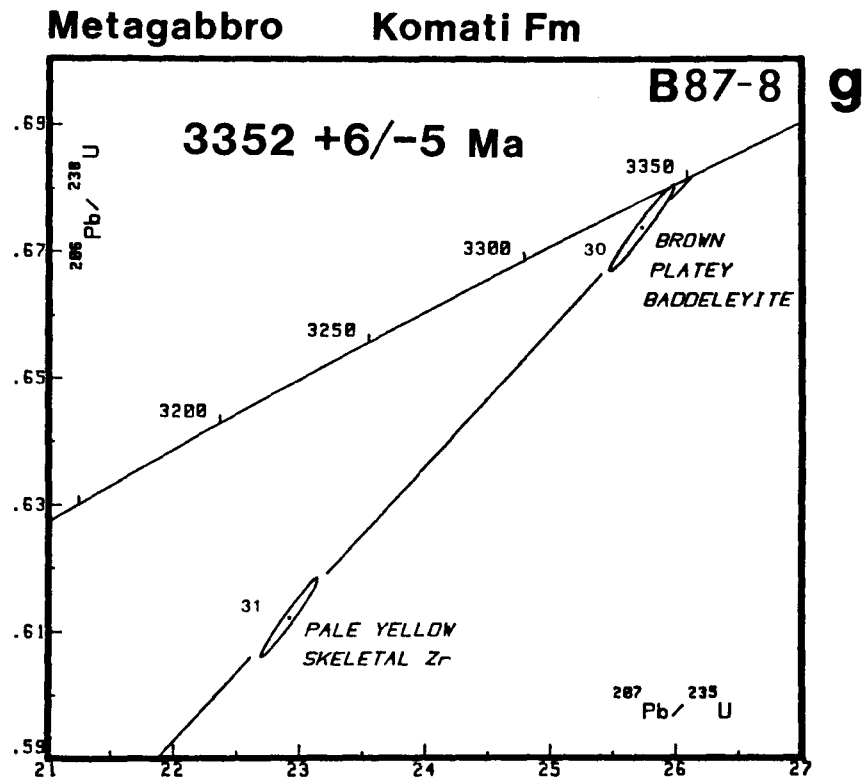
Metagabbro
Komati Fm
B87-8
g
3352 +6/-5 Ma
3350
3300
3250
3200
30
BROWN
PLATEY
BADDELEYITE
31
PALE YELLOW
SKELETAL Zr
206 Pb/ 238 U
207 Pb/ 235 U
.69
.67
.65
.63
.61
.59
21
22
23
24
25
26
27

(b) Table 4: ca. 3230-3200

Kaap Valley Pluton (B87-14; B87-32) (Figure 9a):

This is one of the few samples that yielded a homogeneous population of low U zircons. The concordant, apparently inheritance-free U-Pb systematics reflect this. The zircons analyzed were pale pink, euhedral, mostly stubby (150 um X 150 um) prisms that were not visibly zoned. The border phase (B87-14) and the interior phase (B87-32) gave identical results. Four abraded zircon fractions (two from each phase) and two fractions of clear, brown, blocky fragments of sphene (one from each phase) are concordant and within error of each other (± 1.5 Ma, 1 sigma) at 3227 Ma. The crystallization ages of the two phases are therefore indistinguishable at this level of precision. One non-abraded fraction from B87-14 was also analyzed in order to generate a Pb-loss line; however, this was only 2.6% discordant and the $^{207}Pb/^{206}Pb$ age was 3225 Ma providing only a poorly constrained lower intersection age that indicates Pb-loss was recent.

Th/U ratios for sphene from each phase differed by an order of magnitude. Sphene from the border phase (#4) gave a Th/U ratio typical for minerals that formed in a hydrothermal setting. This may indicate that, although it has an identical $^{207}Pb/^{206}Pb$ age as the magmatic sphene for the interior phase (#7), it did not crystallize under the same magmatic conditions and may reflect a late-stage deuteric effect.

Ignimbrite (Stolzburg Syncline) (B87-11) (Figure 9b):

Five zircon analyses, including both single (#8, #10 & #11) and multi-grain

fractions (#9 & #12), yield consistent and concordant results. A regression line calculation gives a precise age of 3227 ± 1 Ma with a high probability of fit (82%) and a lower intercept age of 53 Ma. The zircon fractions varied in colour and size from very small (-200 mesh) pale pink (#9) to slightly larger darker pink grains with variable U concentrations (36-104 ppm). Th/U ratios are relatively high and are distinctly higher than those for the Kaap Valley pluton.

Feldspar porphyry (Stolzburg Syncline) (B87-10) (Figure 9c):

Three fractions (#19,#20 & #21) of abraded zircon gave a linear regression age of 3223 +3/-2 Ma with a lower intercept age of 203 Ma. One concordant pale pink euhedral zircon (#19) and 20 tiny very pale pink grains (#21) gave the same $^{207}Pb/^{206}Pb$ age, indicating either a zero-age Pb-loss for fraction #21, or a tiny amount of inheritance. Grains from fraction #20 were slightly more brown in colour and plotted to the left and just outside of error of #21. Th/U ratios resemble those for B87-11 (ignimbrite), which it intrudes.

Qtz-fsp porphyry (deformed) (B87-27) (Figure 9d):

The presence of inherited grains was a problem in determining the age of this sample. Three morphologically similar grains (#16, #17 & #18) gave older $^{207}Pb/^{206}Pb$ ages of 3243 Ma, 3279 Ma and 3484 Ma, respectively. Analysis #18 plots outside of Figure 9d. In order to obtain what is interpreted as the crystallization age for this rock, long prisms (4:1 aspect ratio) (#14) and very tiny colourless grains (#15) were selected. These concordant and near-concordant analyses gave a good probability of fit (34%) when regressed with a single pink euhedral grain (#13)

yielding an upper intercept age of 3226 +5/-3 Ma. Analysis #13 plots slightly above the concordia curve which can be attributed to either a poorly defined U peak shape, or an inappropriate assumed U blank. In either case, the data point is still within error of the most concordant fraction (#14).

Th/U ratios for the regressed analyses are highly variable and suggest that these zircons may be from different sources. Nevertheless, the fact that the three youngest near concordant analyses give consistent ages argues for this age as the time of emplacement of the porphyry.

Dalmein Pluton (B87-22) (Figure 9e):

Two fractions of concordant, and near concordant, honey -coloured sphene (#22 and #23) were regressed with one fraction of small, euhedral discordant zircons to yield an upper intercept age of 3216 +2/-1 Ma with a 67% probability of fit. Fraction #24 plots to the left of the regression line with a $^{207}Pb/^{206}Pb$ age of 3194 Ma, but since the $^{207}Pb/^{204}Pb$ ratio varied by 6% during the analysis, it was omitted from the regression calculation. A line regressed through this point and the sphene analyses gives an unusually high lower intercept age of ca. 2100 Ma. The lower intercept age of ca. 500 Ma reported here is typical for the rocks in this study. The Th/U ratios are typical for magmatically-derived sphene.

Stolzburg Pluton (B87-2, younger phase) (Figure 9f):

A concordant $^{207}Pb/^{206}Pb$ age of 3201 Ma for pale yellow sphene (#26) is interpreted to represent a minimum age for this rock. Two single long prismatic colourless zircons (#27, #28) were analyzed and gave $^{207}Pb/^{206}Pb$ ages of 3237 Ma

and 3255 Ma, respectively. Th/U ratios are much lower than expected for magmatic grains and may indicate that these minerals crystallized during a later thermal or hydrothermal event.

TABLE 4.

U-Pb age data for rock samples from ca. 3230-3200 Ma.

(Notes: see Table 3)

TABLE 4

U-Pb data for ca. 3230-3200 Ma rocks from the Barberton Mountain Land.

Description fraction no.	Weight (μg)	Concentration U (ppm)	Concentration Pb (ppm)	Common Pb (pg)	Atomic ratios $^{206}Pb/^{204}Pb$	Atomic ratios $^{208}Pb/^{206}Pb$	$^{206}Pb/^{238}U$	$^{207}Pb/^{235}U$	$^{207}Pb/^{206}Pb$	Age (Ma) $^{207}Pb/^{206}Pb$
KAAP VALLEY PLUTON (border phase) B87-14										
1. Z, 9 gr	40	27	22	3	14940	0.1882	0.6490	22.9789	0.25681	3227
2. Z, 10 gr	30	36	29	2	19995	0.1740	0.6479	22.9216	0.25659	3226
3. Z, 7 gr	20	35	27	7	4339	0.1684	0.6325	22.3669	0.25646	3225
4. S, m-fr	248	106	77	382	2856	0.0500	0.6480	22.9375	0.25671	3227
KAAP VALLEY PLUTON (interior phase) B87-32										
5. Z, 8 gr	59	32	25	3	26366	0.1702	0.6487	22.9889	0.25702	3228
6. Z, 2 gr	7	39	31	27	435	0.1790	0.6582	23.3058	0.25682	3227
7. S, m-fr	358	86	88	413	3100	0.5758	0.6467	22.8803	0.25658	3226
IGNIMBRITE (Stolzburg syncline) B87-11										
8. Z, 1 gr	2	36	29	2	1244	0.1906	0.6472	22.9155	0.25681	3227
9. Z, 20 gr	17	69	57	11	4566	0.2344	0.6464	22.8789	0.25669	3226
10. Z, 1 gr	3	68	57	3	2457	0.2455	0.6453	22.8396	0.25672	3227
11. Z, 1 gr	3	97	82	7	1787	0.2730	0.6448	22.8010	0.25648	3225
12. Z, 2 gr	2	104	89	5	1647	0.3108	0.6370	22.5469	0.25673	3227

QTZ-FSP PORPHYRY B87-27										
13. Z, 1 gr	1	58	44	7	391	0.0906	0.6550	23.2307	0.25722	3230
14. Z, 7 gr	3	31	27	4	962	0.2744	0.6461	22.8921	0.25698	3228
15. Z, m-gr	3	167	125	13	1542	0.1325	0.6410	22.6254	0.25600	3222
16. Z, 1 gr	1	504	363	5	4364	0.0397	0.6448	23.0568	0.25934	3243
17. Z, 1 gr	1	349	259	4	3849	0.0532	0.6550	23.9688	0.26539	3279
18. Z, 1 gr	1	38	33	9	211	0.1226	0.7103	29.6439	0.30269	3484
QTZ-FSP PORPHYRY DYKE (Stolzburg syncline) B87-10										
19. Z, 1 gr	1	61	53	5	4353	0.2882	0.6460	22.8021	0.25601	3222
20. Z, 7 gr	1	256	211	8	3214	0.2812	0.6236	21.9496	0.25526	3218
21. Z, 20 gr	9	113	93	17	3283	0.2817	0.6210	21.9155	0.25595	3222
DALMEIN PLUTON B87-22										
22. S, m-fr	188	80	98	529	1179	0.9592	0.6447	22.6554	0.25487	3215
23. S, m-fr	231	50	69	499	961	1.2463	0.6406	22.4885	0.25460	3214
24. Z, 3 gr	2	96	70	4	1845	0.0844	0.6321	21.9164	0.25145	3194
25. Z, 7 gr	2	151	113	2	5018	0.1617	0.6121	21.4002	0.25355	3207
STOLZBURG PLUTON (younger phase) B87-2										
26. S, m-fr	160	51	37	191	1761	0.0602	0.6371	22.1887	0.25259	3201
27. Z, 1 gr	5	24	16	7	731	0.0006	0.6435	22.9249	0.25839	3237
28. Z, 1 gr	5	29	21	15	431	0.0288	0.6524	23.5177	0.26145	3255

FIGURE 9a-f.

Concordia diagrams for rocks from ca. 3230-3200 Ma.

(Note: abbreviations as in Fig. 8)

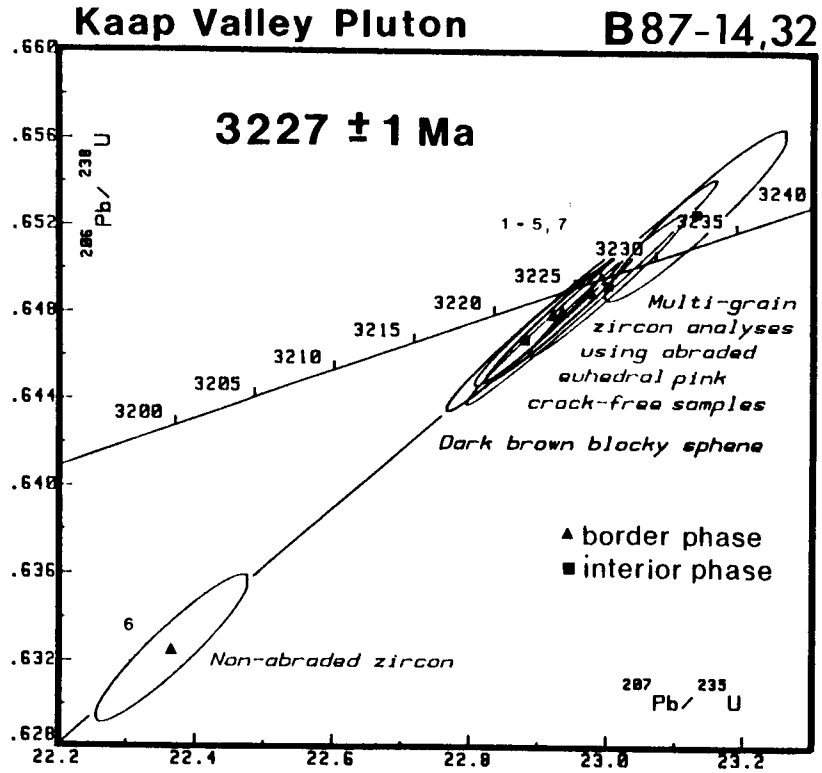
Kaap Valley Pluton
B87-14,32
a
3227 ±1 Ma
206Pb/238U
207Pb/235U
1 - 5, 7
6
3200
3205
3210
3215
3220
3225
3230
3235
3240
Multi-grain zircon analyses using abraded euhedral pink crack-free samples
Dark brown blocky sphene
▲ border phase
■ interior phase
Non-abraded zircon
.660
.656
.652
.648
.644
.640
.636
.632
.628
22.2
22.4
22.6
22.8
23.0
23.2

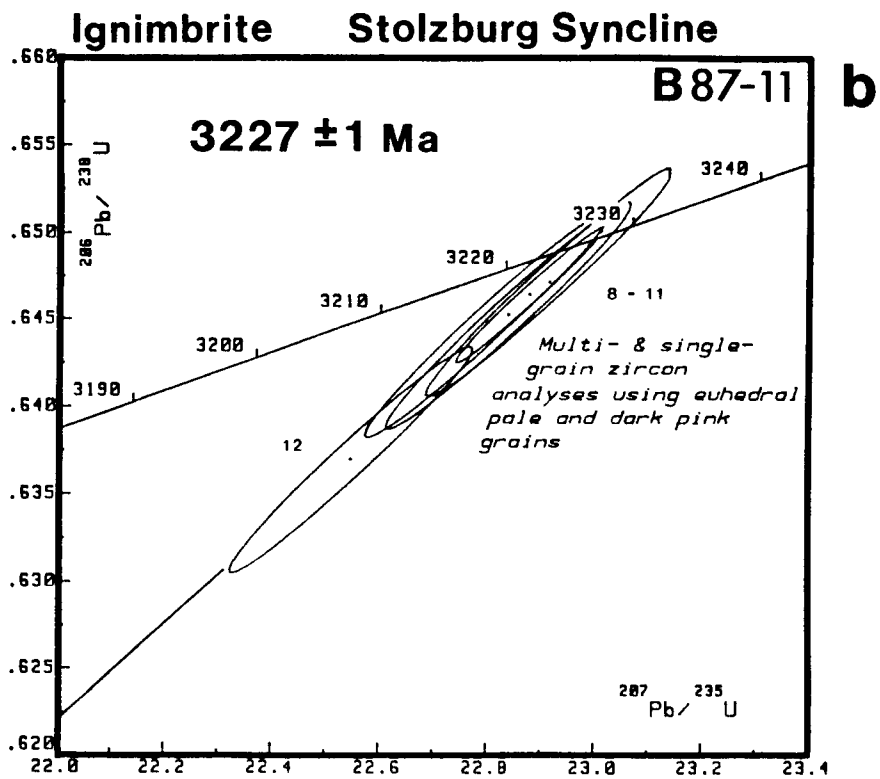
Ignimbrite
Stolzburg Syncline
B87-11
b
3227 ±1 Ma
206Pb/238U
207Pb/235U
8 - 11
12
3190
3200
3210
3220
3230
3240
Multi- & single-grain zircon analyses using euhedral pale and dark pink grains
.660
.655
.650
.645
.640
.635
.630
.625
.620
22.0
22.2
22.4
22.6
22.8
23.0
23.2
23.4

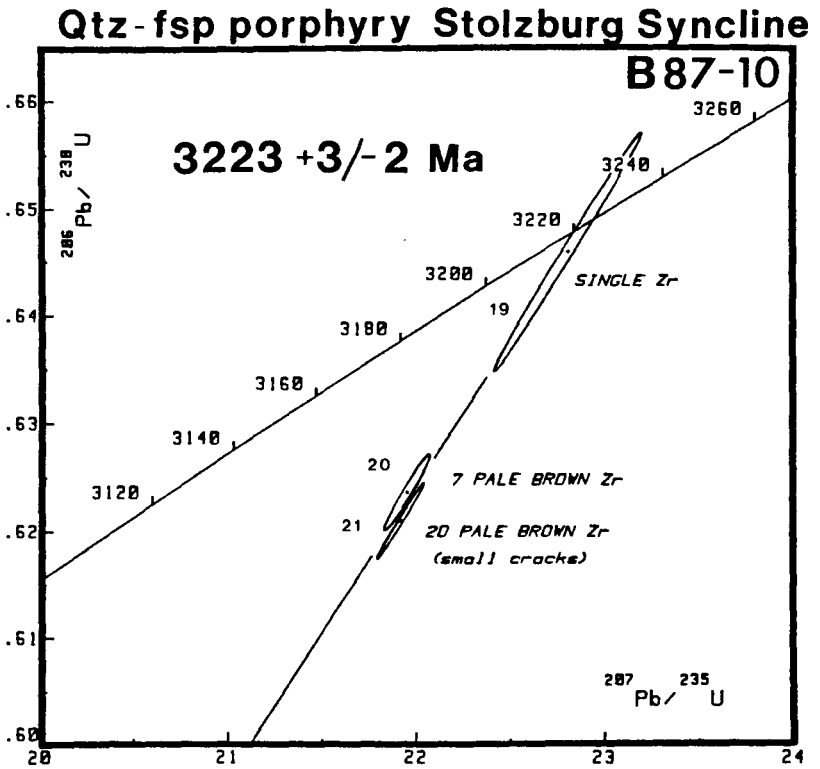
Qtz-fsp porphyry Stolzburg Syncline
B87-10
C
3223 +3/-2 Ma
206 Pb/ 238 U
207 Pb/ 235 U
3260
3240
3220
3200
3180
3160
3140
3120
SINGLE Zr
19
20
7 PALE BROWN Zr
21
20 PALE BROWN Zr
(small cracks)
.66
.65
.64
.63
.62
.61
.60
20
21
22
23
24

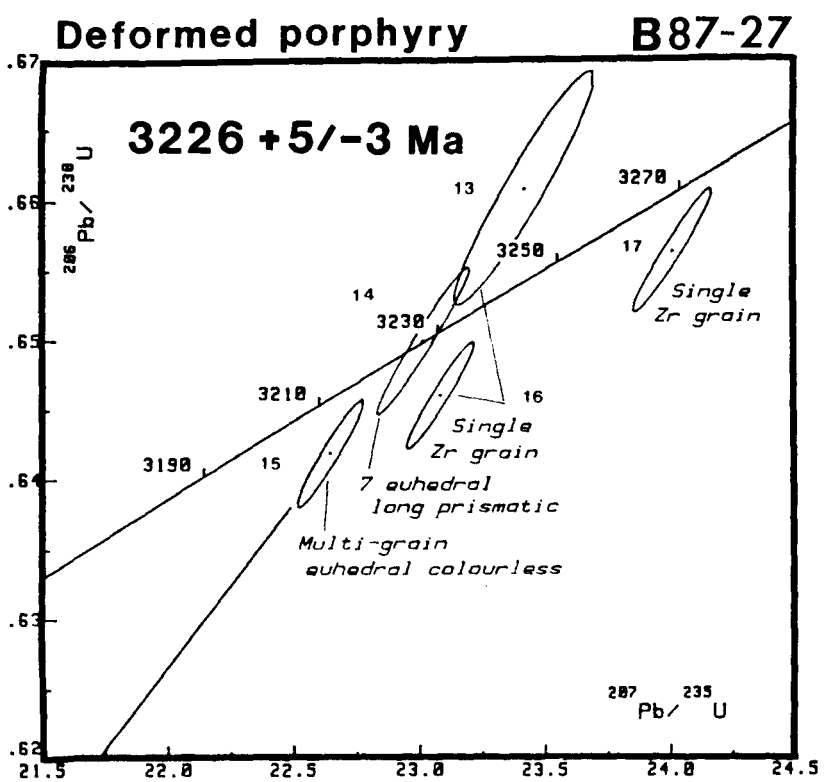
Deformed porphyry
B87-27
D
3226 +5/-3 Ma
206 Pb/ 238 U
207 Pb/ 235 U
13
3270
3250
17
14
3230
Single
Zr grain
3210
16
Single
Zr grain
3190
15
7 euhedral
long prismatic
Multi-grain
euhedral colourless
.67
.66
.65
.64
.63
.62
21.5
22.0
22.5
23.0
23.5
24.0
24.5

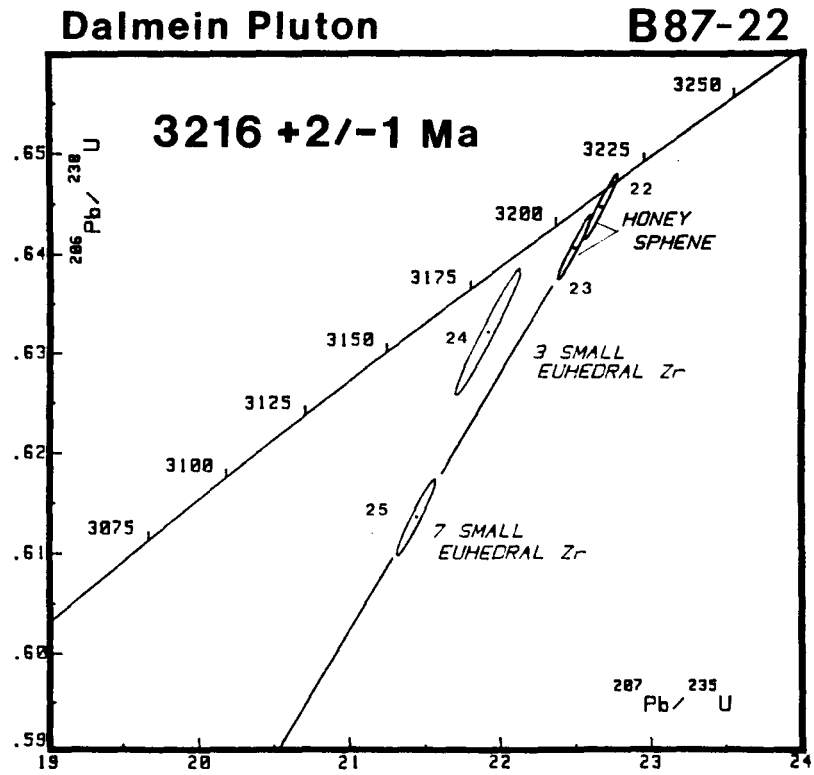
Dalmein Pluton
B87-22
3216 +2/-1 Ma
3250
3225
3200
3175
3150
3125
3100
3075
22
HONEY
SPHENE
23
24
3 SMALL
EUHEDRAL Zr
25
7 SMALL
EUHEDRAL Zr
206 Pb/ 238 U
207 Pb/ 235 U
.65
.64
.63
.62
.61
.60
.59
19
20
21
22
23
24

e

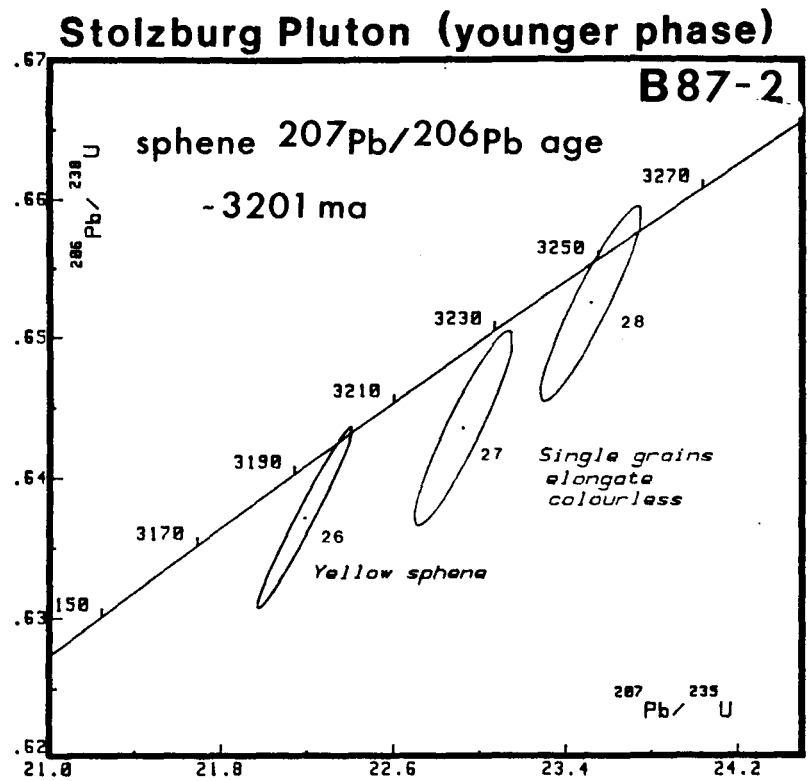
Stolzburg Pluton (younger phase)
B87-2
sphene 207Pb/206Pb age
-3201 ma
3270
3250
3230
3210
3190
3170
3150
28
27
26
Single grains
elongate
colourless
Yellow sphene
206 Pb/ 238 U
207 Pb/ 235 U
.67
.66
.65
.64
.63
.62
21.0
21.8
22.6
23.4
24.2

f

(c) Table 5: ca. 3107-2740 Ma

Potassic sheet-like and associated intrusions

Mpuluzi Pluton (B87-25) (Figure 10a):

The zircons in this population were small, severely cracked and largely altered. A fraction of the clearest grains was analyzed. However, this was still 4.4% discordant (#3). Two fractions of brown, blocky sphene (#1,#2) were less than 1% discordant at 3100 Ma and 3105 Ma, respectively. The upper intercept age of these three analyses is 3107 +4/-2 Ma.

Nelspruit Batholith (B87-17) (Figure 10b):

Both sphene and zircon were analyzed in this sample. Sharply- faceted, pink, low U, unzoned zircons were analyzed in fractions #4 and #6. Together with brown, blocky, clear, crack-free sphene (#5) these analyses yielded a regression age of 3105 +3/-3 Ma. These results were obtained after having first analyzed a multiple zircon fraction (#7) and a single zircon fraction (#8) that both contained inherited components, either in the form of cores that were not visible, or as xenocrystic grains. The older concordant $^{207}Pb/^{206}Pb$ ages of these two analyses (3115 Ma and 3329 Ma, respectively) indicate contamination by an older crustal component. Inherited components such as core-overgrowth relationships were not visible, therefore, in order to determine the crystallization age of the batholith only zircons examined at 100X magnification that showed no indication of resorbed edges or surfaces were chosen.

A gneissic tonalitic xenolith (B87-18) from an agmatitic outcrop located within

the migmatitic - gneissic phase of the Nelspruit batholith has yielded $^{207}Pb/^{206}Pb$ ages of ca. 3300 Ma (#9, #10) which is further evidence for crustal contamination by an older source.

Hebron Pluton (B87-19) (Figure 10c):

Concordant stubby euhedral prisms (#11, #12) and discordant (4.0 %) needles (#14), together with one fraction of brown blocky sphene (#13), were regressed yielding an upper intercept age of 3104 +3/-2 Ma. No inherited components were detected.

Stentor Pluton (B87-15) (Figure 10d):

Five fractions of zircon and one fraction of rutile were regressed to yield an upper intercept age of 3107 +6/-4 Ma. Each zircon fraction represented a different typology specifically chosen to test for the presence of metamorphic zircons. However, all the grains have typical magmatic qualities in terms of morphology and Th/U ratios. Inherited zircon is present as shown by the older age given by #21. Even if the 3107 +6/-4 Ma fractions do contain some inheritance, crystallization and metamorphism of the pluton can be no younger than the 3082 Ma $^{207}Pb/^{206}Pb$ age of the rutile.

Syenitic and granitic plutonism

Boesmanskop Pluton (B87-20) (Figure 10e):

Two abraded fractions (#23, #24) and one non-abraded fraction (#26) of pink, euhedral, low U, crack- and inclusion-free zircons, and one abraded fraction (#25)

of clear, brown, blocky sphene were analyzed. The abraded fractions are all concordant and the non-abraded fraction is 5.3% discordant. The calculated regression age is 3107 +/- 1 Ma.

Mpageni Pluton (B87-16) (Figure 10f):

Three zircon fractions (#27,#28 & #29) are 2.6% to 3.4% discordant. Due to the degree of discordance and the limited spread of the data points, it is necessary to fix a lower intercept for the Pb-loss line. A lower intercept age of 600 ± 400 Ma, typical for late Archean rocks, was chosen which gives an age of 2740 ± 15 Ma.

Late felsic magmatism

Altered feldspar porphyry (B87-6)(not plotted):

Two single grain analyses from a heterogeneous zircon population yielded concordant data points with $^{207}Pb/^{206}Pb$ ages of 3457 and 3080 Ma. The latter age represents an upper limit for emplacement of this pluton.

(V) SUMMARY OF U-Pb RESULTS FROM THE PRESENT STUDY

Age data obtained in this study are summarized in Table 6 (page 64).

TABLE 5.

U-Pb age data for rock samples from ca. 3130-2740 Ma.

(Notes: see Table 3)

TABLE 5

U-Pb data for ca. 3107-2740 Ma rocks from the Barberton Mountain Land.

Description fraction no.	Weight (μg)	Concentration U (ppm)	Concentration Pb (ppm)	Common Pb[a] (pg)	Atomic ratios $^{208}Pb/^{206}Pb^{c}$	$^{206}Pb/^{238}U$	$^{207}Pb/^{235}U$	$^{207}Pb/^{206}Pb$	Age (Ma) $^{207}Pb/^{206}Pb$
MPULUZI BATHOLITH B87-25									
1. S, m-fr	90	60	73	237	907	1.0515	0.6135	20.1094	0.23771	3105
2. S, m-fr	225	86	85	461	1659	0.6251	0.6118	19.9982	0.23708	3100
3. Z, m-gr	5	74	54	2	6025	0.2163	0.5881	19.1188	0.23579	3092
NELSPRUIT BATHOLITH B87-17									
4. Z, 1 gr	4	47	38	3	2462	0.2236	0.6365	20.9704	0.23895	3113
5. S, m-fr	186	164	169	882	1380	0.7000	0.6176	20.2464	0.23777	3105
6. Z, 2 gr	20	49	37	42	935	0.1885	0.6114	19.9815	0.23702	3100
7. Z, 7 gr	10	85	65	21	1636	0.1914	0.6209	20.4853	0.23930	3115
8. Z, 1 gr	5	111	87	18	1376	0.0785	0.6754	25.5203	0.27403	3329
TONALITE XENOLITH B87-18									
9. Z, 2 gr	8	53	44	6	3075	0.1860	0.6645	24.6884	0.26946	3303
10. Z, 5 gr	15	79	64	4	11317	0.1678	0.6572	24.3309	0.26849	3297
HEBRON PLUTON B87-19									
11. Z, 5 gr	4	80	61	7	1697	0.2106	0.6164	20.2059	0.23774	3105
12. Z, m-gr	14	73	58	9	4361	0.2530	0.6139	20.0700	0.23710	3101
13. S, m-gr	136	37	40	366	546	0.8334	0.6107	19.9639	0.23707	3100
14. Z, 3 gr	3	39	30	6	740	0.3030	0.5899	19.1310	0.23522	3088

STENTOR PLUTON B87-15										
15. Z, 4 gr	4	36	28	16	363	0.2071	0.6203	20.3321	0.23772	3106
16. Z, 1 gr	2	27	21	4	609	0.2032	0.6243	20.5658	0.23893	3113
17. Z, 1 gr	1	24	20	16	78	0.3177	0.6460	21.2535	0.23863	3111
18. Z, 6 gr	2	51	38	4	925	0.1981	0.6102	19.9802	0.23747	3103
19. R, m-fr	7	86	54	13	1761	0.0057	0.5921	19.1358	0.23439	3082
20. Z, 1 gr	1	81	57	15	211	0.2196	0.5647	18.0707	0.23210	3067
21. Z, 3 gr	4	26	20	12	1285	0.1643	0.6447	22.1591	0.24928	3180
22. Z, 1 gr	1	15	11	8	85	0.1715	0.5737	18.7795	0.23740	3103
BOESMANSKOP PLUTON B87-20										
23. Z, 17 gr	30	65	51	4	19080	0.2325	0.6184	20.2924	0.23801	3107
24. Z, 6 gr	12	56	45	4	7490	0.2577	0.6170	20.2519	0.23804	3107
25. S, m-fr	107	126	177	846	642	1.3916	0.6193	20.3394	0.23818	3108
26. Z, 6 gr	13	101	76	12	4246	0.2653	0.5852	19.1559	0.23739	3102
MPAGENI PLUTON B87-16										
27. Z, 1 gr	6	64	41	7	1878	0.2633	0.5149	13.4345	0.18924	2736
28. Z, 16 gr	12	125	78	13	3829	0.2335	0.5089	13.1913	0.18801	2725
29. Z, 1 gr	3	51	32	6	807	0.2502	0.5080	13.1594	0.18787	2724
FELSIC INTRUSION B87-6										
30. Z, 1 gr	1	40	34	5	418	0.0854	0.7089	29.0736	0.29742	3457
31. Z, 1 gr	1	116	91	3	1458	0.2488	0.6116	19.7350	0.23402	3080

FIGURE 10a-f.

Concordia diagrams for rocks from ca. 3107-2740 Ma.

(Note: abbreviations as in Fig. 8)

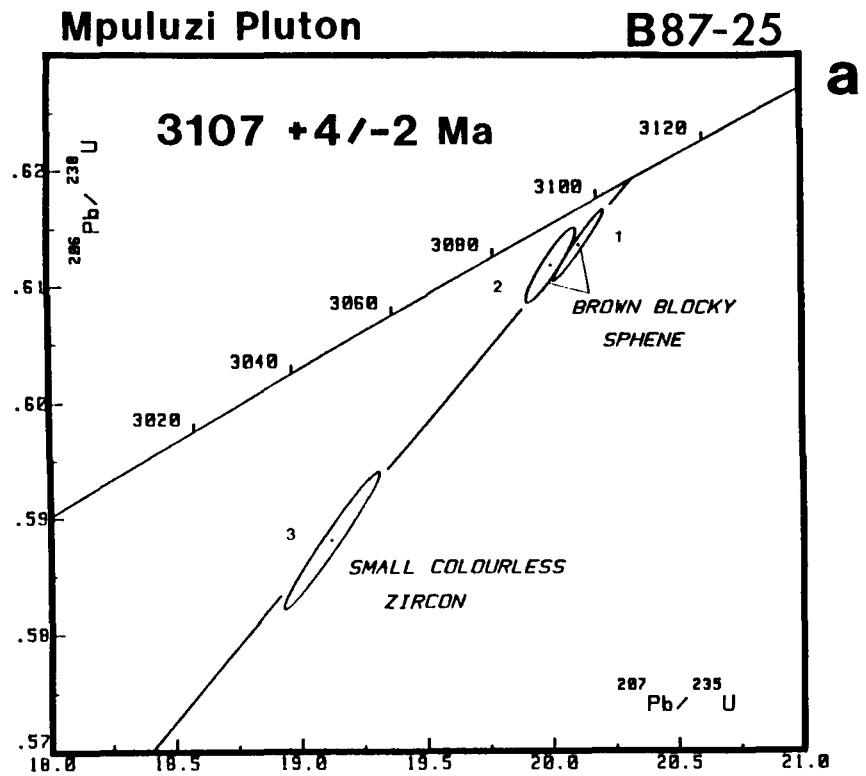
Mpuluzi Pluton
B87-25
a
3107 +4/-2 Ma
3120
3100
3080
3060
3040
3020
1
2
BROWN BLOCKY
SPHENE
3
SMALL COLOURLESS
ZIRCON
.62
.61
.60
.59
.58
.57
18.0
18.5
19.0
19.5
20.0
20.5
21.0
206 Pb/ 238 U
207 Pb/ 235 U

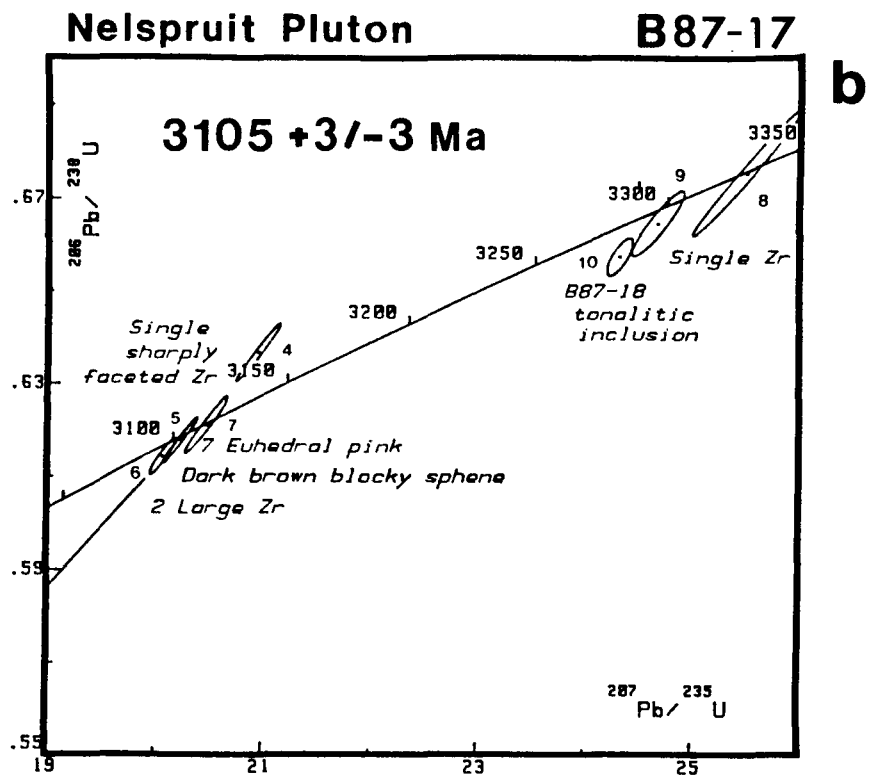
Nelspruit Pluton
B87-17
b
3105 +3/-3 Ma
3350
3300
3250
3200
3150
3100
9
8
10
Single Zr
B87-18
tonalitic
inclusion
Single
sharply
faceted Zr
4
5
7
6
7 Euhedral pink
Dark brown blocky sphene
2 Large Zr
.67
.63
.59
.55
19
21
23
25
206 Pb/ 238 U
207 Pb/ 235 U

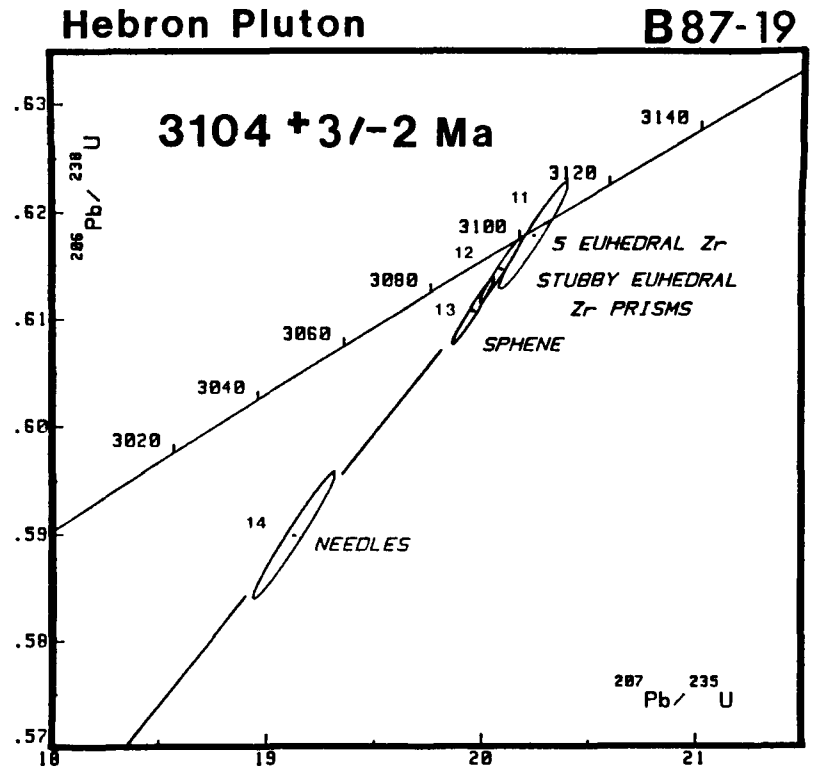
Hebron Pluton
B87-19
c
3104 +3/-2 Ma
206 Pb/ 238 U
207 Pb/ 235 U
3140
3120
3100
3080
3060
3040
3020
11
12
13
14
5 EUHEDRAL Zr
STUBBY EUHEDRAL
Zr PRISMS
SPHENE
NEEDLES
.63
.62
.61
.60
.59
.58
.57
18
19
20
21

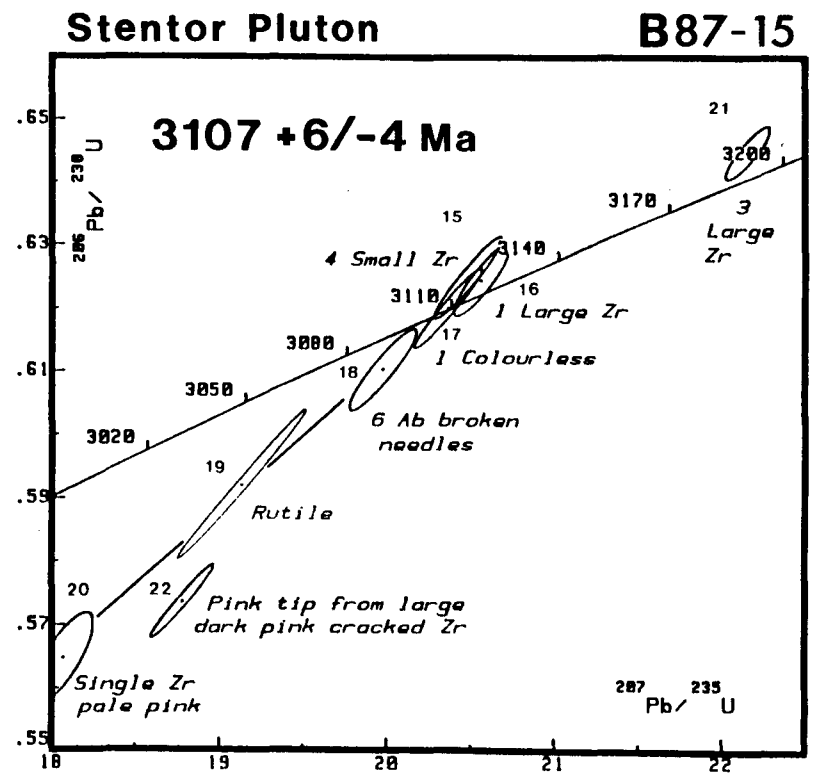
Stentor Pluton
B87-15
d
3107 +6/-4 Ma
206 Pb/ 238 U
207 Pb/ 235 U
3200
3170
3140
3110
3080
3050
3020
15
16
17
18
19
20
21
22
3
Large
Zr
4 Small Zr
1 Large Zr
1 Colourless
6 Ab broken
needles
Rutile
Pink tip from large
dark pink cracked Zr
Single Zr
pale pink
.65
.63
.61
.59
.57
.55
18
19
20
21
22

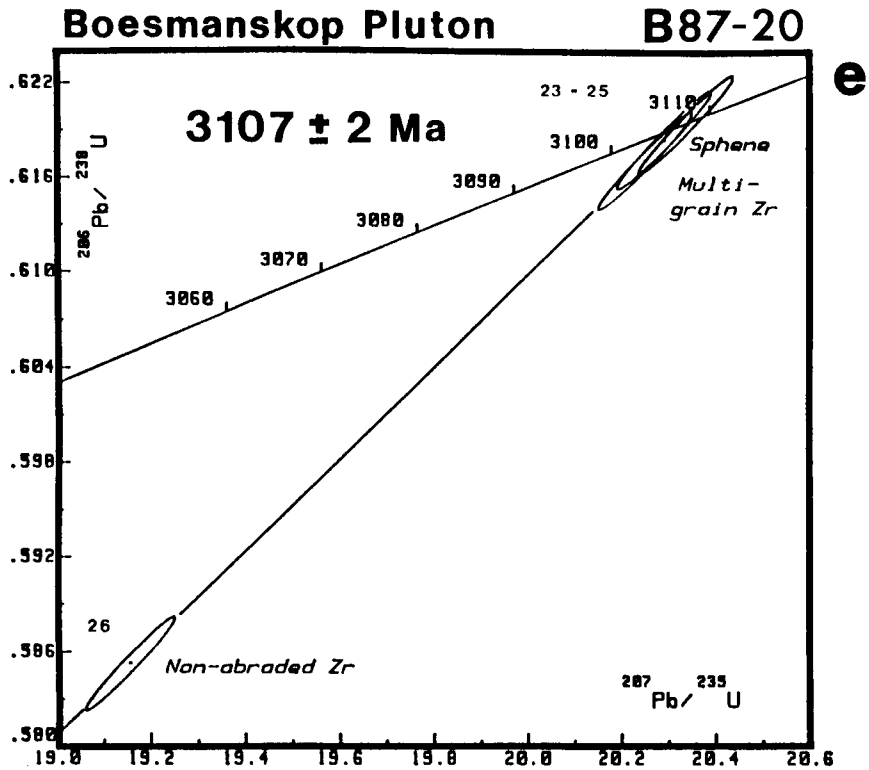
Boesmanskop Pluton
B87-20
e
3107 ± 2 Ma
23 - 25
3110
3100
3090
3080
3070
3060
Sphene
Multi-
grain Zr
Non-abraded Zr
26
.622
.616
.610
.604
.598
.592
.586
.580
19.0
19.2
19.4
19.6
19.8
20.0
20.2
20.4
20.6
206 Pb/ 238 U
207 Pb/ 235 U

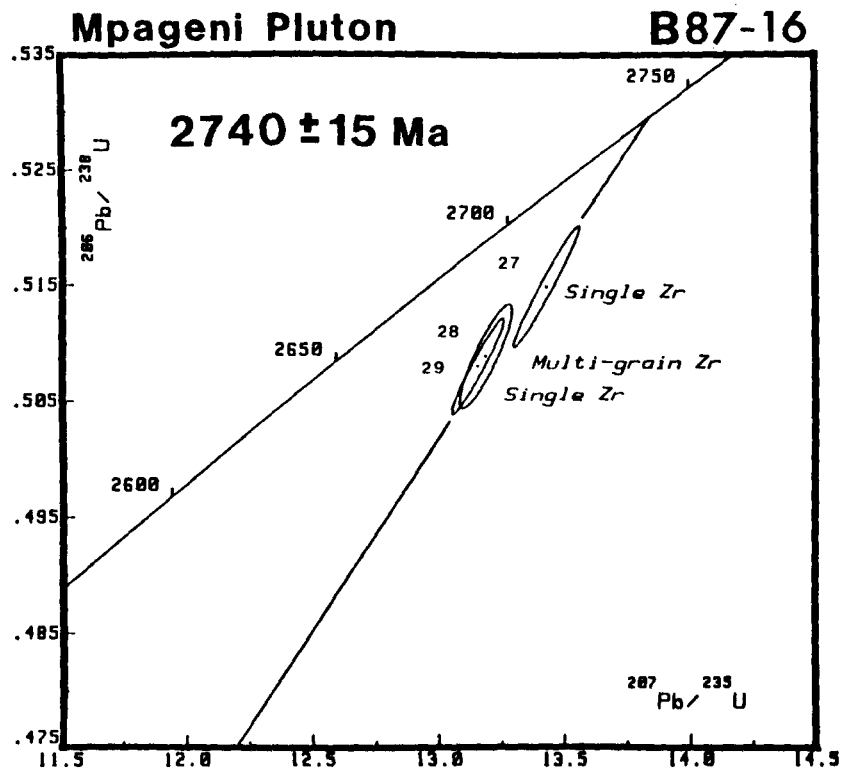
Mpageni Pluton
B87-16
f
2740 ± 15 Ma
206 Pb/ 238 U
207 Pb/ 235 U
.535
.525
.515
.505
.495
.485
.475
11.5
12.0
12.5
13.0
13.5
14.0
14.5
2750
2700
2650
2600
27
28
29
Single Zr
Multi-grain Zr
Single Zr

TABLE 6.

Summary of age data obtained in the present study. Number of points refers to the number of analyses used in the regression calculation. P of F = probability of fit. Asterisks denote regression calculations which utilized the error expansion part of the computer program of Davis (1982) (see Chapter 5ii(c) for explanation).

SAMPLE	Upper intercept age (Ma)	Lower intercept age (Ma)	# of points	P of F (%)
Tonalite gneiss wedge Theespruit formation **B87-5**	3538 +4/-2	348	3	97
Steynsdorp pluton **B87-24**	3509 +8/-7	762	4	*58
Qtz-fsp porphyry **B87-7**	3467 +12/-7	1727	4	31
Stolzburg pluton **B87-1**	3459 +5/-4	954	2	16
Doornhoek pluton **B87-21**	3448 +4/-3	801	3	21
Theespruit pluton **B87-4**	3443 +4/-3	607	5	*41
Metagabbro (Komati fm) **B87-8**	3350 ± 4	849	2	99
Gneissic tonalitic xenolith in Nelspruit pluton **B87-18**	3300		2 analys.	
Deformed feldspar porphyry **B87-27**	3226 +5/-3	861	3	34
Kaap Valley pluton (border phase) **B87-14**	3227 ± 1	220	4	59
Kaap Valley pluton (interior phase) **B87-32**	3228 ± 1	1020	3	68
Ignimbrite (Stolzburg syncline) **B87-11**	3227 ± 1	53	5	67
Feldspar porphyry (Stolzburg syncline) **B87-10**	3223 +3/-2	203	3	42

Dalmein pluton **B87-22**	3216 +2/-1	500	3	67
Stolzburg pluton (younger phase) **B87-2**	3201		3 analys.	
Boesmanskop pluton **B87-20**	3107 ± 2	242	4	69
Mpuluzi pluton **B87-25**	3107 +4/-2	750	3	13
Nelspruit pluton **B87-17**	3105 ± 3	791	3	45
Hebron pluton **B87-19**	3104 +3/-2	827	4	49
Stentor pluton **B87-15**	3107 +6/-4	1115	6	59
Mpageni pluton **B87-16**	2740 ± 15	615	3	47

CHAPTER 6

Sm-Nd ISOTOPE GEOCHEMISTRY

(i) Introduction

The Nd isotopic composition of rocks is important for understanding the source of magmatism and for evaluating the role of processes such as contamination by older crust. It has been used to quantitatively assess the extent and role of assimilation in granitic magmas (e.g. DePaolo 1981a; 1983) and to monitor details of magma chamber processes in mafic layered intrusions (e.g. Stewart and DePaolo, 1987; DePaolo, 1985). In this study, Sm-Nd whole-rock data from rocks from the Barberton Mountain Land, South Africa, in combination with U-Pb geochronology (Chapter 5), are used to gain insight into how one of the earliest exposed remnants of continental crust has evolved through Archean time.

Initial $^{143}Nd/^{144}Nd$ ratios can be calculated when the crystallization age of the sample is known and the present-day $^{143}Nd/^{144}Nd$ and $^{147}Sm/^{144}Nd$ ratios are measured, assuming the sample has remained an isotopically closed system. This approach avoids potential difficulties that can be encountered using the isochron method which requires that all samples be coeval and formed from sources with the same initial $^{143}Nd/^{144}Nd$ ratio as well as remaining closed to the migration of parent and daughter since the time of crystallization. Problems arise in interpreting isochron data when one or more of these requirements are not met. Many published

examples exist where these requirements have been violated because, in order to improve the precision of an isochron, a wide range in Sm/Nd ratios is desirable which may lead to the use of samples with radically different provenances. Examples of apparent Sm-Nd "isochrons" in which the researchers concluded that the ages had no chronological meaning, due to possible mixing of components with different initial $^{143}Nd/^{144}Nd$, have been reported by Cattell et al. (1984) for a mafic-ultramafic suite from Newton Township, Canada, by Chauvel et al. (1985) and Compston et al. (1986) for the Kambalda greenstones, Western Australia, and by Hegener et al. (1984) for the Usushwana gabbroic suite, Swaziland.

(ii) Notation and calculation of ϵ_{Nd} and T_{CHUR} and T_{DM} Model ages

The standard method for presentation of Sm-Nd data is to compare initial $^{143}Nd/^{144}Nd$ ratios of rocks to CHUR (acronym for chondritic uniform reservoir; DePaolo and Wasserburg, 1976) and/or to the "depleted mantle" model curve (DePaolo, 1981b) on an ϵ_{Nd} vs time diagram. The CHUR model assumes that terrestrial Nd has evolved from a uniform reservoir whose Sm/Nd ratio is equal to that of chondritic meteorites thought to represent bulk-Earth Nd compositions or, in other words, a primordial unfractionated mantle. The present $^{143}Nd/^{144}Nd$ ratio in this reservoir is 0.512638 relative to a $^{146}Nd/^{144}Nd$ ratio of 0.7219 (Wasserburg et al., 1981).

ϵ_{Nd} parameter

In order to compare small differences in Nd isotopic ratios between samples and CHUR, the "epsilon parameter" was introduced by DePaolo and Wasserburg (1976) and is defined as follows:

$$\epsilon_{Nd}(T) = \left(\frac{\left(\frac{(^{143}Nd)}{(^{144}Nd)} SAMPLE - \frac{(^{143}Nd)}{(^{144}Nd)} CHUR \right)}{\frac{(^{143}Nd)}{(^{144}Nd)} CHUR} \right) X10^{4}$$

where the $^{143}Nd/^{144}Nd$ ratios are calculated from:

$$\frac{(^{143}Nd)}{(^{144}Nd)} CHUR = \frac{(^{143}Nd)}{(^{144}Nd)} CHUR_{pd} - \frac{(^{147}Sm)}{(^{144}Nd)} CHUR_{pd} X \left(e^{(\lambda T)} - 1 \right)$$

$$\frac{(^{143}Nd)}{(^{144}Nd)} SAMPLE = \frac{(^{143}Nd)}{(^{144}Nd)} SAMPLE_{pd} - \frac{(^{147}Sm)}{(^{144}Nd)} SAMPLE_{pd} X \left(e^{(\lambda T)} - 1 \right)$$

where

$(^{143}Nd/^{144}Nd)_{CHURpd}$ = 0.512638 (Wasserburg et al., 1981),

$(^{147}Sm/^{144}Nd)_{CHUR}$ = 0.1967 (Jacobsen and Wasserburg, 1980),

T = crystallization age of the sample

pd = present-day, and

$$\lambda_{Sm} = 6.54 x 10^{-12} yr^{(-1)}$$

This parameter expresses the difference between the initial $^{143}Nd/^{144}Nd$ ratio of a sample (or suite of samples) and the corresponding value of this ratio for CHUR at the time of crystallization of the sample. A positive ϵ_{Nd} value indicates derivation of the sample from a depleted mantle source (i.e. depleted in LIL elements that are preferentially partitioned into the liquid phase during partial melting); a negative ϵ_{Nd} value indicates derivation from sources that had a lower Sm/Nd ratio (more enriched in LREE) than the chondritic reservoir. In general, it has been observed that rocks derived from juvenile continental crust or upper mantle have positive ϵ_{Nd} values during, and subsequent to, the Archean. Observed upper mantle sources are therefore more depleted than CHUR. Enriched continental crust has $^{143}Nd/^{144}Nd$ values lower than depleted mantle and rocks derived from recycling or mixing with such crust will have lower positive or negative ϵ_{Nd} values. Epsilon neodymium values near zero may be variously interpreted as having been derived either directly from a chondritic source, or from a depleted mantle source that was isotopically enriched through contamination from crustal sources during emplacement.

Model ages

Nd model ages, or "crust-formation" ages, can indicate the time at which samples of continental crust separated from a mantle source. A model age is determined by calculating the time when a sample had an identical isotopic composition to that of its source (which is defined by a given mantle evolution curve). The accuracy of these model ages depends in part on how well the evolution

of the mantle source is known. Model ages can vary by up to 600 Ma for the same sample depending on whether a bulk earth (CHUR) or depleted mantle model is used (Arndt and Goldstein, 1987). Model ages based on a chondritic or depleted mantle source are denoted by T_{CHUR} and T_{DM}, respectively. In this study, T_{CHUR} model ages are calculated as follows:

$$T_{CHUR} = \frac{1}{\lambda} \ln \left[1 + \frac{\frac{(^{143}Nd)}{(^{144}Nd)}sample_{pd} - \frac{(^{143}Nd)}{(^{144}Nd)}CHUR_{pd}}{\frac{(^{147}Sm)}{(^{144}Nd)}sample_{pd} - \frac{(^{147}Sm)}{(^{144}Nd)}CHUR_{pd}} \right]$$

The single-stage depleted mantle model of DePaolo (1981b) describes the effect of progressive long-term depletion of LREE in the mantle and attempts to model such changes with the progressive production of crust from an originally chondritic source. The model is constrained by $\epsilon_{Nd}=0$ (for primordial Earth at 4.5 Ga), $\epsilon_{Nd}=3.7$ (for rocks 1.8 b.y. old) and by $\epsilon_{Nd}=8.5$ (for modern MORB's). Since there is substantial evidence for a depleted mantle in the Archean (see Shirey and Hanson, 1986) this model is widely used for rocks of this age. The calculation of model ages for a depleted mantle reservoir (T_{DM}), as described by DePaolo (1981b), is obtained by solving the following equation for T:

$$\epsilon_{Nd}(T) = 0.25T^2 - 3T + 8.5$$

Implicit in the usage of these ages is the assumption that the Sm/Nd ratio of the rock has not changed since the time of Nd separation from its source. This in effect requires that the time between emplacement of the rock in the continental

crust to the time it acquired its continent-like Sm/Nd ratio, is short. It is also assumed that because Sm and Nd are geochemically similar elements (i.e. both are rare earth elements that are considered to be relatively immobile), they behave similarly under changing geological environments and thus do not fractionate during intra-crustal processes such as metamorphism and crustal remelting. This assumption appears valid in comparison to the Rb-Sr system where the behaviour of the alkaline metal and alkaline earth groups of elements are quite different under various low to high temperature crustal processes. A degree of caution should, nevertheless, be used considering that some REE-rich minerals (e.g. titanite and monazite) are known to have been partially reset or newly grown during a metamorphic event occurring long after original crystallization (e.g. Corfu, 1988; Parrish, 1991). In such a case, the REE's may have been redistributed to varying degrees and Sm-Nd model ages on some accessory minerals may give misleading results. If the process of element redistribution results in very local mobility (i.e. $\gtrsim$ a couple of centimeters), then analyzing whole-rock samples could overcome this potential problem. In a discussion of model ages, Arndt and Goldstein (1987) suggested that if the "true" age (i.e. independently determined reliable crystallization age) of the rock is different from the model age, then the time of crust-mantle separation should be supported by other geological and geochemical information before interpreting the age as representing a specific crust-formation event. The reason given for this is that a sample may be derived from a mixture of two or more isotopically distinct sources, in which case the time significance of the calculated model age would be meaningless in terms of

defining a specific crust-formation event.

The fact that most Archean mantle-derived rocks and many Archean sialic rocks have positive ϵ_{Nd}'s means that they were not derived from a chondritic source ($\epsilon_{Nd}=0$), but rather that most Archean rocks were derived from a LREE depleted mantle source ($\epsilon_{Nd}>0$) (see Shirey, 1991). Furthermore, many of the samples analyzed in this study yield positive values of $\epsilon_{Nd}(t)$. Therefore, it is assumed that T_{CHUR} will not give a reliable mantle-extraction age for most results and model age data in this study are discussed only in reference to a depleted mantle source.

(iii) Previous Sm-Nd studies

The aims of previous Sm-Nd studies in the BGB have been to determine the time of volcanism of rocks from the Onverwacht group and to define petrogenetic models for the Onverwacht komatiites (see Table 7 for a summary of previous results). The age for Onverwacht Group volcanism was previously considered to be ca. 3.56 to 3.53 Ga based on two Sm-Nd whole-rock studies on the Tjakastad Subgroup by Jahn et al. (1982) and Hamilton et al. (1979; 1983). Jahn et al. (1982) obtained an imprecise age of 3560 ± 230 Ma with an $\epsilon_{Nd}(T)= +3.3 \pm 4.5$ (2σ errors) based on five samples of basalt and komatiite. Hamilton et al. (1979; 1983) reported a similar and relatively precise age of 3526 ± 48 Ma with an $\epsilon_{Nd}(T)= +0.7 \pm 0.3$ (both 2σ errors) obtained by using 10 samples ranging in composition from felsic lavas or intrusives to ultrabasic komatiites in which $^{147}Sm/^{144}Nd$ ratios ranged from 0.1036 to 0.2051. It has been suggested that by combining both felsic and mafic

compositions in this isochron, the requisite use of samples with the same initial isotopic composition had been disregarded (e.g. Gruau et al., 1990) leading to erroneous age and initial isotopic values. Further, Gruau et al. suggest that since one of the two felsic samples used in Hamilton et al.'s isochron is a sodic porphyry (i.e. geochemically similar to Archean TTG granitic gneisses that are believed to be derived by remelting of LREE-enriched basaltic or amphibolitic precursors (Jahn et al., 1981; Martin, 1987)), it may have formed later than the mafic-ultramafic rocks and yielded lower initial Nd isotopic ratios. This has since been confirmed in this study by a maximum zircon $^{207}Pb/^{206}Pb$ age substantially younger at 3080 Ma (see Chapter 5) for the same sodic porphyry.

Recently, a third Sm-Nd isotopic study on the Tjakastad subgroup by Gruau et al. (1990) reported an anomolously young age of 3269 ± 84 (2σ) Ma with an $\epsilon_{Nd}(T) = -0.7 \pm 0.6$ using 8 samples of basalt and komatiite to define an apparent "isochron". This age was interpreted by the authors as having no chronological meaning based on (1) independently determined ages for the Onverwacht group that suggest the age of these volcanics is $\approx$3.45 Ga, (2) geochemical arguments that imply source heterogeneity, and therefore probable different initial $^{143}Nd/^{144}Nd$ ratios, solely within the basic-ultrabasic rocks, and (3) an ^{40}Ar-^{39}Ar age of 3440-3450 Ma (Lopez-Martinez et al., 1984), interpreted as a metamorphic age by a chronometer that is considered more sensitive to metamorphic re-setting than the Sm-Nd system (i.e. the 3269 Ma age is not likely a metamorphic age). Gruau et al. concluded that the early Archean mantle beneath the BGB was isotopically heterogeneous with both

depleted and CHUR mantle compositions and that, for the lower Onverwacht mafic-ultramafic suite, the Sm-Nd whole-rock method cannot be used for dating purposes.

TABLE 7.

Summary of published Sm-Nd data on rocks from the Tjakastad Subgroup.

ROCK TYPE	AGE (Ma)	ϵ_{Nd} (T)	Authors interpretation	Reference
Felsic intrusives/ volcanics to ultrabasic komatiites (10 samples)	3526 ± 48	+0.7 ± 0.3	Age is the eruption time for Tjakastad Subgroup volcanics	Hamilton et al. (1979; 1983)
Basalt and komatiite (5 samples)	3560 ± 230	+3.3 ± 4.5	Age is the eruption time for Tjakastad Subgroup volcanics	Jahn et al. (1982)
Basalt and komatiite (8 samples)	3269 ± 84	-0.7 ± 0.6	Age has no chronological meaning	Gruau et al. (1990)

(iv) Results

The Sm-Nd whole rock isotopic data reported here were obtained on a variety of rock types that have precisely measured U-Pb crystallization ages that range from 3467 Ma to 2740 Ma.

Results are summarized in Table 8 and presented graphically in Figure 11. The total range in ϵ_{Nd} for the rocks analyzed in this study is +1.31 to -4.30. In general, the older rock samples tend to give more depleted signatures than younger samples, with the exception of a quartz-feldspar dyke (B87-7). All the depleted mantle model ages exceed the ages of crystallization (as presented in Chapter 5) and the range in T_{DM}'s for all samples is 3.55 Ga to 3.14 Ga. In all samples, T_{DM}'s are outside of error of the crystallization age.

A 3467 Ma quartz-feldspar dyke (B87-7) that intrudes the Komati Formation within the type locality yields a slightly depleted ϵ_{Nd} value of +0.46, which is below the depleted mantle growth curve.

The ϵ_{Nd} value for a 3352 Ma metagabbro plots directly on the depleted mantle curve at +1.31, indicating that the time of crystallization of this rock may also be the time of separation from its mantle source. Depleted mantle source components were also recognized in samples from the Komati Formation by Hamilton et al. (1979), Jahn et al. (1982) and for one other basalt sample from the Komati Formation by Gruau et al. (1990) with an assumed crystallization age of 3450 Ma.

Two Kaap Valley tonalite samples (B87-14, B87-32) yield similar ϵ_{Nd} values

of +0.72 for the border phase and +0.63 for the interior phase. T_{DM}'s for the two samples are 3.31 Ga and 3.32 Ga for the border and interior phases, respectively.

The ignimbritic unit from the Stolzburg syncline (B87-11) is coeval with the Kaap Valley tonalite at 3227 Ma, but has a lower ϵ_{Nd} of -0.48. This value is within error of the values obtained for three potassic intrusions; the Nelspruit, Stentor and Mpuluzi intrusions which yield ϵ_{Nd} values that range from -0.52 to -0.48, but are much younger.

The lowest ϵ_{Nd} value of -4.30 is from the youngest pluton dated in this study, the 2740 Ma Mpageni granite. In general, rocks that are ca. 3230 Ma, ca. 3110 Ma, and 2740 Ma (from Episodes III, IV and V in Fig.11) may represent sources derived predominantly by crustal reworking processes, while rocks from ca. 3450 - 3470 Ma (Episode II in Fig. 11) may represent sources comprised *mainly* of juvenile material. However, the effect of contamination by older crust is evident even in the 3.47 Ga porphyry dyke from the Onverwacht Group.

TABLE 8.

Sm-Nd data for rocks from the present study.

SAMPLE	Nd (ppm)	Sm (ppm)	$^{147}Sm/^{144}Nd$	$^{143}Nd/^{144}Nd$ (measured)	T_{CHUR} (Ga)	T_{DM} (Ga)	ϵ_{Nd}	U-Pb AGE (Ma)
B87-7 QFP dyke	10.91	1.86	0.1031	0.510517 ± 7	3.43	3.55	+0.5	3467
B87-8 Metagabbro	5.95	1.93	0.2080	0.512957 ± 10	NA	NA	+1.3	3352
B87-14 Kaap Valley	16.89	3.34	0.1193	0.511026 ± 6	3.16	3.31	+0.7	3227
B87-15 Stentor	26.09	6.76	0.1567	0.511793 ± 7	3.20	3.45	-0.5	3108
B87-32 Kaap Valley	16.51	3.31	0.1214	0.511066 ± 6	3.16	3.32	+0.6	3227
B87-11 Ignimbrite	NA	NA	0.1179	0.510935 ± 6	3.27	3.42	-0.5	3227
B87-16 Mpageni	NA	NA	0.0786	0.510286 ± 6	3.02	3.14	-4.3	2740
B87-17 Nelspruit	86.4	15.74	0.1100	0.510835 ± 5	3.15	3.30	-0.5	3107
B87-25 Mpuluzi	59.1	8.97	0.0918	0.510465 ± 5	3.14	3.27	-0.4	3107

FIGURE 11.

Epsilon Nd versus Time diagram for rocks from the Barberton Mountain Land. Depleted mantle curve (DM) from DePaolo (1981b). Dotted lines indicate where the two data points from the Komati Formation (Jahn et al., 1982) plot when recalculated at 3.35 Ga (small solid circle) (details in Chapter 7).

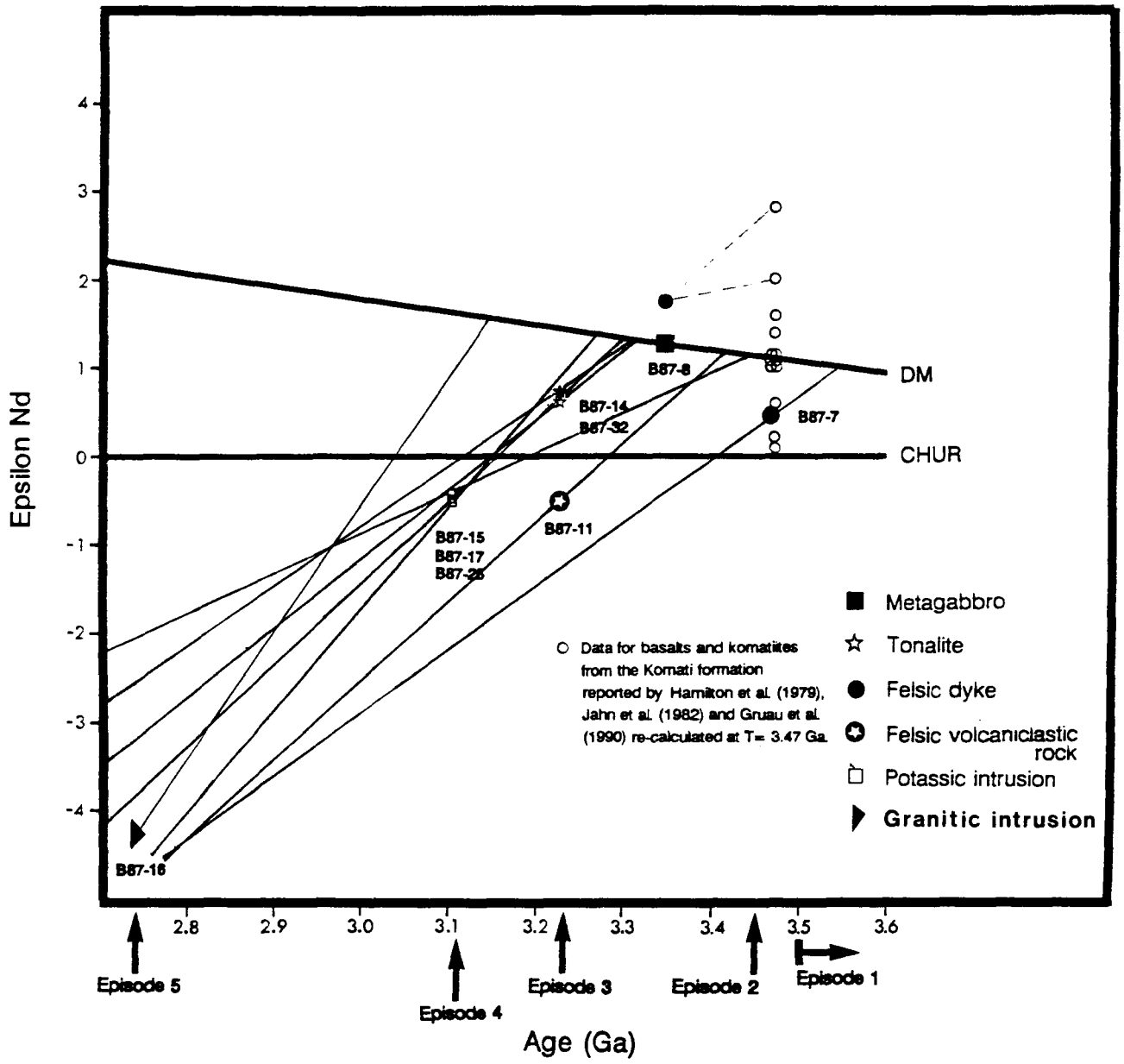
Epsilon Nd
4
3
2
1
0
-1
-2
-3
-4
DM
CHUR
B87-6
B87-14
B87-32
B87-7
B87-15
B87-17
B87-25
B87-11
B87-16
Data for basalts and komatiites from the Komati formation reported by Hamilton et al. (1979), Jahn et al. (1982) and Gruau et al. (1990) re-calculated at T= 3.47 Ga.
Metagabbro
Tonalite
Felsic dyke
Felsic volcaniclastic rock
Potassic intrusion
Granitic intrusion
2.8
2.9
3.0
3.1
3.2
3.3
3.4
3.5
3.6
Episode 5
Episode 4
Episode 3
Episode 2
Episode 1
Age (Ga)

CHAPTER 7:

DISCUSSION

(i) The age of Onverwacht Group volcanism and evidence for pre-Onverwacht crust

Previous age estimates for the lower Onverwacht Group suggest that it formed between ca. 3450-3490 Ma. Ages presented in the present study provide additional constraints on the timing of Onverwacht Group formation. The age of the Komati Formation is now tightly bracketed between 3467 +12 /-7 Ma, based on the zircon age determined for a porphyry dyke (B87-7) that intrudes the Komati Formation, and 3472 ± 5 Ma (Armstrong et al., 1990) based on zircon ages from an interflow sediment within the same formation. An ϵ_{Nd} value of +0.4 for this porphyry dyke suggests that it was derived from a slightly depleted mantle source relative to chondrites, however, the ϵ_{Nd} is enriched relative to the depleted mantle growth curve (DePaolo, 1981b). The T_{DM} age of 3.55 Ga is the earliest mantle-extraction age obtained in this study. If it is assumed that this dyke was contaminated by some older crustal component, then its true ϵ_{Nd} signature may have been subsequently enriched. In this case, 3.55 Ga would be a minimum estimate for mantle-extraction of the enriched component. The T_{DM} age obtained for this rock is comparable to pre-Onverwacht Group ages obtained from the AGC and gneisses within the BGB.

The metagabbro (B87-8) has been interpreted by de Wit et al. (1987b) to intrude the Komati Formation, cut the Middle Marker and merge with pillow lavas

in the lower Hooggenoeg Formation. If correct, the age for this unit corresponds to the age of extrusion of the lower Hooggenoeg Formation volcanic rocks. However, if this interpretation is incorrect, the age for this rock simply represents a time for emplacement of a mafic intrusion. The baddeleyite and zircon age of 3352 +6/-5 Ma for this metagabbro is the first evidence for mafic magmatic activity occurring $\approx$100 m.y. later than the main mafic/ultramafic flows of the Komati Formation. U-Pb SHRIMP data on this rock unit by Armstrong et al. (1990) gave ambiguous results leading to an erroneous interpretation of its age. Since baddeleyite is frequently associated with mafic rocks (e.g. Krogh et al., 1987; Kamo et al., 1989; Heaman and Tarney, 1989; LeCheminant and Heaman, 1989) and is not known to survive crustal melting events, or to form under low grade metamorphic conditions, this age is considered to be the time of crystallization of the metagabbro. Furthermore, skeletal zircon in this rock, although discordant, has an age compatible with that of the baddeleyite. An argument in favour of the zircon having crystallized within the gabbro is its relatively high Th/U ratio, which is typical of zircon crystallizing from mafic melts (Heaman et al., 1990). The age of 3445 Ma for a felsic sub-volcanic sill from the upper Hooggenoeg Formation (Armstrong et al., 1990), is $\approx$100 m.y. older than the metagabbro. Thus, if de Wit et al.'s (1987b) field interpretation is accepted, the age for the metagabbro provides evidence for the presence of a thrust fault separating sequences of vastly different ages within the Hooggenoeg Formation.

The ϵ_{Nd} value of + 1.3 for the metagabbro falls directly on DePaolo's depleted mantle growth curve. A number of other analyses from previous studies using rocks

from the Komati Formation, when recalculated at T= 3.47 Ga (see Fig.11, Chapter 6), also fall on this curve. Some of these plot well above the curve, however, and could be attributed to a unique strongly depleted mantle beneath the Kaapvaal Craton during the mid-Archean. However, if the rocks are from the same generation as the metagabbro (or even younger) then these strongly depleted signatures can be resolved. For example, if the two data points obtained by Jahn et al. (1982), which give ϵ_{Nd} values of +2.7 and +2.0 at 3.47 Ga, are recalculated at 3.35 Ga, identical values of ϵ_{Nd}= +1.7 are obtained which is within 0.4 ϵ_{Nd} units of the depleted mantle growth curve (dotted lines in Fig. 11). The age of this metagabbro, therefore, has important implications for future studies where co-geneticity of rocks, based on rock association and geochemistry, is assumed.

In summary, the Onverwacht Group may consist of two tectonically interleaved sequences, one with an age of about 3.47 Ga and the other at 3.35 Ga. The extent of the younger sequence remains unknown.

Evidence for a pre-Onverwacht Group crustal history is given by U-Pb zircon ages from rocks within the BGB. The oldest units that have been identified in the BGB are sodic intrusive rocks. A tonalitic gneiss sliver (B87-5) dated at 3538 +4/-2 Ma, which is suggested to have been tectonically emplaced within the Theespruit Formation (de Wit et al., 1983), represents the oldest unit yet dated within the BGB; this age agrees precisely with the previously reported SHRIMP data of Armstrong et al. (1990). The age for this gneissic tonalite is important because it provides strong evidence for the current interpretation that an unconformity exists within the

Theespruit Formation between the tonalite and mafic-ultramafic rocks of the lower Onverwacht Group (Armstrong et al., 1990). The strong fabric in this rock records at least one tectono-metamorphic event that pre-dates the early tectonic and thermal history of the greenstone belt (de Wit et al., 1983). This is consistent with the early deformational history and ages reported for the nearby Ancient Gneiss Complex (Compston and Kröner, 1988; Kröner et al., 1989).

The age for the trondhjemitic Steynsdorp pluton (B87-24) at 3509 +8/-7 Ma provides further evidence for early pre-greenstone sialic crust. The contact between this pluton and the greenstone belt is not well exposed but the Steynsdorp pluton has a much stronger fabric than the overlying greenstones which may either unconformably overlie it or have been tectonically emplaced. In general, field relationships between the tonalitic - trondhjemitic plutons and greenstone rocks in the BGB exhibit few intrusive features. An exception to this is the intrusive relationship between the Nelshoogte pluton and the surrounding greenstones of the Nelshoogte schist belt (Anhaeusser, 1982). Some intrusive units, such as the Kaap Valley, Doornhoek, and Stentor plutons, have sheared contacts suggesting structural emplacement as a solid mass (Robb, 1981; Robb and Anhaeusser, 1983).

Pre-Onverwacht Group xenocrystic single zircon ages of ca. 3525 Ma from felsic volcanic-volcaniclastic units related to the Fig Tree Group sediments (Armstrong et al., 1990; Kröner et al., 1991) and 3570 Ma granite clasts in the Moodies Group conglomerates (Kröner and Compston, 1988) provide additional evidence for older sialic components either adjacent to, or possibly as basement to,

the BGB.

(ii) Early TTG magmatism

Ages for TTG rocks from the southwest margin of the BGB, such as the Doornhoek (3448 ± 4 Ma), Theespruit (3443 ± 3 Ma) and Theeboom (3441 ± 5 Ma; de Wit et al., 1987a) plutons, support the suggestion of de Wit et al. (1987a) that these intrusions are contemporaneous with high-level felsic volcanic rocks from the upper Onverwacht Group which have been dated at 3445 ± 3 Ma (Armstrong et al., 1990; Kröner et al., 1991). The ages for these TTG rocks, which structurally underlie the greenstone belt (Fripp et al., 1980; de Wit et al., 1983) and are coeval with sills which intruded up active D_1 thrust faults (de Wit et al., 1987a), are consistent with the hypothesis that the generation of these sodic intrusions is syntectonic, i.e. formed by partial melting of simatic rocks over which the lower Onverwacht Group rocks were thrust during emplacement (de Wit et al., 1987a). If correct, these ages constrain the timing of early D_1 thrusting in this part of the BGB, as noted by Armstrong et al. (1990).

The Stolzburg pluton is distinguished from the other TTG gneisses because it is slightly older, yielding an age of 3459 +5/-4 Ma, and because it contains much younger phases. Kröner et al. (1991) reported a zircon evaporation age of 3440 ± 5 Ma and, in the present study, a late phase that may be as young as ca. 3201 Ma is shown by data from B87-2. This younger phase intrudes the older Stolzburg phase, however, the age may represent a late hydrothermal event as suggested by the extremely low Th/U ratios of the zircons.

(iii) North-central BGB tonalitic magmatism, volcanism, related sedimentation and deformation

A significant time for the geological development of the BGB occurred at 3227 Ma. Tonalitic magmatism, felsic volcanism, sedimentation and D_2 thrust-related deformation in the north-central part of the BGB occurred at this time. The emplacement of the Kaap Valley tonalite at 3227 ± 1 Ma is synchronous with a number of undeformed geochemically similar feldspar porphyries that are considered to be high-level equivalents to the Kaap Valley pluton. These porphyries have been interpreted to intrude along regional shear zones (D_2 thrust faults) and to cross-cut Fig Tree Group sediments which are regionally deformed (de Ronde, 1991; de Ronde et al., 1991). Therefore, they provide a minimum age constraint on D_2 thrust-related deformation. A maximum age for this thrusting event is given by a pre-tectonic feldspar porphyry (B87-27) at 3226 +5/-3 Ma.

An ignimbritic unit (B87-11) from a felsic volcanic-volcaniclastic sequence, located within the Stolzburg Syncline (Fig. 6), yields an age identical to that for the Kaap Valley pluton at 3227 ± 1 Ma. This unit unconformably overlies Fig Tree Group sediments at the sample location, but changes along strike to a conformable contact and has therefore been interpreted as syntectonic (de Wit, 1983; Armstrong et al., 1990). Similar relationships have been shown elsewhere in the BGB (Lamb, 1984; 1987; Paris, 1985). Thus, the age for this rock provides a maximum age for D_3-related deformation i.e. formation of the Stolzburg Syncline which is a large F_3 fold (C. de Ronde, pers. comm., 1991), a minimum age for Fig Tree Group sedimentation

and a maximum age for the deposition of the Moodies Group sediments at this location. The ϵ_{Nd} and zircon Th/U ratios of the ignimbrite differ from those of the Kaap Valley tonalite. The ϵ_{Nd} value suggests that the ignimbrite is more contaminated with older crust. However, this is not evident from the zircon analyses. Armstrong et al. (1990) dated the same unit and found a complex array of $^{207}Pb/^{206}Pb$ ion-microprobe ages. The youngest zircons dated were 3164 ± 12 Ma to 3088 ± 7 Ma which were interpreted to be the maximum age for Moodies Group sedimentation at this locality. These workers emphasized the previously established diachroneity of Moodies Group deposition in the southern part of the BGB by Lamb (1984), and the fact that there may be more than one age for Moodies-like deposition related to separate periods of compressive deformation. The ages of these zircons may, however, reflect contamination during sample processing, as was the case in several of the other samples in the Armstrong et al. (1990) study, or from relatively early Pb loss, since only one of these younger grains was concordant.

Major and trace element geochemical models suggest that TTG rocks are likely produced in two stages where partial melting of mantle produces mafic volcanic rocks, which in turn are partially melted to form tonalites (e.g. Arth et al., 1978; Martin, 1986). Model age calculations in studies of tonalites (e.g. Jahn et al., 1984; Shirey and Hanson, 1986) may place constraints on the age of the mafic metavolcanic source rocks. The difference between the crystallization and model ages can be regarded as the length of time that the sources of the tonalite magmas have been separated from a mantle source ("crustal residence" time) assuming there is no

fractionation of Sm/Nd during the partial melting event which formed the tonalite. However, Sm/Nd is likely to be decreased during this event (LREE enrichment) so measured "crustal residence" times are likely to be minimum estimates. The age difference between the 3227 Ma Kaap Valley tonalite and their T_{DM}'s (3.31 Ga, 3.32 Ga) suggests a crustal residence time for this source of at least 100 m.y.. The depleted mantle model ages for the Kaap Valley tonalite are similar to the age of the metagabbro which could be related to the protolith source of the tonalite. Variations in ϵ_{Nd} values for many TTG rocks indicate that mafic precursors can be separated from a depleted mantle for as long as 300 m.y. (Jahn et al.,1984; Shirey and Hanson, 1986; Schärer, 1989) assuming the mafic protolith has a Sm/Nd ratio close to the derivative TTG's. Much greater crustal residence times are possible if the mafic protolith has a Sm/Nd approaching chondritic Sm/Nd ratios (Shirey and Hanson, 1986). Thus, the Onverwacht Group, which because of its propinquity is the obvious choice for a mafic protolith, may also be related to the source for the Kaap Valley pluton.

(iv) Potassic intrusions

The Nelspruit and Mpuluzi batholiths to the north and south of the BGB, respectively, were emplaced at ca. 3105 Ma and represent the most voluminous episode of magmatism in the BML. Intrusive phases within the batholiths were emplaced closely in time, as shown by the granodioritic Hebron pluton dated at 3104 +3/-2 Ma which cross-cuts the Nelspruit batholith, dated at 3105 ± 3 Ma. The emplacement of these batholiths was also coeval with the syeno-granitic Boesmanskop pluton at 3107 ± 1 Ma.

The Stentor pluton (3107 +6/-4 Ma) is also synchronous with this episode of magmatism. Located at the southern edge of the Nelspruit batholith and its associated migmatites, this unit is cut by thrust faults, indicating that a renewed period of compressional tectonics affected the northern boundary of the BGB during or after emplacement of the Stentor pluton.

These ca. 3105 Ma units are considered to have been derived by extensive partial melting of granitoid (TTG) rocks (Robb et al., 1983), an interpretation that is supported by the negative (ϵ_{Nd} = -0.5) values for the Nelspruit, Mpuluzi and Stentor intrusions. Extensions of the BGB and/or granitoid gneisses may underlie these thin sheet-like batholiths (de Beer et al., 1988). The presence of ca. 3300-3350 Ma xenocrystic and xenolithic (B87-18) components and the ca. 3300 Ma T_{DM}'s together suggest that the source for these rocks is some extensive underlying lithologically evolved crust. These ages are comparable to the 3350 Ma age measured on the Komati metagabbro (B87-8). The age of ca. 3300-3350 Ma may,

therefore, correspond to a major crust forming event in the BML. The extent of this crust exposed in the Onverwacht Group is unknown.

The fact that all these units, the Nelspruit and Hebron, Mpuluzi, Stentor and Boesmanskop intrusions, were emplaced over a very narrow time span, which represents a very large volume of magma, argues for a large-scale, short-duration tectonic event at ca. 3105 Ma. Gold mineralization, bracketed between 3084 Ma and 3126 Ma (de Ronde et al., 1991), could have occurred during this event.

The latest phase of magmatism in the BML is represented by the volumetrically minor Mpageni granite intrusion at 2740 ± 15 Ma. The ϵ_{Nd} value of --4.30 could be interpreted as plotting along an evolution trend with rocks that formed at 3.2 Ga and 3.1 Ga (Episodes III and IV in Fig. 11). However, given the uncertainties in LREE fractionation, it could be derived from crustal rocks produced during any of the earlier episodes.

(v) Comparative summary of recent U-Pb zircon data obtained by three methods

In addition to the data presented here, results from two other U-Pb zircon studies (by SHRIMP and Pb evaporation), which have recently been published on similar rock units as those dated in this study, are summarized in Table 9. For the two plutons dated by all three methods (Kaap Valley and Theespruit) the ages are in agreement. It should be noted that the zircon populations in both cases were simple (i.e. no apparent inherited components and no complex multi-generation zircons), and in the case of the Kaap Valley tonalite, the zircons were relatively low in U (resulting in reduced radiation damage despite its age), crack-free, clear and "gem" quality. For the five units dated in this study by both isotope dilution and by SHRIMP, the ages are either identical, or agree within error.

There are discrepancies in ages for the Stolzburg and Steynsdorp plutons between this study and Kröner et al.'s (1991) zircon Pb evaporation data. The older age obtained here for the Stolzburg pluton may indicate that this intrusion is heterogeneous, giving two slightly different ages of 3459 +5/-4 Ma (this study) and 3445 ± 4 Ma (Kröner et al., 1991). The Steynsdorp pluton, which is separated from the other TTG gneisses by the Dalmein pluton and Onverwacht Group volcanics, in this study gives an age 20 m.y. older than that obtained by zircon evaporation, i.e. 3509 Ma vs. 3490 Ma (Kröner et al., 1991). It is interesting to note that in both cases where the ages do not agree, the zircon populations consisted of cracked poor quality grains. In both cases, using the isotope dilution technique, it was necessary to use very tiny (< 200 mesh or < 50-70 m) multi-grain fractions in order to obtain

more concordant results. Normally, smaller grains give more discordant results, but in these cases the smaller grains were devoid of cracks and inclusions and were generally clear, resulting in more concordant data points. In the case of the Steynsdorp pluton it cannot be argued that the two studies sampled two separate phases of a heterogeneous intrusion because the same zircon separates for Kröner et al.'s study were subsequently analyzed by the SHRIMP (Kröner, A., pers. comm., 1991) giving an older age of 3509 Ma, identical to the isotope dilution result in the present study. There may be problems with the evaporation technique in obtaining crystallization ages of zircons in which severe Pb loss has occurred and insufficient numbers of pristine domains within the grains have survived, giving $^{207}Pb/^{206}Pb$ ages that are too young.

TABLE 9.

Comparative summary of U-Pb zircon data obtained by three methods.

(Note: ** = analysis is unpublished and was determined by A. Kröner (pers.comm., 1991)).

Method / Reference / Rock unit	Isotope dilution This study	Ion-microprobe (SHRIMP) Armstrong et al., 1990	Pb-evaporation (Kober technique) Kröner et al., 1991	Comments
Gneissic tonalite Theespruit fm	3538 +4/-2	3538 ± 6	ND	Zircons low U crack-free, clear
Steynsdorp pluton	3509 +8/-7	** 3509	3490 ± 4	Zircons extremely cracked, altered
Stolzburg pluton	3459 +5/-4	ND	3445 ± 4	
Theespruit pluton	3443 +4/-3	3437 ± 6	3440 ± 5	Simple zircon population
Kaap Valley pluton	3227 ± 1	3226 ± 14	3229 ± 5	"Gem" quality
Metagabbro Komati fm	3350 ± 4	3351 ± 6	ND	Skeletal zircons

(vi) Summary of events in the BML and comparison to other Archean greenstone belts

The duration of evolution of the BML spans 800 m.y. and it appears to have evolved in a series of discrete events widely separated in time (see Fig. 12). The deposition of the Onverwacht sequence was followed shortly by overthrusting onto adjacent sialic crust. TTG gneisses were syntectonically formed beneath the Onverwacht allochthons at ca. 3450 Ma contemporaneous with the emplacement of felsic units higher in the stratigraphy. Sedimentation, represented by Fig Tree rocks in the southern part of the greenstone belt, may have coincided in time as permitted by maximum zircon ages of 3450 Ma determined by Kröner and Compston (1988).

Limited evidence exists for magmatism at 3300 Ma to 3350 Ma. A baddeleyite age of 3352 Ma for a mafic intrusion which apparently feeds volcanism in the Onverwacht Group, zircon ages from a tonalitic xenolith in the Nelspruit batholith, and an ^{40}Ar-^{39}Ar age on serpentinites of the lower Onverwacht Group (York et al., 1981), indicate that there may have been a more extensive magmatic event at this time.

A major event 220 m.y after the extrusion of much of the Onverwacht involved the emplacement of the Kaap Valley tonalite and related high level porphyries at ca. 3230 Ma, northwest directed thrusting, volcanism and sedimentation. Recently Tomkinson and Philpot (1990) have suggested that the northern part of the BGB represents a late rift zone developed on an Onverwacht "basement". If felsic magmatism and mafic/ultramafic volcanism are closely spaced in time as they are in

the southern BGB, the Onverwacht-like volcanics in the north may actually be ≈220 m.y. younger than the type Onverwacht Group.

A large-scale, short-duration, major crust formation event occurred with the volumetrically most significant episode of magmatism at ca. 3105 Ma, ≈110 m.y. later than the Kaap Valley pluton. This event is also characterized by the intrusion of the syeno-granitic Boesmanskop complex. Late granitic plutonism occurred ≈360 m.y. later with the emplacement of the Mpageni pluton.

The long 800 m.y. duration and the episodic nature of the development of the BML characterize the evolution of this part of the Kaapvaal craton. The major crust-formation episodes spanned ≈365 m.y from ca. 3470 Ma to ca. 3105 Ma. In contrast, geochronological studies in the Superior Province, Canada, indicate much shorter greenstone belt development with most of the Abitibi greenstone belt evolving over 30 m.y. (Corfu et al., 1989) and with the bulk of intrusive activity in granite-greenstone terranes of the Wabigoon subprovince occurring between 2740 Ma to 2660 Ma (Blackburn et al., 1991). Thus, superficially similar granite-greenstone terranes may show vastly different time scales for development. The closest comparison to the BML occurs in the Pilbara block of Western Australia. Ages similar to those from the Onverwacht Group have been determined for rocks in the Marble Bar region, Pilbara craton, on lithologically similar units (Thorpe et al., 1990; Pidgeon, 1978) which has led to the suggestion that the Kaapvaal craton and the Pilbara block were once part of the same crustal unit during the mid-Archean (Kröner et al., 1991; Kröner and Layer, in press).

FIGURE 12.

Summary diagram of available age data for rocks from this study. Stars denote ages determined in the present study. 2σ errors are less than or equal to the width of the star unless otherwise noted. Numbers correspond to the following studies:

1. Allsopp et al., 1962
2. Armstrong et al. 1990
3. Barton et al., 1983
4. Brévart et al., 1986
5. De Gasparis, 1976
6. Hamilton et al., 1979
7. Jahn et al., 1982
8. Lopez-Martinez et al., 1984
9. Oosthuyzen, 1970
10. Robb et al., 1986
11. Tegtmeyer and Kröner, 1987

AGE (MA)

2700 2800 2900 3000 3100 3200 3300 3400 3500

TONALITIC GNEISS SLIVER

STEYNSDORP PLUTON

STOLZBURG PLUTON

DOORNHOEK PLUTON

THEESPRUIT PLUTON

Mafic/ultramafic volcanics

KEY

- this study
- Ion microprobe [2]
- bulk conventional

} U-Pb Zircon

- Pb-Pb w-r
- Rb-Sr w-r
- Sm-Nd w-r
- Ar/Ar

KAAP VALLEY PLUTON

DEFORMED PORPHYRY

IGNIMBRITE

STOLZBURG younger phase

DALMEIN PLUTON

MPULUZI PLUTON

NELSPRUIT PLUTON

HEBRON PLUTON

STENTOR PLUTON

BOESMANSKOP PLUTON

MPAGENI PLUTON

EPISODE 5

EPISODE 4

EPISODE 3

EPISODE 2

EPISODE 1

CHAPTER 8

CONCLUSIONS

Magmatism in the BML spanned at least 800 m.y. from 3538 Ma to 2740 Ma (see Fig. 12) and is divisible into at least 5 distinct episodes:

I -- >3500 Ma

II -- ca 3450 Ma

III-- ca 3227 Ma

IV -- ca 3107 Ma

V -- ca 2740 Ma

EPISODE I: Pre-Onverwacht Group rocks are represented within the BGB by the Steynsdorp pluton (3509 +8/-7 Ma) and by a tectonically interleaved tonalitic gneiss sliver (3538 +4/-2 Ma). These units may represent basement to the volcanic sequence or they may have been tectonically juxtaposed with the greenstone sequence.

EPISODE II: The major volcanic event in the BGB is the 3490-3450 Ma Onverwacht Group volcanic rocks. Age constraints on mafic/ultramafic rocks of the Komati Formation indicate that these rocks were emplaced at ca. 3470 Ma. In the southern part of the BGB, Onverwacht Group volcanism was associated in time with the emplacement of early trondhjemitic plutons such as the Doornhoek (3448 ± 4 Ma), Theespruit (3443 +4/-3 Ma) and Stolzburg (3458 +5/-4 Ma) plutons.

Ages for syn-tectonic felsic sills and volcanic rocks from the Hooggenoeg and Theespruit Formations are essentially the same (ca. 3440 Ma) and indicate that the volcanic rocks were affected by an early episode of compression (Armstrong et al., 1990; de Wit et al., 1987). The first evidence for later mafic magmatism is given by a baddeleyite age of 3352 +6/-5 Ma from a pegmatitic gabbro within the Onverwacht Group, interpreted by some workers to feed flows in the lower Hooggenoeg Formation. This indicates a later episode of magmatism and possibly thrusting. The ϵ_{Nd} value for this sample (+1.7) falls on DePaolo's (1981b) depleted mantle growth curve.

EPISODE III: Tonalitic plutonism occurred in the BGB with the emplacement of the Kaap Valley pluton at 3227 ± 1 Ma. This episode was also associated with thrusting in the north-central part of the belt and with deposition of Moodies and Fig Tree Groups sediments as shown by the following data:

-- pre- and syn-tectonic porphyry sills were intruded along thrust faults at 3227 Ma (de Ronde et al., 1991; this study)

-- an ignimbrite deposited during regional deformation between the Moodies and Fig Tree Groups gives an age of 3227 ± 1 Ma

-- dacitic tuffs within the upper Fig Tree Group give ages of ca. 3230 Ma (Kröner et al., 1991)

It therefore appears that ca. 3230 Ma corresponds to a time of major compression, sedimentation, volcanism and plutonism in the northern part of the BGB.

Magmatism at ca. 3200 Ma in the southern BGB is recorded by sphene and zircon in a trondhjemitic phase that intrudes the Stolzburg pluton, by the 3216 +2/-1 Ma Dalmein pluton, and by sphene ages in the Steynsdorp and Doornhoek plutons which may record hydrothermal activity.

Major and trace element geochemical models suggest that TTG rocks are likely produced in at least two stages where partial melting of mantle produces mafic volcanic rocks, which in turn are partially melted to form tonalites (e.g. Arth et al., 1978; Martin, 1986). In this study, ϵ_{Nd} data indicate that the Kaap Valley tonalite was probably derived from mafic crust at least 100 m.y. older than the tonalite.

EPISODE IV: A major plutonic event occurred at ca. 3105 Ma with the emplacement of large sheet-like potassic batholiths such as the Nelspruit batholith (3105 ± 3 Ma) and the Mpuluzi batholith (3107 +4/-2 Ma) to the north and south of the BGB, respectively. This was coeval with the emplacement of the granodioritic Hebron pluton (3104 +3/-2 Ma), the syenitic Boesmanskop pluton (3107 ± 1 Ma), and possibly with gold mineralization (de Ronde et al., 1991). The Stentor pluton (3108 ± 4 Ma) is also part of this event. Since it is affected by thrusting (Fripp, 1980) there appear to be, including Episodes II and III, at least three episodes of compressional events in the BGB.

EPISODE V: The latest phase of magmatism occurred at ca. 2740 Ma with the emplacement of granitic plutons such as the Mpageni pluton (2740 ± 15 Ma) and the Mbabane pluton (2693 ± 8 Ma; Layer et al., 1989). Neodymium data for rocks from Episodes IV and V indicate a source compatible with remelting of older crust.

REFERENCES

Allsopp, H.L., Roberts, H.R., Schreiner, G.D., and Hunter, D.R., 1962. Rb-Sr age measurements on various Swaziland granites. J. Geophys. Res., 67, 5307-5313.

Anhaeusser, C.R., 1973. The evolution of the early Precambrian crust of southern Africa. Phil. Trans. R. Soc. Lond., A, 273, 359-388.

Anhaeusser, C.R., 1975. Precambrian tectonic environments. Ann. Rev. Earth Planet. Sci., 3, 31-53.

Anhaeusser, C.R., 1978. The geological evolution of the primitive earth - evidence from the Barberton Mountain Land, 71-105. *In:* Tarling, D.H., Ed., *Evolution of the Earth's Crust*, Academic Press, London, 443 pp.

Anhaeusser, C.R., 1982. Geological map of a portion of the Nelshoogte schist belt and the Stolzburg layered ultramafic complex, Barberton Mountain Land. *In: A Contribution to the Archean Geology of Southern Africa with Particular Reference to Aspects Involving Metallogeny Granite-greenstone Belt Development and Crustal Evolution.* D.Sc. thesis (unpubl.) Univ. Witwatersrand, Johannesburg.

Anhaeusser, C.R. and Robb, L.J., 1980. Regional and detailed field and geochemical studies of Archean trondhjemitic gneisses, migmatites and greenstone xenoliths in the southern part of the Barberton Mountain Land, South Africa. Precam. Res., 11, 373-397.

Anhaeusser, C.R. and Robb, L.J., 1981. Magmatic cycles and the evolution of the Archean granitic crust in the eastern Transvaal and Swaziland. Spec. Publ. geol. Soc. Aust., 7, 457-467.

Anhaeusser, C.R., Mason, R., Viljoen, M.J. and Viljoen, R.P., 1969. A reappraisal of some aspects of Precambrian shield geology. Bull. Geol. Soc. Am., 80, 2175-2200.

Anhaeusser, C.R., Robb, L.J. and Viljoen, M.J., 1983. Notes on the provisional geological map of the Barberton greenstone belt and surrounding granitic terrane, eastern Transvaal and Swaziland (1:250,000 colour map). Spec.

Publ. Geol. Soc. S. Afr., 9, 221-223.

Armstrong, R.A., Compston, W., de Wit, M.J., and Williams, I.S., 1990. The stratigraphy of the 3.5 - 3.2 Ga Barberton greenstone belt revisited: a zircon ion microprobe study. Earth Planet. Sci. Lett., 101, 90-106.

Arndt, N.T., 1983. Role of a thin, komatiite-rich oceanic crust in the Archean plate-tectonic process. Geology, 11, 372-375.

Arndt, N.T. and Goldstein, S.L., 1987. Use and abuse of crust-formation ages. Geology, 17, 307-310.

Arndt, N.T. and Nisbet, E.G. (Eds.), 1982. *Komatiites*. George Allen and Unwin, London, 526 pp.

Arth, J.G., Barker, F., Peterman, Z., Friedman, I., 1978. Geochemistry of the gabbro - diorite - tonalite - trondhjemite suite of southwest Finland and its implications for the origin of tonalitic and trondhjemitic magmas. J. of Petrol., 19, 289-316.

Barton, J.M., 1983. Isotopic constraints on possible tectonic models for crustal evolution in the Barberton granite-greenstone terrane, Southern Africa. Spec. Publ. geol. Soc. S. Afr., 9, 73-80.

Barton, J.M., Hunter, D.R., Jackson, M.P.A. and Wilson, A.C., 1980. Rb-Sr age and source of the bimodal suite of the Ancient Gneiss Complex, Swaziland. Nat., 283, 756-758.

Barton, J.M., Robb, L.J., Anhaeusser, C.R., and Van Nierop, D.A., 1983. Geochronologic and Sr-isotopic studies of certain units in the Barberton granite-greenstone terrane, South Africa. Spec. Publ. geol. Soc. S. Afr., 9, 63-72.

Beakhouse, G.P., M^{c}Nutt, R.H. and Krogh, T.E., 1988. Comparative Rb-Sr and U-Pb zircon geochronolgy of late- to post-tectonic plutons in the Winnipeg River belt, northwestern Ontario, Canada. Chemical Geol., 72, 337-351.

Bickford, M.E. and Mose, D.G., 1975. Geochronolgy of Precambrian rocks in the St. Francois Mountains, southeastern Missouri. Geol. Soc. Am. Spec. Pap. 165, 48 pp.

Blackburn, C.E., Johns, G.W., Ayer, J.A. and Davis, D.W., 1991. Wabigoon Subprovince. *In: Geology of Ontario*, Ontario Geological Survey, Spec. Vol., 4, Part I, 303-382.

Brévart, O., Dupre, B., and Allegre, C.J., 1986. Lead-lead age of komatiitic lavas and limitations on the structure and evolution of the Precambrian mantle. Earth and Planet. Sci. Lett., 77, 293-302.

Byerly, G.R., Lowe, D.R., Nocita, B.W. and Ransom, B.L., 1983. Apparent volcanic cycles in the Archean Swaziland supergroup, Barberton Mountain Land, South Africa: a result on non-magmatic processes. 14th Lunar and Planetary Science Conference (abstract).

Cattell, A., Krogh, T.E. and Arndt, N.T., 1984. Conflicting Sm-Nd whole rock and U-Pb zircon ages for Archean lavas from Newton Township, Abitibi belt, Ontario. Earth Planet. Sci. Lett., 70, 280-290.

Chauvel , C., Dupré, B. and Jenner, G.A., 1985. The Sm-Nd age of the Kambalda volcanics is 500 Ma too old! Earth Planet. Sci. Lett., 74, 315-324.

Cloete, M., 1990. The metamorphic history of the Komati formation (Barberton, South Africa): a P-T-t path and its tectonic implications. *In*: Glover, G.E. and Ho, S. (comp.), *The Third International Archean Symposium*, Perth, Extended Abstracts Volume, 121-123.

Compston, W, Williams, I.S. and Meyer, C.J., 1984. U-Pb geochronology of zircons from Lunar Breccia 73217 using a sensitive high mass resolution ion microprobe. J. Geophys. Res., 89 Suppl., B525-B534.

Compston, W. and Kröner, A., 1988. Multiple zircon growth within early Archean tonalitic gneiss from the Ancient Gneiss Complex, Swaziland. Earth Planet. Sci. Lett., 87, 13-28.

Compston, W., Williams, I.S., Campbell, I.H. and Gresham, J.J., 1986. Zircon xenocrysts from the Kambalda volcanics: age constraints and direct evidence of older continental crust below the Kambalda-Norseman greenstones. Earth Planet. Sci. Lett., 76, 299-311.

Condie, K.C., 1989. *Plate Tectonics and Crustal Evolution*, 3rd ed., Permagon, Oxford, 476 pp.

Corfu, F., 1988. Differential response of U-Pb systems in coexisting accessory minerals, Winnipeg River Subprovince, Canadian Shield: implications for Archean crustal growth and stabilization. Contrib. Mineral. Petrol., 98, 312-325.

Corfu, F. and Andrews, A.J., 1987. Geochronological constraints on the timing of magmatism, deformation, and gold mineralization in the Red Lake

greenstone belt, northwestern Ontario. Can. J. Earth Sci., 24, 1302- 1320.

Corfu, F. and Muir, T.L., 1989. The Hemlo-Heron Bay greenstone belt and Hemlo Au-Mo deposit, Superior Province, Ontario, Canada: 1. Sequence of igneous activity determined by zircon U-Pb geochronolgy. Chem. Geol., 79, 183-200.

Corfu, F., Krogh, T.E., Kwok, Y.Y. and Jensen, L.S., 1989. U-Pb zircon geochronolgy in the southwestern Abitibi greenstone belt, Superior Province. Can. J. Earth Sci., 26, 1747-1763.

Corliss, J.B., Dymond, J., Gordon, L.I., Edmond, J.M., von Herzen, R.P., Ballard, R.D., Green, K., Williams, D., Bainbridge, A., Crane, K. and van Andel, T.H., 1979. Submarine thermal springs on the Galapagos Rift. Science, 203, 1073-1083.

Davies, R.D., 1971. Geochronology and isotopic evolution of the early Precambrian crustal rocks in Swaziland. Ph.D. thesis (unpubl.), Univ. Witwatersrand, Johannesburg.

Davis, D.W., 1982. Optimum linear regression and error estimation applied to U-Pb data. Can. J. Earth Sci., 19, 2141-2149.

De Beer, J.H., E.H. Stettler, J.G. du Pessis and J. Blume, 1988. The deep structure of the Barberton greenstone belt: a geophysical study. S. Afr. Tydskr. Geol., 91, 184-197.

De Gasparis, A.A., 1967. Rb-Sr studies relating to problems of geochronology on the Nelspruit and Mpageni granites. M.Sc thesis (unpubl.), Univ. Witwatersrand, Johannesburg, 92 pp.

de Ronde, C.E.J., 1991. Structural and geochronolgical relationships and fluid-rock interaction in the central part of the ≈3.2-3.5 Ga Barberton greenstone belt, South Africa. Ph.D. thesis (unpubl.) Univ. Toronto, 370 pp.

de Ronde, C.E.J., Kamo, S.L., Davis, D.W., de Wit, M.J. and Spooner, E.T.C., 1991a. Field, geochemical and U-Pb isotopic constraints from hypabyssal felsic intrusions within the Barberton greenstone belt, South Africa: Implications for tectonics and the timing of gold mineralization. Precam. Res., 49, 261-280.

de Wit, M.J., 1982. Gliding and overthrust nappe tectonics in the Barberton

greenstone belt. J. Struct. Geol., 4, 117-136.

de Wit, M.J., 1983. Notes on a preliminary 1:25,000 geological map of the southern part of the barberton Mountin Land. Geol. Soc. S. Afr. Spec. Publ., 9, 185-187.

de Wit , M.J. and Stern, C.R., 1980. A 3500 Ma ophiolite complex from the Barberton greenstone belt, South Africa. Archean oceanic crust and its geotectonic implications. 2nd Int. Archean Symp., Extended abstracts, Perth, Geol. Soc. Aust., 85-87.

de Wit, M.J., Hart, R., Martin, A. and Abbott, P., 1982. Archean abiogenic and probable biogenic structures associated with mineralized hydrothermal vent systems and regional metasomatism with implications for greenstone belt studies. Econ. Geol., 77, 1783-1802.

de Wit, M.J., Fripp, R.E.P. and Stanistreet, I.G., 1983. Tectonic and stratigraphic implications of new field observations along the southern part of the Barberton greenstone belt. Spec. Publ. geol. Soc. S. Afr., 9, 21-29.

de Wit, M.J., Hart, R.J. and Wilson, A.H., 1987a. Felsic igneous rocks within the 3.3 to 3.5 Ga Barberton greenstone belt: High crustal level equivalents to the surrounding tonalite-trondhjemite terrane, emplaced during thrusting. Tectonics, 6, 529-549.

de Wit, M.J., Hart, R.A. and Hart, R.J., 1987b. The Jamestown ophiolite complex, Barberton mountain belt: a section through 3.5 Ga oceanic crust. J. Afr. Earth Sci., 5, 681-730.

DePaolo, D.J., 1981a. Trace element and isotopic effects of combined wallrock assimilation and fractional crystallization. Earth Planet. Sci. Lett., 53, 189-202.

DePaolo, D.J., 1981b. Neodymium isotopes in the Colorado Front Range and crust-mantle evolution in the Proterozoic. Nat., 291, 193-196.

DePaolo, D.J., 1983. The mean life of continents: estimates of continental recycling rates from Nd and Hf isotopic data and implications for mantle structure. Geophys. Res. Lett., 10, 705-708.

DePaolo, D.J., 1985. Isotopic studies of processes in mafic magma chambers: I. The Kiglapait intrusion, Labrador. J. Petrol., 26, 925-951.

DePaolo, D.J. and Wasserburg, G.J., 1976. Nd isotopic variations and

petrogenetic models. Geophys. Res. Lett., 3, 249-252.

Dokka, R.K. and Lowe, D.R., 1984. Large-scale Phanerozoic-style thrust faulting in the Archean: evidence from the southwestern Barberton greenstone belt, South Africa. Geol. Soc. Am. Abstr. Prgr., 16, 491.

Duchac, K.C. and Hanor, J.S., 1987. Origin and timing of the metasomatic silicification of an early Archean komatiite sequence, Barberton Mountain Land, South Africa. Precam. Res., 37, 125-146.

Edwards, R.L., Chen, J.H. and Wasserburg, G.J., 1986/87. ^{235}U-^{234}U-^{230}Th-^{232}Th systematics and the precise measurement of time over the past 500,000 years. Earth Planet. Sci. Lett., 81, 175-192.

Eriksson, K.A., 1980. Transitional sedimentation styles in the Moodies and Fig Tree groups, Barberton Mountain Land, South Africa: evidence favouring an Archean continental margin. Precam. Res., 12, 141-160.

Fripp, R.E.P., van Nierop, D.A., Callow, M.J., Lilly, P.A. and Plessis, L.U., 1980. Deformation in part of the Archean Kaapvaal craton, South Africa. Precam. Res., 13, 241-251.

Glikson, A.Y., 1979. Early Precambrian tonalite-trondhjemite sialic nuclei. Earth Sci. Rev., 15, 1-73.

Glikson, A.Y. and Jahn, B.M., 1985. REE and LIL elements, eastern Kaapvaal shield, South Africa: evidence of crustal evolution by 3-stage melting. *In*: Ayres, L.D., Thurston, P.C., Card, K.D. and Weber, W., Eds., *Evolution of Archean Supracrustal Sequences*, Geol. Assoc. Can. Spec. Pap., 28, 303-324.

Gruau, G., Chauvel, C. and Jahn, B.M., 1990. Anomalous Sm-Nd ages for the early Archean Onverwacht group volcanics. Contrib. Mineral. Petrol., 104, 27-34.

Hall, A.L., 1918. The geology of the Barberton gold mining district. Mem. Geol. Surv. S. Afr., 9, 324 pp.

Hamilton, P.J., Evenson, N.M., O'Nions, R.K., Smith, H.S., and Erlank, A.J., 1979. Sm-Nd dating of the Onverwacht group volcanics, southern Africa, Nat., 279, 298-300.

Hamilton, P.J., O'Nion's, R.K., Bridgwater, D. and Nutman, A., 1983. Sm-Nd studies of Archean metasediments and metavolcanics from west Greenland and their implications for the Earth's early history. Earth Planet. Sci. Lett.,

62, 263-272.

Hanor, J.S. and Duchac, K., 1990. Isovolumetric silicification of Early Archean komatiites: geochemical mass balances and constraints on origin. J. Geol., 98, 863-877.

Hart, R.A. and de Wit, M.J., 1984. Hydrothermal alteration in the 3.5 Ga old Onverwacht group of South Africa. *In: Workshop on the early Earth: the interval from accretion to the older Archean*, Extended abstract, Lunar and Planetary Inst., Houston, LPI Tech. Rep., 85-01, 23-24.

Heaman, L.H. and Tarney, 1989. U-Pb baddeleyite ages for the Scourie dyke swarm, Scotland: evidence for two distinct intrusion events. Nat., 340, 705-708.

Heaman, L.H., M^{c}Nutt, R.H. and Krogh, T.E., 1986. Geological significance of U-Pb and Rb-Sr ages for two pre-tectonic granites from the central metasedimentary belt, Ontario. Geol. Assoc. Canada Spec. Pap., 31, 209-221.

Heaman, L.H., Bowins, R. and Crocket, J., 1990. The chemical composition of igneous zircon suites: Implications for geochemical tracer studies. Geochim. Cosmochim. Acta, 54, 1597-1607.

Hegener, E., Kröner, A. and Hoffmann, A.W., 1984. Age and isotopic geochemistry of the Archean Pongola and Ushushwana Suites in Swaziland, southern Africa: a case for crustal contamination of mantle-derived magma. Earth Planet. Sci. Lett., 70, 267-279.

Hunter, D.R., 1973. The Ancient Gneiss Complex in Swaziland. Trans. Geol. Soc. S. Afr., 73, 107-150.

Jackson, M.P.A., Eriksson, K.A. and Harris, C.W., 1987. Early Archean foredeep sedimentation related to crustal shortening: a reinterpretation of the Barberton Sequence, Southern Africa. Tectonophys., 136, 197-221.

Jacobsen, S.B. and Wasserburg, G.J., 1980. Sm-Nd evolution of chondrites. Earth Planet. Sci. Lett., 50, 139-155.

Jaffey, A.H., Flynn, K.F., Glendenin, L.E., Bentley, W.C. and Essling, A.M., 1971. Precision measurements of half-lives and specific activities of ^{235}U and ^{238}U. Physical Rev., C4, 1889-1906.

Jahn, B.M., Gruau, G. and Glikson, A.Y., 1982. Komatiites of the Onverwacht

Group, South Africa: REE geochemistry, Sm/Nd age and mantle evolution. Contrib. Mineral. Petrol., 80, 25-40.

Jahn, B.M., Vidal, A.P. and Kröner, A., 1984. Multi-chronometric ages and origin of Archean tonalitic gneisses in Finnish Lapland: a case for long crustal-residence time. Contrib. Mineral. Petrol., 86, 398-408.

Jahn, B.M., Glikson, A.Y., Peucat, J.J. and Hickman, A.H., 1981. REE geochemistry and isotopic data of Archean silicic volcanics and granitoids from the Pilbara Block, Western Australia: implications for early crustal evolution. Geochim. Cosmochim. Acta, 45, 1633-1652.

Kamo, S.L., Gower, G.F. and Krogh, T.E., 1989. Birthdate for the Iapetus ocean? A precise U-Pb zircon and baddeleyite age for the Long Range dikes, southeast Labrador. Geology, 17, 602-605.

Kober, B., 1986. Whole-grain evaporation for $^{207}Pb/^{206}Pb$-age investigations on single zircons using a double filament thermal ion source. Contrib. Mineral. Petrol., 93, 482-490.

Kober, B., 1987. Single-zircon evaporation combined with Pb^{+}emitter-bedding for $^{207}Pb/^{206}Pb$ age investigations using thermal ion mass spectrometry and implications to zirconology. Contrib. Mineral. Petrol., 96, 63-71.

Krogh, T.E., 1973. A low contamination method for the hydrothermal decomposition of zircon and extraction of U and Pb for isotopic age determinations. Geochim. Cosmochim. Acta, 37, 485-494.

Krogh, T.E., 1982. Improved accuracy of U-Pb zircon ages by creation of more concordant systems using an air abrasion technique. Geochim. Cosmochim. Acta, 46, 637-649.

Krogh , T.E., Corfu, F., Davis, D.W., Dunning, G.R, Heaman, L.M., Kamo, S.L., Machado, N., Greenough, J.D. and Nakamura, E., 1987. Precise U-Pb isotopic ages of diabase dykes and mafic to ultramafic rocks using trace amounts of baddeleyite and zircon. *In*: H.C. Halls, ed., *Mafic Dyke Swarms,* Geol. Assoc. Can. Spec. Pap., 34, 147-152.

Kröner, A. and Compston, W., 1988. Ion microprobe ages of zircons from early Archaean granite pebbles and greywacke, Barberton greenstone belt, southern Africa. Precam. Res., 38, 367-380.

Kröner, A. and Layer, P., *in press.* Crust-formation, plate motion and supercontinent assemblage since the early Archean, Science.

Kröner, A. and Todt, W., 1988. Single zircon dating constraining the maximum age of the Barberton greenstone belt, southern Africa. J. Geophys. Res., 93, 15,329-15,337.

Kröner, A., Compston, W. and Williams, I.S., 1989. Growth of early Archaean crust in the Ancient Gneiss Complex of Swaziland as revealed by single zircon dating. Tectonophys., 161, 271-298.

Kröner, A., Byerly, G.R. and Lowe, D.R., 1991. Chronology of early Archaean granite-greenstone evolution in the Barberton Mountain Land, South Africa, based on precise dating by single zircon evaporation. Earth and Planet. Sci. Lett., 103, 41-54.

Lamb, S.H., 1984. Structures on the eastern margin of the Archean Barberton greenstone belt, northwest Swaziland. *In:* Kröner, A. and Greiling, R.O., eds., *Precambrian Tectonics Illustrated*. Schweizerbart, Stuttgart, 19-39.

Lamb, S.H., 1987. Archean synsedimentary tectonic deformation - a comparison with the Quaternary, Geology, 15, 565-568.

LeCheminant, A.N. and Heaman, L.M., 1989. Mackenzie igneous events, Canada: Middle Proterozoic hotspot magmatism associated with ocean opening. Earth and Planet. Sci. Lett., 96, 38-48.

Lopez Martinez, M., York, D., Hall, C.M., and Hanes, J.A., 1984. Oldest reliable $^{40}Ar/^{39}Ar$ ages for terrestrial rocks: Barberton Mountain Land komatiites, Nat., 307, 352-354.

Lowe, D.R., 1982. Comparative sedimentology of the principal volcanic sequences of Archean greenstone belts in South Africa, Western Australia, and Canada: implications for crustal evolution. Precam. Res., 17, 1-29.

Lowe, D.R. and Byerly, G.R., 1986. Archean flow-top alteration zones formed initially in a low-temperature sulfate-rich environment. Nat., 324, 245-248.

Lowe, D.R. and Knauth, L.P., 1977. Sedimentology of the Onverwacht Group (3.4 b.y.), Transvaal, South Africa, and its bearing on characteristics and evolution of the early Earth. J. Geol., 85, 699-723.

Lowe, D.R., Byerly, G.R., Ransom, B.L. and Nocita, B.W., 1985. Stratigraphic and sedimentological evidence bearing on structural repetition in early Archean rocks of the Barberton greenstone belt, South Africa. Precam. Res., 27, 165-186.

Martin, H., 1987. Petrogenesis of Archean trondhjemites, tonalites, and granodiorites from eastern Finland: Major and trace element geochemistry. J. Petrol., 28, 921-953.

Nisbet, E.G., 1987. *The Young Earth*, Allen and Unwin, Boston, 402 pp.

Nisbet, E.G. and Fowler, C.M.R., 1983. A model for Archean plate tectonics. Geology, 11, 376- 379.

Nocita, B.W., 1989. Sandstone petrology of the Archean Fig Tree Group, Barberton greenstone belt, South Africa: Tectonic implications. Geology, 17, 953-956.

Oosthuyzen, E.J., 1970. The geochronology of a suite of rocks from the granitic terrane surrounding the Barberton Mountain Land. Ph.D. thesis (unpubl.), Univ. Witwatersrand, Johannesburg, 94 pp.

Page, R.W., 1978. Response of U-Pb zircon and Rb-Sr total-rock and mineral systems to low-grade regional metamorphism in Proterozoic igneous rocks, Mount Isa, Australia. J. Geol. Soc. Aust., 25, 141-164.

Paris, I., 1985. The geology of the farms Josefsdal, Dunbar and part of Diepgezet in the Barberton greenstone belt, Ph.D. thesis (unpubl.), Univ. of the Witwatersrand, Johannesburg, 239 pp.

Paris, I., Stanistreet, I.G. and Hughes, M.J., 1985. Cherts of the barberton greenstone belt interpreted as products of submarine exhalative activity. J. Geol., 93, 111-129.

Parrish, R.R., 1991. U-Pb dating of monazite and its application to geological problems. Can. J. Earth Sci., 27, 1431-1450.

Parrish, R. and Krogh, T.E., 1987. Synthesis and purification of ^{205}Pb for U-Pb geochronology. Chem. Geol., 66, 103-110.

Pidgeon, R.T., 1978. 3450 m.y.-old volcanics in the Archean layered greenstone succession of the Pilbara Block, Western Australia, Earth Planet. Sci. Lett., 37, 421-428.

Ramsay, J.G., 1963. Structural investigations in the Barberton Mountain Land, eastern Transvaal. Trans. Proc. Geol. Soc. S. Afr., 66, 353-401.

Richards, J.P., Krogh, T.E. and Spooner, E.T.C., 1988. Fluid inclusion characteristics and U-Pb rutile age of late hydrothermal alteration and

veining at the Musoshi stratiform copper deposit, Central African Copper belt, Zaire. Econ. Geol., 83, 118-139.

Reimer, T.O., Condie, K.C., Schneider, G. and Georgi, A., 1985. Petrography and geochemistry of granitoid and metamorphic pebbles from the early Archean Moodies group, Barberton Mountain Land, South Africa. Precam. Res., 29, 383-404.

Robb, L.J., 1981. The geological and geochemical evolution of the tonalite-trondhjemite gneisses and migmatites in the Barberton region, Eastern Transvaal. Ph.D. thesis (unpubl.), Univ. Witwatersrand, Johannesburg, 342 pp.

Robb, L.J., 1983a. The nature, origin and significance of Archean migmatites in the Barberton Mountain Land: a new approach in the assessment of early crustal evolution. Spec. Publ. geol. Soc. S. Afr., 9, 81-102.

Robb, L.J., 1983b. Geological and chemical characteristics of late granite plutons in the Barberton region and Swaziland with an emphasis on the Dalmein pluton - a review. Spec. Publ. geol. Soc. S. Afr., 9, 153-167.

Robb, L.J., Anhaeusser, C.R. and Van Nierop, D.A., 1983. The recognition of the Nelspruit batholith north of the Barberton greenstone belt and its significance in terms of Archean crustal evolution. Geol. Soc. S. Afr. Spec. Publ., 9, 117-130.

Robb, L.J. and Anhaeusser, C.R., 1983. Chemical and petrogenetic characteristics of Archean tonalite-trondhjemite gneiss plutons in the Barberton Mountain Land. Geol. Soc. S. Afr. Spec. Publ., 9, 103-116.

Robb, L.J., Barton, J.M., Kable, E.J., and Wallace, R.C., 1986. Geology, geochemistry and isotopic characteristics of the Archean Kaap Valley pluton, Barberton Mountain Land, South Africa. Precam. Res., 31, 1-36.

SACS (South African Committee for Stratigraphy), 1980. Part 1 (comp. L.E. Kent), Stratigraphy of South Africa. Handb. Geol. Survey S. Afr. 8, 690 pp.

Schärer, U., 1989. Age, origin and metamorphic overprint of volcanic and plutonic rocks in the central Uchi Subprovince, Superior Province, Canada. Geol. Assoc. Canada - Mineral. Assoc. Canada Joint Annual Meeting, Montreal, 14, p.A55.

Shirey, S.B., 1991. The Rb-Sr, Sm-Nd, Re-Os isotopic systems: a summary and

comparison of their applications to the cosmochronology and geochronology of igneous rocks. *In:* Heaman, L.H. and Ludden, J.N., eds., *Short Course Handbook on applications of radiogenic isotope systems to problems in geology*, Mineral. Assoc. Canada, May 1991, Toronto, 498 pp.

Shirey, S.B. and Hanson, G.N., 1986. Mantle heterogeneity and crustal recycling in Archean granite-greenstone belts: Evidence from Nd isotopes and trace elements in the Rainy Lake area, Superior Province, Ontario, Canada. Geochim. Cosmochim. Acta, 50, 2631-2651.

Sleep, N.H. and Windley, B.F., 1982. Archean plate tectonics: Constraints and inferences. J. of Geology, 90, 363-379.

Stacey, J.S. and Kramers, J.D., 1975. Approximation of terrestrial lead isotope evolution by a two-stage model. Earth Planet. Sci. Lett., 26, 207-221.

Stanistreet, I.G., de Wit, M.J. and Fripp, R.E.P., 1981. Do graded units of accretionary spheroids in the Barberton greenstone belt indicate Archean deep water environment? Nat., 293, 280-283.

Stewart, B.W. and DePaolo, D.J., 1987. Nd and Sr isotopic evidence for open system behaviour in the Skaergard intrusion. Geol. Soc. Am. Abs., 18, 764.

Tegtmeyer, A.R. and Kroner, A., 1987. U-Pb zircon ages bearing on the nature of early Archean greenstone belt evolution, Barberton Mountain Land, Southern Africa. Precam. Res., 36, 1-20.

Thorpe, R.I., Hickman, A.H., Davis, D.W., Mortensen, J.K. and Trendall, A.F., 1990. Application of recent zircon U-Pb geochronology in the Marble Bar region, Pilbara craton, to modelling Archean lead evolution. *In*: Glover, G.E. and Ho, S. (comp.), *The Third International Archean Symposium*, Extended abstract, Perth, 11-13.

Tompkinson, M.J. and Philpott, 1990. Fault-bounded tectonostratigraphic units in the northern portion of the Barberton greenstone belt and evidence for more than one phase of greenstone belt development. *In*: Glover, J.E. and Ho, S.E. (comp.), *The Third International Archean Symposium*, Extended abstract, Perth, 377-380.

Viljoen, M.J., 1964. The geology of the Lily syncline and portion of the Eureka syncline between the Consort Mine and Joe's Luck Siding, Barberton Mountain Land. M.Sc. thesis (unpubl.), Univ. Witwatersrand, Johannesburg, 131 pp.

Viljoen, M.J. and Viljoen, R.P., 1969a. An introduction to the geology of the Barberton granite-greenstone terrane. Geol. Soc. S. Afr., Spec. Publ., 2, 9-28.

Viljoen, M.J. and Viljoen, R.P., 1969b. The geology and geochemistry of the lower ultramafic unit of the Onverwacht group and a proposed new class of igneous rock. Spec. Publ. geol. Soc. S. Afr., 2, 55-86.

Viljoen, M.J. and Viljoen, R.P., 1969c. The geological and geochemical significance of the Upper formation of the Onverwacht group. Spec. Publ. geol. Soc. S. Afr., 2, 113-152.

Viljoen, M.J. and Viljoen, R.P., 1969d. The effects of metamorphism and serpentinization on the volcanics and associated rocks of the Barberton region. Spec. Publ. geol. Soc. S. Afr., 2, 29-53.

Viljoen, M. J., Viljoen, R.P., Smith, H.S., and Erlank, A.J., 1983. Geological , textural and geochemical features of komatiite flows from the Komati formation. Spec. Publ. geol. Surv. S. Afr., 9, 1-20.

Visser, D.J.L. (comp.), van Eden, O.R., Joubert, G.K., Sohnge, A.P.G., van Zyl, J.S., Rossow, P.J. and Taljaard, J.J., 1956. The geology of the Barberton area. Spec. Publ. geol. Survey. S. Afr., 15, 242 pp.

Wasserburg, G.J., Jacobsen, S.B., DePaolo, D.J., M^{c}Culloch, M.T. and Wen, T., 1981. Precise determination of Sm/Nd ratios, Sm and Nd isotopic abundances in standard solutions. Geochim. Cosmochim. Acta, 45, 2311-2323.

Williams, D. and Furnell, R.G., 1979. Reassessment of part of the Barberton type area, South Africa. Precam. Res., 9, 325-347.

Williams, I.S., Compston, W., Black, L.P., Ireland, T.R. and Foster, J.J., 1984. Unsupported radiogenic lead in zircon: a cause of anomalously high Pb-Pb, U-Pb and Th-Pb ages. Contrib. Mineral. Petrol., 88, 322-327.

Windley, B.F., 1984. *The Evolving Continents*, 2nd ed., J. Wiley, London, 399 pp.

York, D., Hall, C.M., Masliwec, R.L. and Hale, C.J., 1981 [abs.]. ^{40}Ar-^{39}Ar age measurements on the Onverwacht volcanics. Eos, 62, p.429.

APPENDIX 1

Sm-Nd whole rock procedure

Concentrations of Sm and Nd were determined by isotope dilution and chemical separation was performed using standard cation and reverse-phase column techniques. Descriptions of all processes involved in determining Sm/Nd data are presented in this Appendix.

Sample preparation

Sm-Nd analyses were performed on samples free of weathered surfaces. Approximately 2-4 kg was selected from the rock sample collected for the U-Pb study. This amount was crushed to 0.5-0.7 mm^3 rock chips and subsequently pulverized to a fine powder (<300 mesh) in a tungsten - carbide shatterbox. Both the jaw crusher and shatterbox were stringently cleaned between samples to avoid contamination.

Sample dissolution and chemical separation

Rock powders weighing approximately 100 mg (i.e. >70 mg and <150 mg) were placed in clean PFA Teflon Savillex capsules with ≈10 ml of 48% HF. As a precaution against HF leakage, these capsules were placed inside a second (FEP Teflon) Savillex capsule. These were placed in an oven at 150° for 72 hours after

which the capsules were removed, cooled to room temperature, and evaporated on a hot plate overnight. In order to dissolve the fluorides, approximately 5 ml of 16N HNO_3 were added to the capsules and these were placed in the oven, again at 150°, overnight. After cooling the capsules and evaporating the solution to dryness, the samples were converted in 5 ml of 6N HCl in the oven overnight. Once removed and cooled, 5 ml of triply distilled water (Milli-Q 3-cartridge system) was added to the HCl solution which was then split into two aliquots, one of which was spiked with a mixed REE spike enriched in ^{149}Sm and ^{150}Nd for determining Sm and Nd concentrations by isotope dilution. The Sm and Nd concentrations of the spike were previously calibrated to the international rock standard BCR-1 which yielded a $^{147}Sm/^{144}Nd$ ratio of 0.2280. The two aliquots were evaporated, re-dissolved in 2 ml of 2.5N HCl, and centrifuged to ensure that there was no residue remaining before ion exchange column separation. Rb, Sr, and the bulk REE's were separated using cation exchange resin (Dowex Bio-Rad AG50W, 200-400 mesh) in quartz columns. The REE aliquot was evaporated and redissolved in 1 ml of 0.155N HCl before loading onto a separate set of columns containing Teflon powder (200 mesh) coated with 2,2 diethyl-hexyl-orthophosphoric acid (HDEHP). This procedure, called reverse phase ion exchange chromatography, is used to purify Sm and Nd. After chemical separation of these two REE's (Nd in 0.155N HCl and Sm in 0.5N HCl) the two aliquots were evaporated and redissolved in a mixture of 0.3N H_3PO_4 and 3N HNO_3 (1.3:100) in preparation for mass spectrometric analysis. Blanks in the M^{c}Master laboratory typically average 0.1 ng for Sm and 0.5 ng for Nd.

Mass spectrometry

Sm and Nd were loaded separately in a 1 μl solution of H_3PO_4 onto outgassed Ta side filaments of a triple filament assembly. Isotopic ratios were measured using a VG354, 5-collector, solid source mass spectrometer (27 cm radius, 90° magnetic sector) in dynamic multi-collector mode controlled by an HP 9121 computer. using 4 collectors. The La Jolla standard gave an average value of 0.51184 ± 0.00002 (2σ mean) over 24 runs during the course of this work. The average within- run precision on Nd isotopic ratios was ± 0.000012 (2σ) with 180 ratios in a typical run. The $^{143}Nd/^{144}Nd$ ratios were normalized to $^{146}Nd/^{144}Nd$ = 0.7219 and variations in the Sm/Nd ratios between repeat dissolutions of unknowns was less than ± 0.5%. The mean intensity of the ^{143}Nd peak was $\approx 1.1ex10^{-11}$ amps. The analytical uncertainty on each model age totals $\approx$ ± 20 Ma (2σ).